1-1-2013

Developmental Regulation of Strongyloides Stercoralis infectious Third-Stage Larvae by Canonical Dauer Pathways

Jonathan David Chaffee Stoltzfus
University of Pennsylvania, jonathan.stoltzfus@gmail.com

Developmental Regulation of Strongyloides Stercoralis infectious Third-Stage Larvae by Canonical Dauer Pathways

Abstract
Parasitic nematodes inflict a vast global disease burden in humans as well as animals and plants of agricultural importance; understanding how these worms infect their hosts has significant health and economic implications. In humans, soil-transmitted parasitic nematodes cause hookworm disease and strongyloidiasis, and vector-transmitted parasitic nematodes cause filariasis. The infectious form of the species causing these diseases is a developmentally arrested third-stage larva (L3i). Molecular mechanisms governing L3i developmental arrest and activation within a host have been poorly understood. An analogous developmentally arrested third-stage larva--the dauer larva--forms during stressful environmental conditions in the free-living nematode *Caenorhabditis elegans* and is controlled by four cellular signaling pathways. The "dauer hypothesis" posits that similar mechanisms regulate dauer and L3i development. The parasitic nematode *Strongyloides stercoralis* was used to test the dauer hypothesis because its life cycle includes both parasitic and free-living forms. To investigate the role of canonical dauer pathway homologs in regulating L3i arrest and activation, this study utilized transcriptome sequencing (RNAseq), transgenesis, and pharmacological studies. Transcripts encoding cyclic guanosine monophosphate (cGMP) pathway components were coordinately up-regulated in L3i. Application of membrane-permeable 8-bromo-cGMP resulted in activation of L3i and modulation of ligand transcripts in other pathways. In comparison to *C. elegans*, *S. stercoralis* has few genes encoding insulin/IGF-1 -like signaling (IIS) ligands, several of which have transcripts modulated during L3i development. Application of the phosphatidylinositol-3 kinase inhibitor, LY294002, prevented L3i activation in host-like conditions. The *S. stercoralis* transcriptome includes seven homologs of the single *C. elegans* dauer transforming growth factor &beta (TGF&beta) ligand, three of which are only expressed in L3i. Although the *C. elegans* nuclear hormone receptor ligand delta7-dafachronic acid (DA) stimulates L3i activation, putative DA biosynthetic genes were not coordinately regulated in L3i development. These data demonstrate that *S. stercoralis* has homologs for nearly every component in the four canonical dauer pathways, that cGMP signaling may transduce host cues during L3i activation, and that IIS regulates L3i arrest and activation. However, dauer TGF&beta signaling appears to function in L3i arrest, an opposite role than in *C. elegans*, and endogenous DA regulation of L3i development remains largely unexplored.

Degree Type
Dissertation

Degree Name
Doctor of Philosophy (PhD)

Graduate Group
Cell & Molecular Biology

First Advisor
James B. Lok

Keywords
Caenorhabditis elegans, dauer, L3i, RNAseq, Strongyloides stercoralis

Subject Categories
Cell Biology | Molecular Biology | Parasitology

DEVELOPMENTAL REGULATION OF *STRONGYLOIDES STERCORALIS* INFECTIOUS THIRD-STAGE LARVAE BY CANONICAL DAUER PATHWAYS

Jonathan David Chaffee Stoltzfus

A DISSERTATION

in

Cell and Molecular Biology

Presented to the Faculties of the University of Pennsylvania

in

Partial Fulfillment of the Requirements for the

Degree of Doctor of Philosophy

2013

Supervisor of Dissertation

_____

James B. Lok, Ph.D.
Professor of Parasitology

Graduate Group Chairperson

_____

Daniel S. Kessler, Ph.D.
Associate Professor of Cell and Developmental Biology

Dissertation Committee

David Abraham, Ph.D.
Professor of Microbiology and Immunology

Robert M. Greenberg, Ph.D.
Research Associate Professor

S. Todd Lamitina, Ph.D.
Assistant Professor of Physiology

David S. Roos, Ph.D. (Chair)
E. Otis Kendall Professor of Biology

DEVELOPMENTAL REGULATION OF *STRONGYLOIDES STERCORALIS* INFECTIOUS THIRD-STAGE LARVAE BY CANONICAL DAUER PATHWAYS

ACKNOWLEDGMENT

As with any significant undertaking, this thesis would not have been possible without a great deal of encouragement. First, I have appreciated the generous support of my thesis committee, including David Abraham, Robert Greenberg, Todd Lamitina, and David Roos. Additionally, I would like to thank my friends and colleagues in the Cell and Molecular Biology Graduate Group for their camaraderie. To my dear friends Christie Helfer, Stacey Lehman, and Keeley Mui - thank you for always being willing to try a new restaurant, commiserate with my failed experiments, and share the experience of graduate school with me. You all really helped to make these four years enjoyable.

A special "thank you" to my family for encouraging my exploration of the natural world and helping foster my sense of curiosity as to how things work. Your tolerance of my experiments, which often involved explosions, is truly unsurpassed. Likewise, to my many science professors throughout my undergraduate studies - thank you for teaching and challenging me to think critically and carefully about the world!

I am additionally grateful for all the technical assistance, conversations about worms, and support from Tom Nolan and members of the Lok lab. The assistance of other friends and colleagues, particularly Sam Minot, has greatly facilitated this thesis project.

I owe a debt of gratitude to two people in particular, without whom this thesis would never have been completed. To my thesis advisor Sparky Lok - thank you for your guidance and patience in teaching me the ways of the worms, for always being available to answer my questions, and for your willingness to let me explore all manner of scientific questions. To my partner Kristina Lewis - thank you for listening to my science banter for so many years, for your endless encouragement during the many dark days, and for allowing me to share this journey with you. Your support is sincerely appreciated.

Last, but certainly not least, I wish to thank the worms and the research animals that hosted them.

ABSTRACT

DEVELOPMENTAL REGULATION OF *STRONGYLOIDES STERCORALIS* INFECTIOUS THIRD-STAGE LARVAE BY CANONICAL DAUER PATHWAYS

Jonathan David Chaffee Stoltzfus

James Barron Lok

Parasitic nematodes inflict a vast global disease burden in humans as well as animals and plants of agricultural importance; understanding how these worms infect their hosts has significant health and economic implications. In humans, soil-transmitted parasitic nematodes cause hookworm disease and strongyloidiasis, and vector-transmitted parasitic nematodes cause filariasis. The infectious form of the species causing these diseases is a developmentally arrested third-stage larva (L3i). Molecular mechanisms governing L3i developmental arrest and activation within a host have been poorly understood. An analogous developmentally arrested third-stage larva—the dauer larva—forms during stressful environmental conditions in the free-living nematode *Caenorhabditis elegans* and is controlled by four cellular signaling pathways. The "dauer hypothesis" posits that similar mechanisms regulate dauer and L3i development. The parasitic nematode *Strongyloides stercoralis* was used to test the dauer hypothesis because its life cycle includes both parasitic and free-living forms. To investigate the role of canonical dauer pathway homologs in regulating L3i arrest and activation, this study utilized transcriptome sequencing (RNAseq), transgenesis, and pharmacological studies. Transcripts encoding cyclic guanosine monophosphate (cGMP) pathway components were coordinately up-regulated in L3i. Application of membrane-permeable 8-bromo-cGMP resulted in activation of L3i and modulation of ligand transcripts in other pathways. In comparison to *C. elegans*, *S. stercoralis* has few genes encoding insulin/IGF-1 -like signaling (IIS) ligands, several of which have transcripts modulated during L3i development. Application of the phosphatidylinositol-3 kinase inhibitor, LY294002, prevented L3i activation in host-like conditions. The *S. stercoralis* transcriptome includes seven homologs of the single *C. elegans* dauer transforming growth factor β (TGFβ) ligand, three of which are only expressed in L3i. Although the *C. elegans* nuclear hormone receptor ligand Δ7-dafachronic acid (DA) stimulates L3i activation, putative DA biosynthetic genes were not coordinately regulated in L3i development. These data demonstrate that *S. stercoralis* has

homologs for nearly every component in the four canonical dauer pathways, that cGMP signaling may transduce host cues during L3i activation, and that IIS regulates L3i arrest and activation. However, dauer TGFβ signaling appears to function in L3i arrest, an opposite role than in *C. elegans*, and endogenous DA regulation of L3i development remains largely unexplored.

TABLE OF CONTENTS

LIST OF TABLES

LIST OF FIGURES

CHAPTER 1 - Introduction

1.1 Parasitic nematodes developmentally arrest as infectious third-stage larvae

Parasitic nematodes, including many species of major importance to human and veterinary medicine [1,2], inflict a vast global disease burden and significant agricultural losses [3]. Approximately one in four people worldwide are infected with a parasitic nematode [4], often resulting in significant morbidity and mortality [5]. The infectious form of many human parasitic nematodes is a developmentally arrested third-stage larva (L3i). These parasitic nematodes include the major species that cause hookworm disease (*Necator americanus* and *Ancylostoma duodenale*, 576-740 million people currently infected), lymphatic filariasis (*Wuchereria bancrofti* and *Brugia malayi*, 120 million infected), onchocerciasis (*Onchocerca volvulus*, 37 million infected), and strongyloidiasis (*Strongyloides stercoralis*, 30-100 million infected) [5,6]. L3i for the species that cause these diseases can be transmitted through either the bite of an insect, in the case of filarial diseases (lymphatic filariasis and onchocerciasis) [6], or by skin penetration, in the case of certain soil-transmitted nematodes (species that cause hookworm disease and strongyloidiasis) [5]. Other soil-transmitted parasitic nematode species of significant human health importance include *Ascaris lumbricoides* (807-1221 million infected) and *Trichuris trichiura* (604-795 million) [5], where infection occurs from ingestion of an embryonated egg. In the case of *A. lumbricoides*, the parasites that hatch from these eggs in the host gut penetrate the intestinal wall as third-stage larvae [1,2]. The exception to the rule of the infective third-stage larva is *T. trichiura* and related parasitic nematodes, such as *Trichinella* species, where transmission occurs by ingestion of an embryonated egg and the infectious form is a first-stage larva [2].

The life cycles of human parasitic nematodes that infect as L3i include both intra-host stages, such as parasitic adults, and eggs or larval stages that develop outside the human host in either the external environment (hookworms, *S. stercoralis*) or inside an insect vector (filarial worms) [1,2]. The life cycle of *S. stercoralis* (Figure 1.1) is unique in comparison to other human parasitic nematode genera, in that it includes an alternative free-living generation outside the host [7]. In contrast, other human parasitic nematode species develop directly to the infectious form without additional generations or population expansion outside the host [1,2]. This unique feature of the *S. stercoralis* life cycle allows for replication outside the host and expansion of the number of L3i. *S. stercoralis* post-parasitic larvae can develop either directly to L3i (homogonic

development) or to the alternative free-living generation, consisting of males and females (heterogonic development); the post-free-living generation invariably develops into L3i, which are exclusively female (as are the parasitic adults) [8]. These features of the *S. stercoralis* life cycle and the multiple "checkpoints" in larval development, along with ease of maintenance in prednisone-treated dogs [9], make it an ideal model for the interrogation of factors regulating L3i development [10].

S. stercoralis post-parasitic larvae can also precociously develop to auto-infective third-stage larvae (L3a) entirely within the host. The L3a can penetrate the gut wall, migrate through the host, and develop into adult parasitic females, thereby allowing for successive complete generations of development. When well regulated in immunocompetent hosts, this process, called autoinfection, allows for maintenance of an infection for several decades by gradual replacement of dying parasitic females [8]. When unregulated in immunocompromised or corticosteroid treated hosts, autoinfection may result in disseminated hyperinfection with geometric expansion of the parasite load, multi-organ involvement, and potentially fatal consequences for the host [11]. Although more difficult to study, this additional "checkpoint" in infective larval development is of obvious importance in understanding strongyloidiasis.

L3i of soil-transmitted helminths are not only developmentally arrested, non-feeding, and non-aging, but are also characterized by an ability to survive for weeks (*S. stercoralis*) or months (hookworm species) in the external environment [8,12]. This resistance to environmental stresses, such as heat and desiccation, is imparted by an extremely durable cuticle [13]. Since L3i are non-feeding and have a plugged buccal cavity, they must metabolize lipid stores in the gut as their sole source of energy [14,15]. Advantageous for finding a host, L3i are highly motile and exhibit rapid chemotaxis [16-18] and thermotaxis [19] to host cues. They also exhibit negative geotaxis, which facilitates dispersal and host contact [20]. Upon encountering a permissive host, the radially constricted L3i can quickly penetrate the skin by secretion of hydrolytic enzymes, including proteases [21] and hyaluronidase [22]. Once the L3i has entered the host, it rapidly resumes development and migrates through the host tissue to its final site, completing development to the parasitic adult. However, the molecular mechanisms regulating developmental arrest of L3i outside the host and their activation upon entry into the host are poorly understood and remain some of the large unanswered questions in the field. Specifically, this thesis has sought to leverage facets of the *S. stercoralis* life cycle to investigate mechanisms regulating L3i arrest and activation in parasitic nematodes.

1.2 The "dauer hypothesis"

Nearly four decades ago, it was observed that the free-living nematode *Caenorhabditis elegans* can also undergo developmental arrest at the third larval stage and that these "dauer larvae" were, like parasitic L3i, non-feeding, radially constricted, long-lived, and stress-resistant [23]. It was later posited that most parasitic nematodes, such as hookworms, mimic a "dauer constitutive" (Daf-c) route of development in *C. elegans*, and that the pathways governing *C. elegans* dauer entry similarly regulate hookworm L3i arrest [13]. This paradigm has been broadened to suggest that the same pathways regulating *C. elegans* dauer entry and exit may also regulate L3i arrest and activation in parasitic nematodes generally [24-27], in what has become known as the "dauer hypothesis."

In *C. elegans*, dauer larvae form during stressful environmental conditions, including high temperature, decreased food availability, and high population density mediated by a mixture of pheromones [28-30]. When conditions improve, dauer larvae exit their developmentally arrested state and resume reproductive development. Many of the environmental cues regulating dauer entry and exit in *C. elegans* are sensed and processed by amphidial neurons, which have cell bodies in the posterior portion of the head and dendrites that lead to the anterior tip of the worm, where they contact the external environment through amphidial pores [31]. Careful laser ablation studies revealed that ADF, ASI, and possibly ASG amphidial neurons regulate the switch between dauer entry and development to adulthood by providing a signal that blocks dauer entry when conditions are favorable [32], while ASK and ASJ neurons provide a signal promoting dauer entry when conditions are unfavorable [33,34]. Dauer exit is promoted by ASJ and AWC neurons, which provide a signal that environmental conditions have improved [32,35], while IL2 neurons produce a signal inhibiting dauer exit when unfavorable environmental conditions persist [35].

Multiple mutant screens have identified nearly 40 genes that control *C. elegans* dauer arrest, including dauer-formation abnormal (Daf) mutants that have either "dauer defective" (Daf-d) or Daf-c phenotypes [36,37]. While some Daf mutants have abnormal amphidial neurons or cilia, resulting in a loss of perception of environmental cues [37-40], most of these mutations are in genes that constitute one of four signaling pathways: a cyclic guanosine monophosphate (cGMP) signaling pathway, an insulin/IGF-1-like signaling (IIS) pathway, a dauer transforming growth factor β (TGFβ) signaling pathway, and a DAF-12 nuclear hormone receptor (NHR) regulated by dafachronic acid (DA) steroid ligands [41]. In a simplified analysis, epistasis

experiments have placed the cGMP pathway upstream of parallel IIS and dauer TGFβ pathways, which together regulate DA production and DAF-12 signaling [41].

1.3 Regulation of L3i arrest and activation in *S. stercoralis* and other parasitic nematodes

Study of the factors controlling L3i development is facilitated by developmental "checkpoints" in parasitic nematode species that do not follow the "Daf-c" paradigm. Animal parasitic nematodes in both the *Strongyloides* and the closely related *Parastrongyloides* genera can have a single (most *Strongyloides* spp.) or multiple free-living generations (*S. planiceps* and *P. trichosuri*) outside the host [1,2,7]. Larvae may develop to L3i in either the post-parasitic generation or in a subsequent post-free-living generation. Stressful environmental conditions are thought to bias development directly towards L3i [8], similar to the conditions promoting dauer entry. Entering a permissive host (e.g. "favorable" conditions) triggers resumption of development by L3i.

In *C. elegans*, temperatures in excess of 25°C promote dauer entry [28]. The temperature at which *Strongyloides* spp. post-parasitic larvae develop regulates whether the female larvae proceed to L3i by the direct or indirect (free-living) route of development; male larvae always develop indirectly in *Strongyloides* spp. For *S. stercoralis* post-parasitic female larvae, temperatures below 34°C promote indirect development, while temperatures greater than 34°C promote development directly to L3i [42,43]. However, the opposite trend is observed for *S. ratti*, *S. planiceps*, and *S. papillosus*, where direct development is favored at 13-15°C and indirect development favored at 30°C or above [44-46]. Provided food is abundant and the population density is low, culture temperature does not appear to affect the proportion of *P. trichosuri* larvae developing to L3i, which include both males and females for this genus [47,48].

Both the genetics of individual *Strongyloides* spp. strains as well as the host immune response also impact the percentage of post-parasitic larvae developing directly to L3i [8,49]. Different geographical isolates of *S. ratti* have vastly different homogonic indices (proportion of female larvae developing directly to L3i), with some strains having females that develop almost exclusively to free-living adults, while other strains almost exclusively develop directly to L3i [49]. Similar findings have been observed in *S. stercoralis*, with some strains having females that predominantly develop directly to L3i [50], while other strains predominantly develop indirectly to free-living adults [9].

Host immunity also regulates direct versus indirect development of female larvae in *Strongyloides* species. In *S. ransomi* [51], *S. ratti* [46], and *S. planiceps* [52], post-parasitic female larvae from a recently acquired infection in an immunologically naive host predominantly develop directly to L3i. In *S. stercoralis*, post-parasitic female larvae from patients with disseminated infection almost exclusively develop directly to L3i [50].

In *C. elegans*, several pairs of amphidial neurons control dauer entry and exit [32-35]. Maps of the amphidial neurons have been constructed for *S. stercoralis* [53,54], which have been used as a basis for laser ablation studies to determine their function in controlling L3i development [55,56]. In *S. sterocoralis*, both ASF (homologous to ADF in *C. elegans*) and ASI act together to control the switch between homogonic and heterogonic development, and ablation of these two cells results in formation of L3i in a hetergonically developing strain [54]; these data are consistent with the role of their homologs in regulating *C. elegans* dauer entry [32]. Additionally, in *S. stercoralis*, ALD neurons control thermotaxis [19] and the switch to L3i formation at high temperatures [43]. ASJ amphidial neurons in *S. stercoralis* regulate L3i activation [57], similar to their role in regulating *C. elegans* dauer exit [32]. Together, these data support the hypothesis that amphidial neuron positions and functions are conserved across divergent nematode species [58].

Similar to studies examining dauer regulation in *C. elegans*, pharmacological methods have also been utilized to explore conditions and compounds that control L3i activation in parasitic nematodes, particularly hookworms [59,60]. In *A. caninum*, L3i are activated, as evidenced by resumption of feeding [61], when exposed to 37°C, canine serum, and/or reduced glutathione [62-65]. Specific compounds, including the muscarinic agonists arecoline and oxotremorine, the *C. elegans* DAF-12 agonist Δ7-DA, and the membrane-permeable cGMP analog 8-bromo-cGMP, stimulate feeding of *A. caninum* L3i [66-69]. In contrast, the muscarinic antagonist atropine, the metalloprotease inhibitor 4,7-phenanthroline, the AKT inhibitor IV, and the PI3 kinase inhibitor LY294002 all inhibit *A. caninum* L3i feeding [66-68,70]. Several of these compounds can also influence L3i activation in other hookworm species, including *A. ceylanicum* and *Nippostrongylus brasiliensis* [68,71]. Prior to the commencement of this thesis, only Δ7-DA and a combination of DMEM, serum and reduced glutathione were known to initiate feeding in *S. stercoralis* L3i [57,69].

1.4 Canonical dauer pathways in parasitic nematodes and *S. stercoralis*

Whether canonical dauer signaling pathways are fully recapitulated in parasitic nematodes and whether they regulate L3i development are questions that have not been thoroughly examined; where components of these pathways have been studied, results have been mixed. While some pathways seem to function similarly in parasitic nematodes as in *C. elegans*, others do not. In several studies examining the transcript abundance of a dauer TGFβ ligand (DAF-7) homolog throughout *Stronglyoides*, *Ancylostoma*, and *Brugia* species life cycles, the parasitic nematodes' transcripts encoding *daf-7* homologs were up-regulated in arrested forms - the exact opposite of the pattern observed in *C. elegans*, where *Ce-daf-7* transcripts are down-regulated in dauer larvae [72-76]. These studies have suggested that dauer TGFβ signaling plays a different role in parasitic nematodes than in *C. elegans* [77], thereby diminishing support for the dauer hypothesis.

In contrast, studies of the IIS pathway, which have examined the DAF-16 transcription factor homolog, have suggested mechanisms similar to *C. elegans* in *Ancylostoma* spp., *S. stercoralis*, and *Haemonchus contortus* [78-84]. More specifically, heterologous complementation experiments have demonstrated that expression of parasitic nematode *daf-16* homolog cDNA in *C. elegans* complements *Ce-daf-16* mutants [79,83,84]. Additionally, trafficking of *S. stercoralis* and *A. caninum* DAF-16 orthologs in and out of the nucleus is controlled by putative AKT phosphorylation sites [78,84], similar to *C. elegans* [85]. Most strikingly, a dominant negative *Ss-daf-16* transgene expressed in the post-free-living generation of *S. stercoralis* antagonizes L3i morphogenesis and arrest [78]. However, upstream IIS pathway components had not yet been described, nor had their regulation of L3i development been assessed, in parasitic nematodes prior to the commencement of this thesis.

The DAF-12 NHR homolog has been cloned from *S. stercoralis*, and it has been demonstrated that *C. elegans* DA steroid ligands regulate L3i development in *Strongyloides* and *Ancylostoma* species [69,86,87]. Application of Δ7-DA to post-free-living *Strongyloides papillosus* or *S. stercoralis*, which have similar life cycles outside the host, results in bypass of L3i arrest, and in *S. papillosus*, results in formation of a second free-living generation of females [69,86]. Additionally, exogenous application of Δ7- or Δ4-DA to *S. stercoralis* or *A. caninum* L3i results in potent activation [69]. Together, these data suggest that *C. elegans* DAF-12 ligands can influence L3i development in parasitic nematodes; however, it is unclear whether parasitic nematodes endogenously synthesize DAs or if the ligands of parasite DAF-12 NHR homologs are structurally similar to *C. elegans* DAs.

Homologs of *C. elegans gpa-2* and *gpa-3* have been cloned in *S. stercoralis* [88]. These genes encode G protein alpha subunits that are members of a putative cGMP signaling pathway and in *C. elegans* are required for dauer arrest in response to dauer pheromone [89]. Additionally, the promoter for *Ss-gpa-3* is active in amphidial neurons [90], an anatomical location analogous to *Ce-gpa-3* [91,92], suggesting a conserved function. However, whether other cGMP signaling pathway elements are present and whether this pathway regulates L3i development in *S. stercoralis* was unknown prior to this thesis.

Therefore, at the inception of this thesis, the data were equivocal as to whether all members of the four canonical dauer pathways are fully conserved in parasitic nematodes. While components of each of the four pathways had been cloned from parasitic nematodes, this did not confirm that the entire pathways are fully present. Other evolutionarily conserved pathways have critical components that are absent in parasitic nematodes, a prime example being the RNAi pathway [93]. It was also equally unclear whether, if present, these pathways regulate parasitic nematode L3i arrest and activation.

1.5 Molecular tools in *S. stercoralis*

S. stercoralis was chosen as the organism in which to investigate factors regulating L3i development not only due to unique aspects of the life cycle, but also due to a comparatively large set of available molecular tools with which to address these questions in a parasitic nematode. Perhaps one of the most valuable tools with which to interrogate gene function in *S. stercoralis* is the ability to express transgenes in the parasite [94]. Using both native promoter and terminator sequences, fluorescent reporter transgenes can be expressed in the post-free-living generation as extra-chromosomal arrays [90,95]. Plasmid constructs are micro-injected into the distal gonads of gravid free-living females [94] by methods similar to those developed in *C. elegans* [96]. Additionally, dominant loss- or gain-of-function transgenes can also be expressed in the post-free-living generation [78]. In *S. stercoralis*, transgenes in extra-chromosomal arrays are transmitted to, but are potently silenced in, the post-parasitic generation [97]. Most recently, it has been demonstrated in the closely related parasitic nematode *S. ratti* that transgenes integrated into the genome can be inherited and expressed for many generations [98]. Together, this system for transgenesis facilitates investigation of temporal/anatomical regulation of promoters, over-expression of transgenes, and expression of dominant loss- or gain-of-function proteins.

Additional techniques to ascertain gene function in *S. stercoralis* include application of pharmacological inhibitors/activators, laser ablation of specific neurons, and quantification of gene expression. An *S. stercoralis* L3i activation assay [57,69], adapted from a similar hookworm assay [63], can be used to assess resumption of feeding (a hallmark of activation) in the presence of host-like cues and to determine whether pharmacological compounds can modulate this activation. Laser ablation of specific neurons to determine their function, first developed in *C. elegans* to assess the role of amphidial neurons in the head of the worm in the regulation of dauer development [31,32,34], has been adapted for *S. stercoralis* to determine the role of specific neurons in regulating L3i development [19,43,54,57]. Transcript quantification of specific genes by reverse transcription quantitative PCR (RT-qPCR) as well as genome-wide studies using microarrays [26,99], based on a limited cDNA library [26], have been used to examine gene regulation in different *S. stercoralis* developmental stages. Recent advances in sequencing technology, including next-generation deep-sequencing of the transcriptome (RNAseq), in other parasitic nematodes has allowed for true genome-wide transcript regulation studies [100-105]. However, prior to this thesis, RNAseq had yet to be applied to *S. stercoralis*.

Noticeably lacking from this list of techniques to assess gene function in *S. stercoralis* is a method of targeted gene silencing, specifically RNA interference (RNAi). *S. stercoralis*, as well as many other parasitic nematodes, appear to be largely refractory to the gene silencing effects of double-stranded RNA (dsRNA) [106]. This may be due to the loss of multiple conserved components in the RNAi pathway during the evolution of parasitism [93]. One large limitation to investigating gene function in *S. stercoralis* was the lack of a sequenced genome. However, with our lab's participation, progress towards this goal has been made, and the first genome contigs were made available by the Wellcome Trust Sanger Institute in December 2011. Additionally, despite the significant progress towards transgenesis, there is not yet a system for inducible transgene expression in *S. stercoralis*. These technical limitations have slowed research and have constrained the types of experimental approaches available to assess the mechanisms regulating L3i development in *S. stercoralis*.

1.6 Summary

This thesis leverages unique aspects of the *S. stercoralis* life cycle as well as molecular tools developed in this organism to explore the pathways regulating L3i arrest and activation. These studies are guided by the work in *C. elegans* on four canonical dauer pathways that regulate dauer larva development in a life stage similar to L3i, which forms the basis of the

"dauer hypothesis." Chapter 2 recounts RNAseq on seven *S. stercoralis* developmental stages, which both establishes the presence of all principle components of the four canonical dauer pathways and examines the regulation of these genes' transcripts throughout the life cycle. Chapter 3 focuses on the *S. stercoralis age-1* ortholog, a principle component in the *C. elegans* IIS pathway; this work establishes a role for IIS in *S. stercoralis* L3i activation. In Chapter 4, observations from the RNAseq data lead to a study of the role of cGMP pathway signaling in regulating *S. stercoralis* L3i activation; this work demonstrates that this pathway is upstream of IIS signaling in regulating L3i activation. Together, these studies present a complete survey of the four canonical dauer pathways in *S. stercoralis* and demonstrate the role of several components in the regulation of L3i arrest and activation.

1.7 Figure

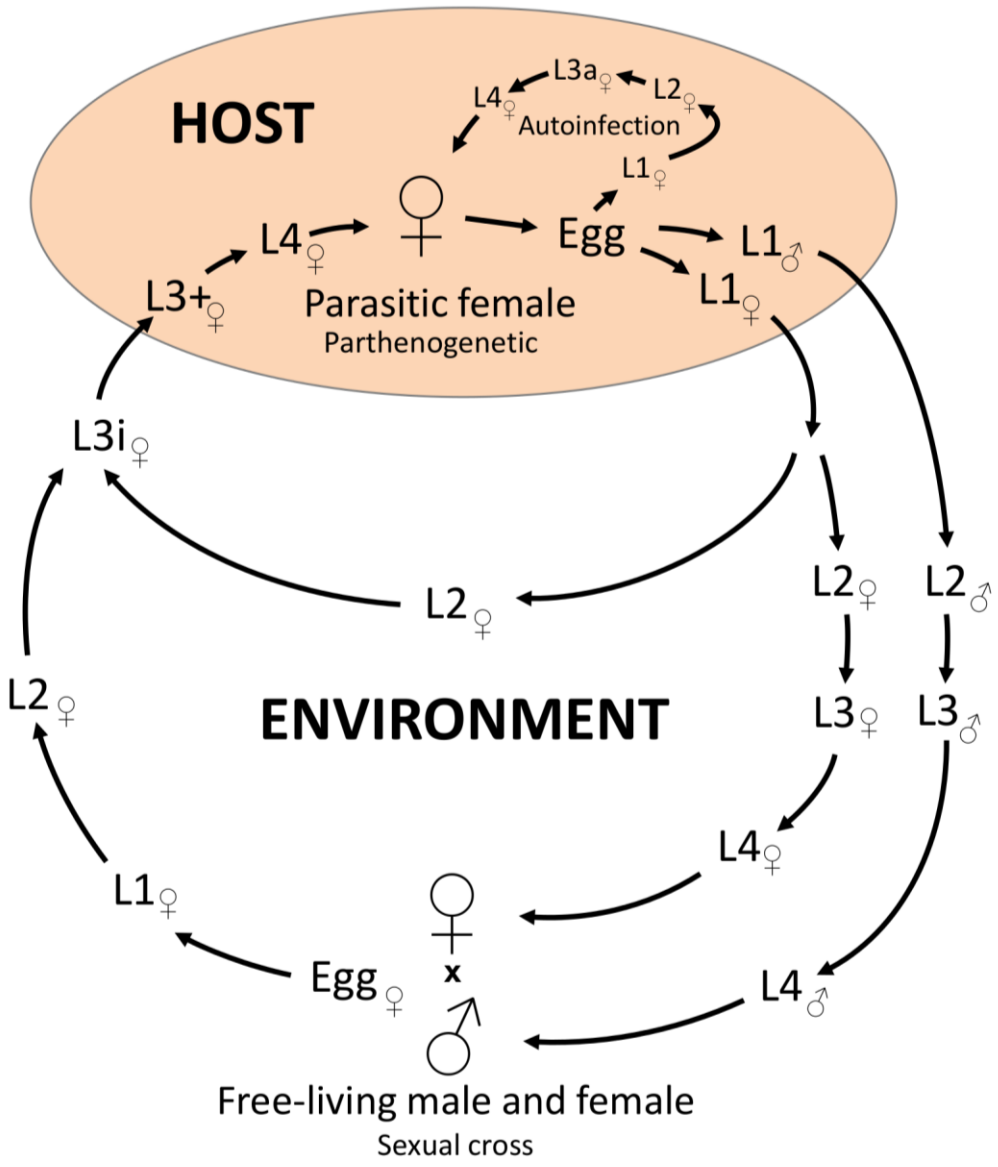

Figure 1.1 Diagram of the *Strongyloides stercoralis* life cycle.
Developmentally arrested infective third-stage larvae (L3i) can form by either a homogonic (direct) route or a heterogonic (indirect) route. Female post-parasitic first-stage larvae (L1) passed in the feces of the infected host can either develop through two larval molts directly to L3i or through four larval molts to free-living females. Post-parasitic L1 males invariably develop through four molts to free-living males. Post-free-living L1, which are all female, molt twice and develop exclusively to L3i. Upon encountering and penetrating a susceptible host, activated third-stage larvae (L3+) resume feeding and development, migrate to the intestines, and molt twice into parasitic females. Post-parasitic L1 larvae can also precociously develop into auto-infective third-stage larvae (L3a) entirely within the host. Adapted from [8].

CHAPTER 2 - RNAseq Analysis of the Parasitic Nematode *Strongyloides stercoralis* Reveals Divergent Regulation of Canonical Dauer Pathways

The contents of this chapter has been published as:

Stoltzfus JD, Minot S, Berriman M, Nolan TJ, and Lok JB (2012) RNAseq analysis of the parasitic nematode *Strongyloides stercoralis* reveals divergent regulation of canonical dauer pathways. PLoS Negl Trop Dis 6(10): e1854. doi:10.1371/journal.pntd.0001854

2.1 Abstract

The infectious form of many parasitic nematodes, which afflict over one billion people globally, is a developmentally arrested third-stage larva (L3i). The parasitic nematode *Strongyloides stercoralis* differs from other nematode species that infect humans, in that its life cycle includes both parasitic and free-living forms, which can be leveraged to investigate the mechanisms of L3i arrest and activation. The free-living nematode *Caenorhabditis elegans* has a similar developmentally arrested larval form, the dauer, whose formation is controlled by four pathways: cyclic GMP (cGMP) signaling, insulin/IGF-1-like signaling (IIS), transforming growth factor β (TGFβ) signaling, and biosynthesis of dafachronic acid (DA) ligands that regulate a nuclear hormone receptor. We hypothesized that homologous pathways are present in *S. stercoralis*, have similar developmental regulation, and are involved in L3i arrest and activation. To test this, we undertook a deep-sequencing study of the polyadenylated transcriptome, generating over 2.3 billion paired-end reads from seven developmental stages. We constructed developmental expression profiles for *S. stercoralis* homologs of *C. elegans* dauer genes identified by BLAST searches of the *S. stercoralis* genome as well as *de novo* assembled transcripts. Intriguingly, genes encoding cGMP pathway components were coordinately up-regulated in L3i. In comparison to *C. elegans*, *S. stercoralis* has a paucity of genes encoding IIS ligands, several of which have abundance profiles suggesting involvement in L3i development. We also identified seven *S. stercoralis* genes encoding homologs of the single *C. elegans* dauer regulatory TGFβ ligand, three of which are only expressed in L3i. Putative DA biosynthetic genes did not appear to be coordinately regulated in L3i development. Our data suggest that while dauer pathway genes are present in *S. stercoralis* and may play a role in L3i development, there are significant differences between the two species. Understanding the mechanisms governing L3i development may lead to novel treatment and control strategies.

2.2 Introduction

Parasitic nematodes infect over one billion people worldwide, resulting in vast morbidity [5], as well as causing significant agricultural losses from infections of both animals and plants [3]. The infectious form of many parasitic nematodes, including those causing hookworm disease, filariasis, and strongyloidiasis, is a developmentally arrested third-stage larva (L3i), which is both stress-resistant and long-lived [12,27,107]. Upon entering a suitable host, L3i quickly resume development (activation), eventually forming parasitic adults [27,107]. The genes and proteins constituting the pathways that control the developmental arrest and activation of L3i represent potential targets for chemotherapy as well as environmental control strategies.

Our lab uses the parasitic nematode *Strongyloides stercoralis*, which infects 30-100 million people globally [5], to study mechanisms controlling L3i arrest and activation [10]. *S. stercoralis* has a complex life cycle (Figure 2.1), which includes both an obligatory parasitic generation as well as a facultative free-living generation. Parasitic females reproduce parthenogenetically to produce post-parasitic larvae, which develop either directly to L3i (homogonic/direct development) or to free-living males and females (heterogonic/indirect development). Post-free-living larvae constitutively form L3i [8]. This life cycle allows us to investigate the mechanisms underlying different developmental fates for similar larval forms. Additionally, we have developed molecular tools in *S. stercoralis*, which are unavailable in other parasitic nematodes, to investigate molecular mechanisms involved in L3i regulation [78,90,95].

The free-living nematode *Caenorhabditis elegans* has a developmentally arrested third-stage dauer larva, morphologically similar to L3i, which forms during conditions of low food abundance, high temperature, and high dauer pheromone levels reflecting high population density. Dauer larvae quickly resume development into reproductive adults once environmental conditions improve. Mutant screens in *C. elegans* have identified over 30 genes that are involved in dauer formation (*daf*), and mutations in these genes result in either dauer constitutive (daf-c) or dauer defective (daf-d) phenotypes. Extensive study has placed many of these *daf* genes into four dauer pathways (Figure 2.2): a cyclic guanosine monophosphate (cGMP) signaling pathway, an insulin/IGF-1-like signaling (IIS) pathway regulated by insulin-like peptide (ILP) ligands, a dauer transforming growth factor β (TGFβ) pathway regulated by the *Ce*-DAF-7 ligand, and a nuclear hormone receptor (NHR) regulated by a class of steroid ligands known as dafachronic acids (DAs) [30]. Epistatic analysis places the cGMP signaling pathway upstream of the parallel IIS and dauer TGFβ pathways, which converge on the DA biosynthetic pathway, ultimately regulating the NHR *Ce*-DAF-12 (Figure 2.2) [41]. A long-standing paradigm in the field, known

as the "dauer hypothesis," proposes that similar molecular mechanisms regulate the developmental arrest and activation of both *C. elegans* dauer larvae and L3i of parasitic nematodes [13,24,27,108], despite their high degree of evolutionary divergence [109,110].

Members from each of the four dauer pathways have been cloned in *S. stercoralis* [76,79,87,88,111]; however, it is unclear whether all members from each of the *C. elegans* pathways are present in this parasite, whether their anatomical and temporal regulation is similar to *C. elegans*, and whether they control L3i development in *S. stercoralis*. While we have demonstrated that *S. stercoralis* IIS plays a crucial role in post-free-living L3i arrest and activation [78,111], we have also shown that an *S. stercoralis* TGFβ ligand encoding gene, *Ss-tgh-1*, is transcriptionally regulated in a manner opposite to that of the *C. elegans* TGFβ ligand encoding gene *Ce-daf-7* [73,76]. Studies examining the global transcriptional changes during *S. stercoralis* L3i development have failed to identify specific pathways regulating L3i development and have not directly shown whether pathways regulating dauer in *C. elegans* are similarly regulated in *S. stercoralis* [26,99]. However, these studies have been hindered by a small expressed sequence tag (EST) database, which does not include homologs for many *C. elegans* dauer genes.

To overcome these obstacles, we used a next-generation RNA sequencing (RNAseq) approach aided by the concurrent release of draft *Strongyloides ratti* and *S. stercoralis* genome sequences. Similar to recent work in other parasitic nematode species [100-103,112,113], we isolated polyadenylated RNA from seven different *S. stercoralis* developmental stages (Figure 2.1), from which we constructed dsDNA libraries that were subjected to high-throughput sequencing. Using both *S. ratti* and *S. stercoralis* genomic contigs as well as *de novo* assembled RNAseq transcripts, we identified *S. stercoralis* homologs of *C. elegans* genes involved in dauer regulation and examined their temporal regulation throughout the *S. stercoralis* life cycle using a collection of over 2.3 billion paired-end reads.

While we identified *S. stercoralis* homologs of nearly all *C. elegans* dauer genes, some of which appear to have similar developmental regulation between the two species, we also identified multiple differences between *C. elegans* dauer genes and their *S. stercoralis* homologs, including protein structure, developmental regulation, and expansion of gene families. Both IIS and cGMP signaling appear to be regulated in a manner consistent with a role in L3i regulation, while genes putatively involved in DA biosynthesis were not coordinately regulated during L3i development. *S. stercoralis* dauer-like TGFβ signaling was regulated oppositely to that observed

in *C. elegans*; nevertheless, this pathway may play a unique role in *S. stercoralis* L3i development.

2.3 Materials and Methods

Ethics statement

The *S. stercoralis* PV001 strain was maintained in prednisolone-treated beagles in accordance with protocols 702342, 801905, and 802593 approved by the University of Pennsylvania Institutional Animal Care and Use Committee (IACUC). Experimental infections of *S. stercoralis* were conducted in Mongolian gerbils under the same IACUC-approved protocols, and animals were sacrificed by CO_2 asphyxiation in accordance with standards established by the American Veterinary Medical Association. All IACUC protocols, as well as routine husbandry care of the animals, were carried out in strict accordance with the *Guide for the Care and Use of Laboratory Animals of the National Institutes of Health*.

S. stercoralis maintenance and RNA isolation

The *S. stercoralis* PV001 line, derived from a single female worm [111], was maintained and cultured as previously described [9,10,114]. *S. stercoralis* developmental stages were isolated as previously described [111]. Both L3+, which had resumed development as evidenced by changes in morphology and resumption of feeding (Figure 2.S1), and parasitic females were derived from experimental infections of Mongolian gerbils, a permissive host [114]. All developmental stages, except for parasitic females and L3+, were rendered free of fine particle debris by migration through agarose [115] into BU buffer [116]. Worms were snap-frozen in TRIzol reagent (Life Technologies, http://www.lifetechnologies.com) in liquid nitrogen; total RNA was extracted using the manufacturer's protocol. Total RNA was quantified using the Bioanalyzer 2100 (Agilent Technologies, Inc., http://www.agilent.com), and only samples with an RNA integrity number (RIN) greater than 8.0 were used.

S. stercoralis polyadenylated RNA library construction and sequencing

Libraries were constructed using the TruSeq RNA Sample Preparation Kit (Illumina, Inc., http://www.illumina.com) according to the manufacturer's protocol. For each of the 21 libraries, 500 ng of total RNA, diluted to 10 ng/µl in de-ionized water, was used as starting material. Polyadenylated RNA enrichment was performed first using olido-dT beads and eluted polyadenylated RNA fragmented at 94°C for eight minutes to approximately 170 ± 50 (standard

deviation) bp. Subsequently, first and second strand cDNA was synthesized; unique adapters for each replicate were then ligated. dsDNA fragments with ligated adapters were enriched using 15 cycles of PCR. Libraries were assessed for fragment size distribution using the Bioanalyzer 2100.

The concentration of the dsDNA adapter-ligated libraries was then determined by quantitative PCR (qPCR) using the Kapa SYBR Fast qPCR Kit for Library Quantification (Kapa Biosystems, Inc., http://www.kapabiosystems.com) using the manufacturer's protocol. Three dilutions, at 1:4,000, 1:8,000, and 1:16,000, were used to calculate the concentration of each of the 21 libraries using a calibration curve of Kapa standards. Each library was then diluted to 15 nM, and libraries from each developmental stage were pooled in equal volume quantities. The concentration of each of these pools was determined using qPCR and diluted to a final concentration of 10 nM.

The quality of the pooled libraries from each of the seven developmental stages was assessed using the High Sensitivity DNA Assay (Agilent Technologies). Pooled libraries were loaded on individual lanes of the Illumina HiSeq 2000 flow cell at 4 pM for all libraries, except for the post-free-living L1 and parasitic female libraries, which were loaded at 3 pM. Samples were then sequenced on the Illumina HiSeq 2000 with 100 bp paired-end reads, with image analysis and base calling performed with HiSeq Control Software. Raw flow-cell data was processed and demultiplexed using CASAVA version 1.8.2 (Illumina) for each of the 21 samples (ArrayExpress accession number E-MTAB-1164; http://www.ebi.ac.uk/arrayexpress/experiments/E-MTAB-1164).

Alignment of *S. stercoralis* RNAseq reads to genomic contigs

Raw reads from each of the 21 samples were independently aligned to *S. stercoralis* genomic contigs (6 December 2011 draft; ftp://ftp.sanger.ac.uk/pub/pathogens/HGI/) using TopHat version 1.4.1 (http://tophat.cbcb.umd.edu/), which utilized the Bowtie aligner version 0.12.7 (http://bowtie-bio.sourceforge.net/index.shtml) and SAMtools version 0.1.18 (http://samtools.sourceforge.net/). We refined the alignment parameters until TopHat accurately predicted introns and exons of several known *S. stercoralis* genes. Default parameters were used, but with the following options: mate inner distance of 25; mate standard deviation of 50; minimum anchor length of 6; minimum intron length of 30; maximum intron length of 20,000; micro exon search; minimum segment intron of 30; and maximum segment intron of 20,000.

Aligned reads from each developmental stage were inspected using the Integrated Genome Viewer (IGV) version 2.0.34 (http://www.broadinstitute.org/igv/).

De novo assembly of developmental stage-specific *S. stercoralis* transcripts

RNAseq reads from the sample with the greatest number of reads for each stage were independently *de novo* assembled into transcripts. First, forward and reverse read pairs were merged to form a single "contig" using SeqPrep (https://github.com/jstjohn/SeqPrep), with a quality score cutoff of 35, a minimum merged read length of 100 bp, and no mismatches in the overlapping region. The two read contigs were then trimmed with the FASTX toolkit quality trimmer (http://hannonlab.cshl.edu/fastx_toolkit/) to remove bases from the ends with a quality score less than 35. These high quality contigs were then *de novo* assembled via Trinity release 2012-04-27 (http://trinityrnaseq.sourceforge.net/) using "jellyfish" for k-mer counting. The *de novo* assembled transcripts from each developmental stage (ArrayExpress accession number E-MTAB-1184; http://www.ebi.ac.uk/arrayexpress/experiments/E-MTAB-1184) were tagged with the name of the developmental stage from which they were derived and merged into a single FASTA file. This FASTA file was then searched using the custom BLAST feature in Geneious version 5.5.6 (http://www.geneious.com/) [117] to search for *S. stercoralis* homologs of *C. elegans* genes.

Identification and annotation of *S. stercoralis* genes

BLAST searches of the *S. stercoralis* (ftp://ftp.sanger.ac.uk/pub/pathogens/HGI/) and *S. ratti* (http://www.sanger.ac.uk/resources/downloads/helminths/strongyloides-ratti.html) genomic contigs using *C. elegans* protein sequences (http://www.wormbase.org/) were performed using Geneious set to the least restrictive parameters. Putative *S. stercoralis* homologs were identified through reverse BLAST searches using NCBI's pBLAST (http://blast.ncbi.nlm.nih.gov/Blast.cgi) [118] against *C. elegans* and/or phylum Nematoda sequences. Putative homologs were then manually annotated using aligned reads from all seven developmental stages by a combination of IGV and Geneious. Manually annotated *S. stercoralis* transcripts were used to determine predicted protein sequences.

Additional searches for ILP motifs in the *S. stercoralis* and *S. ratti* genomes were performed by translating the contigs in all six reading frames and searching for conserved A and B peptide motifs using Geneious. Similarly, we searched the *S. stercoralis de novo* assembled transcripts for ILP motifs by assembling the contigs from all developmental stages using

Geneious, translating into all six reading frames, and searching for the B peptide motifs, C-11X-C and CPPG-11X-C, as well as the A peptide motifs, C-12X-CC, C-13X-CC, C-14X-CC, CC-3X-C-8X-CC, CC-4X-C-8X-CC, CC-3X-C-8X-C, and CC-3X-C-9X-C, where X represents any amino acid except for cysteine.

Protein alignments and phylogenetic analysis

Protein alignments and phylogenetic analyses were performed when several *S. stercoralis* or *C. elegans* homologs with similar e-values were identified in an attempt to resolve the homology of the *S. stercoralis* genes. Predicted protein sequences for *S. stercoralis* genes were derived from manually annotated transcripts using Geneious. Protein alignments using related S. *stercoralis*, *C. elegans*, phylum Nematoda, and other kingdom Animalia protein sequences were generated with Clustal W, using a BLOSUM matrix, or MUSCLE and neighbor-joining phylogenetic trees constructed using Geneious.

A protein alignment for full-length guanylyl cyclases, similar to *Ce*-DAF-11, was performed with Clustal W in Geneious. A neighbor-joining tree with 100 iterations of boot-strapping was constructed using Geneious and inspected for clear homology between *Ce*-DAF-11 and nematode homologs (Figure 2.S2).

A protein alignment for the TGFβ super-family ligands was performed using only the ligand domain, truncated at the first conserved cysteine residue [119], with Clustal W in Geneious. A neighbor-joining tree with 100 iterations of boot-strapping was constructed using Geneious (Figure 2.6A). A protein alignment for the TGFβ ligand domains that included all cysteine residues was performed using MUSCLE in Geneious and manually corrected (Figure 2.S3).

A protein alignment for the full-length SMADs using every publicly available phylum Nematoda sequence was performed with Clustal W in Geneious. A neighbor-joining tree with 100 iterations of boot-strapping was constructed using Geneious and inspected for clear homology between *C. elegans* proteins and other nematode homologs (Figure 2.S4). Similarly, a protein alignment for full-length short-chain dehydrogenases related to *Ce*-DHS-16 was used to construct a neighbor-joining phylogenetic tree (Figure 2.S5) to find an *S. stercoralis* homolog most similar to *Ce*-DHS-16. A similar approach was used for cytochrome P450 proteins related to *Ce*-DAF-9 to generate a protein alignment and construct a neighbor-joining phylogenetic tree (Figure 2.S6) to find the *S. stercoralis* homolog most similar to *Ce*-DAF-9.

Differential analysis of *S. stercoralis* transcripts

Transcript abundances of manually annotated *S. stercoralis* genes were calculated using Cufflinks version 2.0.0 (http://cufflinks.cbcb.umd.edu/) as fragments per kilobase of exon per million mapped reads (FPKM), with paired-end reads counted as single sampling events [120]. FPKM values for coding sequences (CDS) were calculated for each gene in each of the 21 samples and FPKM values for entire transcripts were calculated for each isoform in each of the 21 samples. Log transformed values, ± 95% confidence intervals, were plotted in Prism version 5.03 (GraphPad Software, Inc., http://www.graphpad.com/), and the y-axis was scaled from zero to 3.5 to aid comparisons between genes. Significant differences in FPKM values between developmental stages and p-values were determined using Cuffdiff version 1.3.0, a program with the Cufflinks package [121].

2.4 Results

RNAseq of seven *S. stercoralis* developmental stages

Many genes involved in *C. elegans* dauer regulation are transcriptionally regulated, including genes encoding ILPs [122], the dauer TGFβ ligand-encoding gene *Ce-daf-7* [123], and the genes encoding biosynthetic enzymes for DA [124] that regulate the NHR *Ce*-DAF-12 [125]. To acquire a comprehensive transcriptomic profile of the *S. stercoralis* homologs of these genes, as well as other genes potentially involved in *S. stercoralis* L3i developmental regulation, we undertook a next-generation RNA sequencing (RNAseq) approach using Illumina HiSeq technology.

Since *S. stercoralis* has a unique life cycle with a single free-living generation (Figure 2.1), several pair-wise comparisons can be made between life stages fated for free-living versus parasitic development. For RNAseq analysis, we examined the following developmental stages: gravid free-living females (FL Females), post-free-living first-stage larvae (PFL L1), infectious third-stage larvae (L3i), *in vivo* activated third-stage larvae (L3+), gravid parasitic females (P Females), predominantly (>95%) heterogonically developing post-parasitic first-stage larvae (PP L1), and post-parasitic larvae at approximately the third-stage developing heterogonically to free-living adults and enriched for females (PP L3).

We isolated total RNA, in biological triplicate, from these seven developmental stages, using an *S. stercoralis* strain derived from a single free-living female [111] to decrease the number of nucleotide polymorphisms, which can confound alignment [103]. Using these samples, we constructed 21 polyadenylated RNA libraries, which we sequenced with 100 base-

pair (bp) paired-end reads on an Illumina HiSeq 2000 instrument, generating a total of 2.36 billion reads (Figure 2.3). We independently aligned reads from each sample to *S. stercoralis* genomic contigs using TopHat [121,126,127], a strategy used in the clade III parasitic nematode species *Ascaris suum* [113] and *Brugia malayi* [100]. Of the 2.36 billion reads initially sequenced, 1.75 billion (74%) aligned to genomic contigs (Figure 2.3). The roughly one quarter of reads that did not align to the genome may have come from contaminants such as gut bacteria or the gerbil host, contained sequencing errors, or originated from parts of the *S. stercoralis* genome that remain unsequenced.

Identification of *S. stercoralis* genes encoding homologs of *C. elegans* dauer genes

To identify *S. stercoralis* homologs of the critical components involved in cGMP signaling, IIS, TGFβ signaling, as well as DA biosynthesis and NHR regulation, we performed BLAST searches of the *S. stercoralis* draft genome using *C. elegans* protein sequences. To confirm hits, we performed reverse BLAST searches to compare the manually annotated *S. stercoralis* sequences with *C. elegans* and phylum Nematoda databases [93]. When several homologs with similar e-values were present, we performed protein alignments and phylogenetic analysis to attempt to resolve the homology of *S. stercoralis* genes using related *S. stercoralis*, *C. elegans*, and phylum Nematoda protein sequences. For a few genes, we were unable to identify clear *C. elegans* homologs in *S. stercoralis* due to the lack of sequence similarity between the two species. We also noted several cases where either *S. stercoralis* or *C. elegans* had several closely related genes for which there was a single homolog in the other species, highlighting the evolutionary divergence between these two species, which are members of clade IV and clade V, respectively [109,110].

We were unable to identify *S. stercoralis* homologs of several *C. elegans* genes within the *S. stercoralis* or closely related *S. ratti* genome sequences. To determine if these genes are absent from the genome assemblies, but present in the transcriptome, we performed *de novo* assembly of *S. stercoralis* transcripts with Trinity [128]. Using one sample from each developmental stage, we first merged each forward and reverse read pair to form a single, high quality "contig." These merged single-read contigs were quality filtered and independently assembled to form expressed transcripts for each developmental stage. The seven expressed transcript libraries were merged to form a database on which we performed BLAST searches for *C. elegans* homologs not present in the draft *S. stercoralis* or *S. ratti* genomes. This *S. stercoralis* expressed transcript database contains a total of 210,709 developmental stage-specific transcripts;

however, this includes redundant, fragmented, and un-spliced transcripts as well as contaminating sequences from gerbil and other environmental sources.

Due to the compactness of the *S. stercoralis* genome, we were unable to use Cufflinks [121,129] to reliably predict transcripts because this program merged transcripts with untranslated region (UTR) overlap into single transcripts. Thus, we used aligned reads from all seven developmental stages to manually annotate exons and predict coding sequences for all isoforms of transcripts of interest. We then determined transcript abundances using Cufflinks to calculate fragments per kilobase of exon per million mapped reads (FPKM), with paired-end reads counted as single sampling events [120]. FPKM values were calculated for each gene or isoform in each developmental stage, and significant differences between developmental stages were determined using the three biological replicates and Cuffdiff [121].

Cyclic GMP signaling components are up-regulated in *S. stercoralis* L3i

In *C. elegans*, formation of dauer larvae is regulated by dauer pheromone [28,130], a constitutively produced complex mixture of ascarosides [131,132], which is indicative of population density. Dauer entry is promoted by dauer pheromone, which is sensed by several GTP-binding protein (G protein)-coupled receptors (GPCRs), including *Ce*-SRBC-64, *Ce*-SRBC-66, *Ce*-SRG-36, and *Ce*-SRG-37 [33,133]. When bound by specific ascarosides, GPCRs activate G protein alpha subunits [33], including *Ce*-GPA-2 and *Ce*-GPA-3 [89], resulting in repression of the transmembrane guanylyl cyclase *Ce*-DAF-11 [60] and a decrease in cGMP levels. Intracellular cGMP levels regulate cyclic nucleotide-gated ion channels [134], composed of the *Ce*-TAX-4 α subunits [135] and *Ce*-TAX-2 β subunits, which result in neuron depolarization when activated. The *C. elegans* cGMP signaling pathway is epistatic to the TGFβ pathway [136] (Figure 2.2) and may regulate the production of the *Ce*-DAF-7 TGFβ ligand [137] as well as the IIS agonists *Ce*-DAF-28 and *Ce*-INS-7 [138,139]. Other *daf* mutants have been identified that are critical both in the localization of these cGMP signaling pathway proteins to the cilia as well as in the formation of proper ciliary structures [140]. Developmental regulation of *C. elegans* cGMP signaling pathway genes during dauer arrest has not been well studied, although *Ce-gpa-2*, *Ce-gpa-3*, *Ce-daf-11*, *Ce-tax-2*, and *Ce-tax-4* are all down-regulated following dauer recovery in microarray analysis [124].

Outside of *C. elegans*, the role of ascarosides and cGMP pathway signaling in parasitic nematodes has been nearly overlooked. Muscarinic agonists and the cGMP analog 8-bromo-cGMP have been shown to activate *Ancylostoma caninum* L3i [66,67], and we have previously

cloned *S. stercoralis* homologs of *Ce-gpa-2* and *Ce-gpa-3* [88]. Recently, several groups have reported the presence of ascarosides in parasitic nematodes, which appear to differ in structure and composition between species and may play a role in L3i formation [48,141,142]. Thus, we sought to determine whether the components of a cGMP signaling pathway are present in *S. stercoralis* and whether these transcripts are developmentally regulated (Table 2.1).

We identified an *S. stercoralis* gene encoding a putative guanylyl cyclase that phylogenetically groups with *Ce*-DAF-11, which we termed *Ss-gyc-11* (Figure 2.S2). We also identified genes encoding homologs of the two cGMP-gated ion channels, *Ce*-TAX-2 and *Ce*-TAX-4, which we termed *Ss-tax-2* and *Ss-tax-4* respectively. We were unable to identify clear homologs of the GPCR genes, as many of the seven transmembrane receptor families have undergone rapid expansion in *C. elegans* [33]. Examination of the transcript abundance profiles for each of the five *S. stercoralis* genes putatively involved in cGMP pathway signaling revealed strikingly similar temporal regulation (Figure 2.4), with the steady-state level of each transcript at its peak in L3i and its nadir in both free-living and parasitic females. Interestingly, this developmental transcript abundance profile was also observed for two other guanylyl cyclases similar to *Ss-gyc-11* (Figure 2.4).

Insulin-like peptide transcripts are regulated during *S. stercoralis* development

IIS plays a critical role in both dauer arrest and recovery in *C. elegans*. Both microarray [143] and careful transcript quantification experiments [122] have shown that regulation of *C. elegans* IIS transcripts during dauer development takes place at the level of the ILPs, while the intracellular signaling component transcripts are always present. We have previously shown that IIS in *S. stercoralis* plays a crucial role in L3i arrest [78] and activation [111]. However, neither the presence nor regulation of ILPs has been reported in *S. stercoralis* or any other parasitic nematodes.

In *C. elegans*, 40 ILPs have been discovered and are thought to play redundant and complex roles in regulating dauer as well as other forms of development, with some ILPs agonizing and others antagonizing IIS [138,144]. To find *S. stercoralis* ILPs, we performed BLAST searches of the draft genomes of *S. stercoralis* and *S. ratti* as well as our *de novo* assembled *S. stercoralis* transcripts using both *C. elegans* ILP protein sequences and conserved cysteine motifs in the A and B peptides [144]. In total, we identified seven *S. stercoralis* ILPs (Figure 2.5A, Table 2.2), which are also present in *S. ratti* (data not shown). The predicted protein sequences of the *S. stercoralis* ILPs are highly divergent from *C. elegans* homologs,

except for several conserved cysteine residues which are predicted to form disulfide bonds. In contrast to both *C. elegans* and *Homo sapiens*, *S. stercoralis* ILPs lack the conserved intron located between the N-terminal B peptide and C-terminal A peptide, and all but one lack a predicted furin cleavage site [144-146]. Furthermore, cleavable C peptides, located between the B and A peptides, are not conserved between species.

The *S. stercoralis* putative ILPs—*Ss*-ILP-3, *Ss*-ILP-4, and *Ss*-ILP-6—have type β cysteine architecture [144]. In *C. elegans*, the type β family includes several agonistic ligands including *Ce*-DAF-28 [138], *Ce*-INS-6 [138,147,148], and *Ce*-INS-7 [149], as well as the antagonistic ligand *Ce*-INS-1 [144,147,150-152]. The type β family also includes the *Lymnaea stagnalis* molluscan insulin-related peptide I (MIP-1) [153]. In contrast, *Ss*-ILP-1 and *Ss*-ILP-7 have type γ cysteine architecture, similar to that found in human insulin [144]. In *C. elegans*, the type γ family includes the putative antagonist *Ce*-INS-18, which has a PPG motif between the conserved cysteine and glycine residues in the B peptide [144,154]. Interestingly, *Ss*-ILP-7 is the only *S. stercoralis* ILP to share this motif (Figure 2.5A). Unlike the six cysteine residues found in type α and γ ILPs or the eight found in type β ILPs, *Ss*-ILP-2 and *Ss*-ILP-5 have 10 cysteine residues. We propose that *Ss*-ILP-2 and *Ss*-ILP-5 represent a novel class of nematode ILPs, which we term type δ.

To determine whether *S. stercoralis* ILP transcripts are developmentally regulated, we compared FPKM values for each transcript between developmental stages (Figure 2.5B-H). In contrast to many *C. elegans* ILPs which are only expressed at one or a few developmental stages [122], transcripts encoding all seven *S. stercoralis* ILPs were detected in all developmental stages examined. We noted that *Ss-ilp-1* transcripts are decreased in L3i and significantly down-regulated in L3+ and parasitic females compared to the other developmental stages examined ($p<0.001$). We also noted that transcripts for both *Ss-ilp-4* and *Ss-ilp-7*, encoding the only two *S. stercoralis* ILPs with predicted C peptides that are cleaved, are at their peak in L3i. Additionally, we observed high variability in the transcript abundances of several ILP-encoding genes in the L3i developmental stage, evidenced by the large 95% confidence intervals. Since we isolated L3i incubated at 21°C after 8 and 10 days of culture or 25°C after 7 of days of culture, we plotted transcript abundance for each *ilp* gene by relative age for each biological replicate (Figure 2.S7). This analysis revealed that the error was not stochastic, but rather a developmental trend dependent upon the relative age of the L3i. In this analysis, we observed a one log increase in the transcript abundance of *Ss-ilp-6* from the oldest L3i to the L3+.

Intracellular IIS component transcripts are always present in *S. stercoralis*

While *C. elegans* ILPs are developmentally regulated, intracellular IIS components are always present [122,143]. We have previously cloned and detected transcripts throughout the life cycle of *S. stercoralis* homologs of both the forkhead transcription factor *daf-16* [80] and the *age-1* catalytic subunit of the phosphatidylinositol-3 kinase (PI3K) [111]. Recently, we have also cloned and characterized the *S. stercoralis* genes encoding the *Ss*-AAP-1 PI3K accessory/regulatory subunit [111] and the *Ss*-DAF-2 insulin-like receptor [155]. In this study, we asked whether homologs of the remaining IIS components are present in *S. stercoralis* and, if so, whether their transcripts are also present throughout the life cycle (Table 2.2).

Downstream of the DAF-2 IIS receptor, we identified two genes encoding homologs of the insulin receptor substrate *Ce*-IST-1 [156], which we termed *Ss-ist-1* and *Ss-ist-2*. Interestingly, we also found two homologs of the gene encoding the *C. elegans* phosphatase and tensin (PTEN) homolog *Ce*-DAF-18, which opposes the function of the PI3K *Ce*-AGE-1 when IIS is activated [157]. We termed these genes *Ss-pten-1* and *Ss-pten-2*. We also identified *Ss-pdk-1* as a homolog of the gene encoding the 3-phosphoinositide-dependent kinase *Ce*-PDK-1, which phosphorylates and activates *Ce*-AKT-1 and -2 when IIS is activated [158]. We identified *Ss-akt-1* as a single homolog of the genes encoding the *C. elegans* serine/threonine kinases *Ce*-AKT-1 and *Ce*-AKT-2 [159], which phosphorylate *Ce*-DAF-16 when IIS is activated [85,160]. In *C. elegans*, AKT-1 is negatively regulated by *Ce*-PPTR-1, a B56 regulatory subunit of the PP2A phosphatase [161]. We identified an *S. stercoralis* gene encoding a similar phosphatase, which we termed *Ss-pptr-1*. We also found a gene encoding the *C. elegans* homolog of the serum- and glucocorticoid-inducible kinase *Ce*-SGK-1 that regulates *Ce*-DAF-16 [162], which we termed *Ss-sgk-1*. We identified a homolog of the gene encoding the 14-3-3 protein *Ce*-FTT-2 [163] that regulates *Ce*-DAF-16 [164], which we termed *Ss-ftt-2*. Additionally, we found *Ss-asna-1*, a homolog of the gene encoding the ATPase *Ce*-ASNA-1, which regulates ILP secretion in *C. elegans* [165]. Together, these *S. stercoralis* homologs reconstruct a complete IIS pathway similar to that found in *C. elegans* and other metazoans [166].

Transcripts for each of the *S. stercoralis* genes encoding IIS cytoplasmic signaling proteins, except for *Ss-sgk-1*, were detected in every developmental stage examined (Figure 2.S8), suggesting that the IIS cytoplasmic signaling proteins are present throughout the *S. stercoralis* life cycle. We observed varying degrees of transcript up-regulation in the post-free-living generation of genes encoding the core IIS cytoplasmic signaling proteins *Ss*-DAF-2, *Ss*-AGE-1, *Ss*-PDK-1, *Ss*-AKT-1, and *Ss*-DAF-16. Interestingly, the increases in *Ss-akt-1* transcripts

in the L3i and L3+ stages were largely due to expression of a second isoform, *Ss-akt-1b*, which encodes a predicted peptide with a shortened N-terminus that results in a 33 amino acid deletion from the AKT pleckstrin homology (PH) domain and which is only present in these two stages (Figure 2.S9). Conversely, we noted an absence of *Ss-sgk-1* transcripts in L3i and L3+ (Figure 2.S8).

Homologs of *Ce*-DAF-16-regulated genes are not similarly regulated in *S. stercoralis* development

To determine whether IIS regulates similar genes in *S. stercoralis* and *C. elegans*, we then asked whether homologs of genes transcriptionally regulated by *Ce*-DAF-16 were similarly regulated over the course of *S. stercoralis* development (Table 2.2). In *C. elegans*, multiple studies have examined the genes regulated by the transcription factor *Ce*-DAF-16 [149,167-170]. The superoxide dismutase encoding gene *Ce-sod-3* is a well-characterized gene that is up-regulated by *Ce*-DAF-16 in the dauer stage [122,171,172], while the RAPTOR ortholog-encoding gene *Ce-daf-15* is down-regulated by *Ce*-DAF-16 in low IIS conditions [173]. We identified a single superoxide dismutase-encoding gene in *S. stercoralis* that phylogenetically grouped with *Ce-sod-2* and *Ce-sod-3*, which we termed *Ss-sod-1*, as well as a homolog of *Ce-daf-15*, which we termed *Ss-daf-15*. Additionally, we identified *S. stercoralis* homologs of *Ce-acs-19*, *Ce-ldb-1*, *Ce-pitp-1*, and *Ce-Y105E8B.9*, all of which were identified as *Ce*-DAF-16 targets by ChIPseq, are differentially regulated in *Ce-daf-16(mu86)* mutants, and have a phenotype associated with loss of *Ce*-DAF-16 function upon RNAi knock-down [170]. We termed these homologs *Ss-acs-19*, *Ss-limdb-1* and *-2*, *Ss-pitp-1*, and *Ss-Y105E8B.9*, respectively.

Surprisingly, transcript abundance profiles for each of these six genes (Figure 2.S10) revealed that neither *Ss-sod-1*, *Ss-daf-15*, nor the other five genes were up- or down-regulated in L3i. In fact, no large differences in *Ss-sod-1* or *Ss-daf-15* transcript levels were observed among any of the seven developmental stages examined.

The DAF-7-like TGFβ ligand family is expanded in *S. stercoralis*

In *C. elegans*, mutation of the TGFβ ligand-encoding gene *daf-7* results in temperature sensitive dauer arrest and is the only TGFβ ligand in the *C. elegans* genome in the same family as human TGFβ1, Inhibin/Activin, and Myostatin [123,174]. *Ce-daf-7* transcripts are at their peak in L1 larvae and are up-regulated during recovery from both L1 and dauer arrested states

[73,123,124]. In *C. elegans*, DAF-7 is most likely produced in response to food cues and functions in parallel with other pathways to promote continuous development.

Previous work in *S. stercoralis*, *S. ratti*, and *Parastrongyloides trichosuri* has identified *Ce*-DAF-7-like TGFβ ligand-encoding genes, named *Ss-tgh-1*, *Sr-daf-7*, and *Pt-daf-7*, respectively [73,76]. In stark contrast to *C. elegans*, these clade IV parasitic nematode TGFβ ligands are significantly up-regulated in the developmentally arrested L3i and down-regulated in activated L3i—a pattern directly opposite to that predicted under the dauer hypothesis. Similarly, transcripts encoding a DAF-7-like TGFβ ligand, termed *tgh-2*, have been described in the clade V parasitic nematodes *Ancylostoma caninum* [72,74], *Heligmosomoides polygyrus*, *Nippostrongylus brasiliensis*, *Haemonchus contortus*, and *Teladorsagia circumcincta* [175], as well as the clade III parasitic nematodes *Brugia malayi* and *Brugia pahangi* [75]. For many of these nematode species, the *tgh-2* transcripts are up-regulated in the L3i. These observations have led some groups to question the relevance of using *C. elegans* dauer pathways to predict pathways regulating infectious larval development in parasitic nematodes [77].

In addition to *Ce*-DAF-7, *C. elegans* also has four other TGFβ ligands that have different cysteine architecture and are not involved in dauer regulation; thus, we sought to identify homologs of all the TGFβ ligands in *S. stercoralis* to ensure proper classification. To our surprise, we discovered a total of 10 TGFβ ligands in both the *S. stercoralis* draft genome (Figure 2.6A) and *S. ratti* draft genome (data not shown). Protein alignment and phylogenetic analysis placed seven of these ligands in the same family as *Ce*-DAF-7, which also includes the previously described *Ss*-TGH-1 (Figure 2.6A, Figure 2.S3). We named these additional *Ss-tgh-1*-like genes *Ss-tgh-2* through *-7* (Table 2.3). Interestingly, the putative *Ss*-TGH-6 and *Ss*-TGH-7 ligands are not predicted to have propeptides, an observation previously reported in TGH-2 from *N. brasiliensis* [175], *Schistosoma mansoni* SmInAct [176], and a few TGFβ ligands from Ctenophores (marine invertebrates commonly called comb jellies) [119]. The three additional *S. stercoralis* TGFβ ligands grouped with homologs of *Ce*-DBL-1, *Ce*-UNC-129, and *Ce*-TIG-2 [177] by both phylogenetic analysis (Figure 2.6A) and protein alignment (Figure 2.S3). We termed the genes encoding these ligands *Ss-dbl-1*, *Ss-dbl-2*, and *Ss-tigl-1*, respectively.

We investigated whether the transcript abundance patterns of the seven genes encoding *S. stercoralis* TGH ligands were similar to *Ss-tgh-1* (Figure 2.6B-H). Interestingly, *Ss-tgh-1*, *-2*, and *-3* transcripts were detected exclusively in L3i, while *Ss-tgh-4* and *-5* were not detected in any of the life stages examined. *Ss-tgh-6* and *-7* had more complex transcript abundance patterns; *Ss-tgh-6* was up-regulated in L3+ in comparison to L3i ($p<0.001$), while *Ss-tgh-7* was not expressed

in either the free-living or parasitic females. Similar to the ILP-encoding genes, the *tgh* genes also had a high degree of variability in the transcript abundances in the L3i developmental stage. As with the *ilp* genes, the variability of the *tgh* genes in L3i represented developmental trends that are dependent upon the relative age of the L3i (Figure 2.S7). We also determined transcript abundances for *Ss-dbl-1*, *Ss-dbl-2*, and *Ss-tigl-1*, which are not predicted to signal through the dauer TGFβ signaling pathway (Figure 2.S11).

Dauer TGFβ signaling pathway components are present in *S. stercoralis*, but have high sequence divergence

Components of the *C. elegans* dauer TGFβ signaling pathway all have a temperature sensitive dauer phenotype when mutated [136]. Recent studies have presented an integrated model for dauer TGFβ signaling [178,179], where under well-fed conditions, the *Ce*-DAF-7 ligand is expressed [34,123] and binds the type I receptor *Ce*-DAF-1 [180] and type II receptor *Ce*-DAF-4 [181], overcoming the inhibition of *Ce*-DAF-1 by *Ce*-BRA-1 [182]. This results in phosphorylation and activation of the cytoplasmic R-SMADs *Ce*-DAF-8 [178] and *Ce*-DAF-14 [183], which together repress the Co-SMAD *Ce*-DAF-3 [184] and allow for reproductive development. However, when the *Ce*-DAF-7 ligand is not present, *Ce*-DAF-3 is active [178] and, together with the Sno/Ski-like transcriptional co-factor *Ce*-DAF-5 [185], represses expression of *Ce-daf-7* and *Ce-daf-8* [178], thereby promoting dauer development (Figure 2). In *C. elegans*, *Ce*-DAF-8 and *Ce*-DAF-14 are also inhibited by the phosphatase *Ce*-PDP-1, which also appears to control components of IIS, including ILPs, suggesting cross-talk between these pathways [179].

Proteins of the *C. elegans* dauer TGFβ pathway have diverged from those of other metazoans in both structure and function. *Ce*-DAF-1 can signal to some extent without *Ce*-DAF-4 [186], and a truncated *Ce*-DAF-4 protein expressed in dauers can negatively regulate *Ce*-DAF-7 signaling [187]. Consensus SMADs have both an MH1 (DNA-binding) and an MH2 (protein-protein interacting) domain and are activated by TGFβ signaling [188]; however, *Ce*-DAF-14 does not contain a consensus MH1 domain [183] and *Ce*-DAF-3 is repressed by *Ce*-DAF-7 signaling [184]. Temporal regulation of multiple components has been observed, including an up-regulation of *Ce*-DAF-1 [186] and *Ce*-DAF-8 [178] in L1 similar to *Ce-daf-7* transcriptional regulation [123], as well as a decrease in full-length *Ce-daf-4* transcripts in dauer larvae [187].

Since we observed a marked increase in the number of *Ce*-DAF-7-like TGFβ ligands in *S. stercoralis*, we asked whether the dauer TGFβ cytoplasmic signaling components were

conserved in both protein structure and temporal regulation (Table 2.3). We sought to differentiate these components from those in the *C. elegans* small body size and male tail abnormal (Sma/Mab) TGFβ pathway. We identified homologs of the genes encoding the *Ce*-DAF-1 type I receptor and the *Ce*-DAF-4 type II receptor, which we termed *Ss-daf-1* and *Ss-daf-4*, respectively. We also identified a homolog of the gene encoding the *Ce*-DAF-1 negative regulator *Ce*-BRA-1, which we termed *Ss-bra-1*. The *C. elegans* Sma/Mab TGFβ pathway, which uses the *Ce*-DBL-1 ligand [189,190], also utilizes the *Ce*-DAF-4 type II receptor but with *Ce*-SMA-6 as the type I receptor [191]. To ensure proper classification of the type I receptors, we identified a gene encoding a homolog of *Ce*-SMA-6, which we termed *Ss-sma-6*.

Identification of homologs for each of the SMADs proved difficult and was confounded by structurally similar SMADs involved in the dauer and Sma/Mab TGFβ signaling pathways present in *C. elegans* [174]. We identified a gene encoding a homolog of *Ce*-DAF-14 that did not include a MH1 domain, which we termed *Ss-smad-1*. We identified three *S. stercoralis* genes, termed *Ss-smad-5*, *Ss-smad-7*, and *Ss-smad-8*, which encode SMADs similar to *Ce*-DAF-3 and *Ce*-DAF-8; however, we were unable to resolve homology further by protein alignment or phylogenetic analysis (Figure 2.S4). Interestingly, we were able to clearly resolve genes encoding Sma/Mab TGFβ pathway SMADs similar to *Ce*-SMA-2, *Ce*-SMA-3, and *Ce*-SMA-4, which we termed *Ss-smad-2*, *Ss-smad-3*, and *Ss-smad-4*, respectively.

We identified a gene encoding a dauer TGFβ pathway *Ce*-DAF-5-like transcriptional co-factor, which we termed *Ss-daf-5*. The gene encoding a homolog of the Sma/Mab TGFβ pathway *Ce*-SMA-9-like transcriptional co-factor, which we termed *Ss-sma-9*, was clearly differentiable from *Ss-daf-5*. We also identified a gene encoding a phosphatase similar to *Ce*-PDP-1, which we termed *Ss-pdp-1*.

Examination of the transcript abundance patterns of the *S. stercoralis* genes encoding dauer pathway TGFβ homologs revealed several interesting trends (Figure 2.S12). In direct contrast to the down-regulation of the type I and type II receptors observed in *C. elegans* dauer larvae [186,187], *Ss-daf-1* and *Ss-daf-4* transcripts are at their peak in L3i and L3+. Likewise, *Ss-smad-8* transcripts were also at their peak in L3i. These observations are consistent with the expression of the *Ss-tgh-1*, *Ss-tgh-2*, and *Ss-tgh-3* transcripts exclusively in L3i (Figure 2.6B-D). We also noted a significant decrease in *Ss-smad-5* transcripts in parasitic females in comparison to the other six developmental stages examined ($p<0.001$). We did not observe any changes greater than one log in the transcript abundance of *Ss-bra-1*, *Ss-smad-1*, *Ss-smad-7*, or *Ss-daf-5* in the seven developmental stages examined. Additionally, we examined the transcript abundances

of the components in the Sma/Mab TGFβ pathway and noted that transcript levels for the receptor-encoding genes, *Ss-sma-6* and *Ss-daf-4*, as well as the *Ss-sma-9* transcriptional co-factor, are at their peak in L3i (Figure 2.S12).

A putative dafachronic acid biosynthetic pathway is present in *S. stercoralis*

In *C. elegans* dauer development, epistatic analysis has placed both the IIS and dauer TGFβ pathways upstream of the NHR *Ce*-DAF-12 [192] (Figure 2.2). *Ce*-DAF-12 is broadly expressed [193] and is regulated by at least two steroid-like ligands, known as Δ^4- and Δ^7-dafachronic acid (DA) [125]. These DAs are synthesized from cholesterol, which is trafficked intracellularly by *Ce*-NCR-1 and -2 [194]. For Δ^7-DA synthesis, cholesterol is first modified by the Rieske-like oxygenase *Ce*-DAF-36 [195], followed by the short-chain dehydrogenase *Ce*-DHS-16 [196]. In the final step, the cholesterol side chain is oxidized by the cytochrome P450 *Ce*-DAF-9 [197,198], with likely assistance from the cytochrome P450 reductase *Ce*-EMB-8 [196]. The enzymes that synthesize the precursors of Δ^4-DA are unknown, although the final oxidation step(s) are carried out by *Ce*-DAF-9 and *Ce*-EMB-8, similarly to Δ^7-DA [196]. The 3β-hydroxysteriod dehydrogenase/Δ^5-Δ^4 isomerase *Ce*-HSD-1 has previously been reported to play a role in Δ^4-DA biosynthesis [199]; however, a recent study has shown that this is not the case and that *Ce*-HSD-1 may be involved in synthesizing other DAs [196]. Additionally, the *Ce*-STRM-1 methyltransferase modifies DA precursors and can influence dauer development [200].

In favorable environmental conditions and when dauer larvae resume development, DAs are synthesized and bind *Ce*-DAF-12 [125] to promote reproductive development. However, in unfavorable environmental conditions, DAs are not synthesized and *Ce*-DAF-12, along with its co-repressor *Ce*-DIN-1 [201], promotes dauer development. Expression of GFP reporter constructs from *Ce-daf-36* [195] and *Ce-daf-12* [193] promoters is down-regulated in dauers, while microarray evidence has shown that *Ce-daf-9* and *Ce-daf-36* transcripts are up-regulated during dauer recovery [124]. Somewhat contradictorily, *Ce-daf-12* transcripts have been shown to be up-regulated during dauer formation [202].

The *S. stercoralis* homolog of DAF-12 has been cloned [87], and recent evidence from our lab has demonstrated that exogenous application of Δ^7-DA to *S. stercoralis* L3i results in potent activation, as measured by resumption of feeding, in the absence of all host-like cues [69]. Furthermore, Δ^7-DA applied to *S. stercoralis* post-free-living larvae results in failure to arrest as L3i and development to free-living L4, which we have termed an "L3i bypass" phenotype [69]. In the closely related parasite *Strongyloides papillosus*, which has a life cycle outside the host

very similar to that of *S. stercoralis*, application of Δ^7-DA to post-free-living larvae results in a second free-living generation of reproductively competent females [86]. In both *S. stercoralis* and *S. papillosus*, Δ^7-DA results in stronger L3i activation or L3i bypass phenotypes than does Δ^4-DA [69,86].

Therefore, we asked whether a biosynthetic pathway for NHR DA ligand(s) similar to that found in *C. elegans* was present in *S. stercoralis* and had similar developmental regulation (Table 2.4). We identified a single *S. stercoralis* gene encoding a homolog of *Ce*-NCR-1 and -2, which we termed *Ss-ncr-1*, as well as a gene encoding a homolog of *Ce*-DAF-36, which we termed *Ss-daf-36*. We identified several *S. stercoralis* genes encoding putative short-chain dehydrogenases similar to *Ce*-DHS-16; one of these genes, which we termed *Ss-scdh-16*, encoded a predicted protein that phylogenetically grouped closely with *Ce*-DHS-16 (Figure 2.S5). Similarly, we identified several *S. stercoralis* genes putatively encoding cytochrome P450s similar to *Ce*-DAF-9; one of these, which we termed *Ss-cyp-9*, encoded a putative peptide that grouped with *Ce*-DAF-9 by phylogenetic analysis (Figure 2.S6). We also identified a gene encoding a homolog of *Ce*-EMB-8, which we termed *Ss-emb-8*, as well as a gene encoding a homolog of *Ce*-STRM-1, which we termed *Ss-strm-1*. Curiously, we were unable to identify genes encoding *S. stercoralis* homologs of *Ce*-HSD-1 or *Ce*-DIN-1 in the *S. stercoralis* draft genome, the *S. ratti* draft genome, or our *de novo* assemblies of *S. stercoralis* transcripts. We also found that the *Ss-daf-12* locus encoded a total of seven transcripts encoding three different proteins, with the variability confined to the N-terminus of the predicted protein before the DNA-binding domain, similar to that found in *Ce-daf-12* [193,202].

We then examined the developmental regulation of the *S. stercoralis* genes potentially involved in a DA biosynthetic pathway (Figure 2.7). We found that *Ss-ncr-1* transcripts peak in L3+ and then significantly decrease in parasitic females ($p<0.001$), while *Ss-daf-36* transcripts are at their nadir in L3i and L3+ developmental stages. Counterintuitively, we also found that *Ss-cyp-9* transcripts are down-regulated in both free-living and parasitic females compared to the other developmental stages examined. Perhaps our most interesting observation was that *Ss-daf-12* transcript levels peak in L3i and that the differences in expression also reflected significant changes in the promoter usage and coding forms (Figure 2.S9).

Homologs of *Ce*-DAF-12-regulated genes are not similarly regulated in *S. stercoralis* development

We asked whether homologs of genes transcriptionally regulated by *Ce*-DAF-12 during dauer development were similarly regulated during *S. stercoralis* L3i development. We selected *C. elegans* genes that are directly linked to DAF-12 response elements, are differentially regulated during dauer development [203], and for which we could identify clear homologs in *S. stercoralis* (Table 2.4). We identified *S. stercoralis* homologs of *Ce-lev-9* and *Ce-gck-2*, which are up-regulated during both dauer induction [203] and following dauer recovery [124], that we termed *Ss-lev-9* and *Ss-gck-2*, respectively. We also identified two *S. stercoralis* homologs of *Ce-lit-1*, which is up-regulated in dauers [203], that we termed *Ss-lint-1* and *Ss-lint-2*. Additionally, we identified two *S. stercoralis* homologs of *Ce-ugt-65*, a gene down-regulated during dauer formation by *Ce*-DAF-12 [203], which we termed *Ss-udpgt-1* and *Ss-udpgt-2*. Intriguingly, we were unable to identify *S. stercoralis* homologs of the *Ce-let-7* microRNA family [204] in the *S. stercoralis* or *S. ratti* draft genomes or in our *de novo* assembled *S. stercoralis* transcripts. Members of this microRNA family are directly regulated by DAF-12 in *C. elegans* and control several dauer developmental programs [205].

We did not observe any consistent regulation of the *S. stercoralis* homologs during L3i formation (Figure 2.S13). In the seven developmental stages examined, *Ss-gck-2* and *Ss-lint-2* had no differences in transcript abundance greater than one log, *Ss-udpgt-1* and *Ss-udpgt-2* were expressed at very low levels in all stages examined, and *Ss-lev-9* and *Ss-lint-1* appeared to have decreased transcripts in parasitic and free-living females in comparison to the other developmental stages. This lack of consistent regulation of target genes between the two species appeared similar to that observed in *S. stercoralis* homologs of genes regulated by *Ce*-DAF-16 in *C. elegans*.

2.5 Discussion

In this study, we determined which homologs of *C. elegans* genes involved in dauer arrest and/or activation (Figure 2.2) are present in *S. stercoralis* and whether these *S. stercoralis* genes are developmentally regulated in a manner consistent with the regulation of their *C. elegans* counterparts. Our results have provided important insights into which developmental pathways are conserved between the morphologically similar dauer and L3i stages, thereby illuminating potential mechanisms governing L3i development. In our searches of the *S. stercoralis* and *S. ratti* draft genomes as well as our *de novo* assembled *S. stercoralis* transcript database, we were able to identify *S. stercoralis* homologs for nearly every *C. elegans* gene directly involved in the four canonical dauer pathways. While these pathways are well conserved

in metazoans, they regulate a wide variety of functions; thus, we were specifically interested in whether they regulate *S. stercoralis* L3i arrest and/or activation.

In previous work, we demonstrated that both IIS and DAs play a role in *S. stercoralis* L3i arrest and activation [69,78,111]. However, we have also found that an *S. stercoralis* TGFβ ligand similar to *Ce*-DAF-7 is transcriptionally regulated in opposition to its *C. elegans* homolog [76]. A recent study found that genes involved in dauer recovery differ considerably between the clade V nematodes *Pristionchus pacificus* and *C. elegans* [206], further suggesting potential developmental differences between *S. stercoralis* and *C. elegans*, which are far more evolutionarily divergent [109]. Together, these studies, along with others in multiple parasitic nematode species, have demonstrated that while some *C. elegans* dauer pathway genes and metabolites appear to play a role in L3i development, others appear to be uninvolved [27]. Therefore, in this study, we used an RNAseq approach to globally examine the developmental regulation of *S. stercoralis* homologs in each of the four canonical dauer pathways and to gain key insights into their potential role in regulating *S. stercoralis* L3i development.

The role of cGMP signaling in *S. stercoralis* development

The pronounced up-regulation in L3i and the striking similarity of the transcriptional profiles of the *S. stercoralis* genes putatively involved in a cGMP signaling pathway (Figure 2.4) suggest a role in transducing host cues during the infective process. The similar up-regulation of putative guanylyl cyclases that do not phylogenetically group with *Ce*-DAF-11 suggests broad up-regulation of cGMP pathway components in *S. stercoralis* L3i and is reminiscent of studies in *C. elegans* showing that genes with similar temporal regulatory patterns often have similar genetic functions [207]. Since *S. stercoralis* L3i are attracted to chemical and thermal host cues [17-19] and are activated in host-like conditions [69], "priming" L3i for infection by up-regulating signaling components that relay these host cues would impart a selective advantage. Therefore, we hypothesize that cGMP signaling plays an important role in transducing signals of host recognition, consistent with studies in *A. caninum*, which demonstrated that a cGMP analog can stimulate L3i activation [66,70].

This proposed role for cGMP signaling in *S. stercoralis* is somewhat at odds with the role of cGMP pathway signaling in *C. elegans*, where dauer pheromone, composed of a complex mixture of ascarosides, utilizes the cGMP signaling pathway to control dauer arrest [130-132]. This would suggest that an as yet undiscovered ascaroside helps to control *S. stercoralis* L3i formation. Recent reports suggest that ascarosides play a role in L3i formation in the closely

related nematode *P. trichosuri* [48] as well as the entomopathogenic nematode *Heterorhabditis bacteriophora* [141]. Both of these species have multiple free-living generations, allowing ascaroside concentration to build up over time. In contrast, *S. stercoralis* has only one free-living generation, the progeny of which invariably form L3i regardless of the population density. This makes it difficult to envisage a role for an environmentally secreted ascaroside by either the parasitic or free-living female, although an ascaroside that acts *in utero* on the developing embryo remains a possibility.

The role of IIS in *S. stercoralis* development

In previous studies, we have demonstrated that *S. stercoralis* IIS is crucial to both L3i arrest [78] and activation [111]. Down-regulation of IIS is necessary for L3i formation, since a *Ss*-DAF-16 dominant interfering construct designed to block the function of native *Ss*-DAF-16 results in L3i bypass phenotypes [78]. Furthermore, up-regulation of IIS is important during L3i activation, since pharmacological inhibition of PI3Ks, which include *Ss*-AGE-1, results in a dramatic decrease in L3i activation [111].

In this study, we demonstrate that the transcripts of intracellular IIS signaling components are always present in all developmental stages examined, with the exception of *Ss-sgk-1* (Figure 2.S8). These results are consistent with findings in *C. elegans*, where IIS signaling is thought to be regulated at the level of the ILPs, while intracellular signaling components are always present [122]. However, we did observe developmental regulation of several IIS signaling component transcripts in the post-free living generation, including increases in the transcript abundances for *Ss-daf-2*, *Ss-age-1*, *Ss-pdk-1*, *Ss-akt-1*, and *Ss-daf-16* (Figure 2.S8). We also noted an absence of *Ss-sgk-1* transcripts in L3i and L3+ (Figure 2.S8). In *C. elegans*, loss of *Ce-sgk-1* results in increased stress resistance and lifespan extension [162]. These two attributes are key features of *S. stercoralis* L3i and we postulate that *Ss-sgk-1* plays a role in these processes. Perhaps our most interesting observation is that *Ss-akt-1b* transcripts, encoding an isoform that is predicted to have a truncated PH domain and may not be subject to regulation by phosphatidylinositol lipids, are found almost exclusively in L3i and L3+ (Figure 2.S9). We hypothesize that *Ss*-AKT-1B modulates *S. stercoralis* IIS during L3i development, potentially by interfering with *Ss*-AKT-1A or its substrates. Together, these data suggest that *S. stercoralis* IIS may be modulated at the level of the intracellular signaling proteins; however, the developmental transcript abundance profiles suggest that the core components are always present.

Upstream regulation of IIS by ILPs has never been demonstrated in parasitic nematodes, and it has generally been assumed that such regulation would be highly complex and redundant, similar to that of *C. elegans*, which has 40 known ILPs [122,144]. In this study, extensive searches of the *S. stercoralis* and *S. ratti* draft genomes as well as *de novo* assembled *S. stercoralis* transcripts identified only seven ILPs (Figure 2.5A). These are conserved between these two parasite species but are highly divergent from the ILPs in *C. elegans*. We do not discount the possibility that other ILPs may be present in *S. stercoralis*; however, they would almost certainly have non-canonical cysteine architecture, given our search algorithm. Although we have no direct evidence to support their role in L3i development, we hypothesize that *Ss-ilp-1*, *Ss-ilp-6*, and *Ss-ilp-7* encode ligands that regulate *S. stercoralis* IIS during L3i development. Determining whether an ILP acts as an agonist or antagonist is complicated by the fact that IIS regulates functions other than dauer development in *C. elegans*, including life-span [149].

We hypothesize that *Ss-ilp-7* encodes a type γ antagonistic IIS ligand that promotes developmental arrest, due to the conservation of a unique PPG motif found in *Ce*-INS-18, which acts as an IIS antagonist in *C. elegans* [144,154]. This hypothesis is supported by our observation that *Ss-ilp-7* transcripts are significantly up-regulated in the post-free-living generation and peak in L3i, which are developmentally arrested (Figure 2.5H). However, *Ss-ilp-7* transcripts remain at an elevated level in L3+, which are developmentally activated. The similar levels of *Ss-ilp-7* transcripts in L3i and L3+ may reflect the fact that both forms are third-stage larvae and that the L3+ has yet to complete all the developmental programs associated with activation, which may only commence after molting and establishment in the intestine.

We also hypothesize that *Ss-ilp-1* encodes an agonistic ligand that, when down-regulated, allows parasitic development, as it is the only other gene we identified to encode a type γ ILP, a family that also includes the human agonists insulin and IGF-1 [144]. The fact that *Ss-ilp-1* transcripts are significantly down-regulated in L3i, L3+, and parasitic females supports this characterization (Figure 2.5B). Continued down-regulation of *Ss-ilp-1* transcripts in L3+ and parasitic females is difficult to reconcile with a strictly developmental regulatory role in L3i. However, it should be noted that parasitic females retain characteristics of L3i, including an extended lifespan. Parasitic females live for many months in contrast to a lifespan of a few days for their free-living counterparts [208]. We hypothesize that negative regulation of lifespan by IIS is reversed in the long-lived parasitic forms and that *Ss*-ILP-1 participates in this effect.

We also speculate that *Ss-ilp-6* encodes an agonistic ligand that promotes larval growth and development in both homogonic and heterogonic phases of the life cycle. This is based on

our observation that *Ss-ilp-6* transcript levels decrease during post-free-living development, reaching a minimum in physiologically older L3i, and then increase by one log in L3+, which have resumed feeding (Figure 2.S7). Additionally, *Ss-ilp-6* transcripts appear to increase in rapidly developing post-parasitic larvae (Figure 2.5G).

In future studies, we will test whether these three *S. stercoralis* ILPs, and possibly others, directly regulate L3i development. Due to the significantly smaller number of ILPs in *S. stercoralis* compared to *C. elegans*, as well as their highly divergent amino acid sequences and even novel cysteine architecture, we believe that these two species differ in the diversity and complexity of ligands regulating the DAF-2 receptor. Nevertheless, the data we report here are consistent with roles for *S. stercoralis* ILPs in the regulation of larval development and lifespan via the IIS pathway.

Differences in IIS regulated genes between *S. stercoralis* and *C. elegans* are suggested by our observation that none of the *S. stercoralis* homologs of *Ce*-DAF-16-regulated genes we examined, including *Ss-sod-1* and *Ss-daf-15*, had transcript abundance differences greater than one log between any of the *S. stercoralis* developmental stages examined (Figure 2.S10). We found this observation interesting because *Ss*-DAF-16 can heterologously complement *C. elegans daf-16* mutants [79], suggesting similar biochemical capabilities. These results illustrate the important caveat that heterologous rescue does not prove that homologous genes fulfill similar genetic functions. However, no *Ce*-DAF-16-regulated genes have been shown to be "master regulators" of dauer development, and thus it is difficult to determine which target genes are most important. *Ce*-DAF-16 regulates several biological processes in addition to dauer development, including longevity, stress responses, and metabolism, and this has complicated the identification of target genes for specific processes [170]. The *S. stercoralis* genes in this study were selected because in *C. elegans*, the homologs are transcriptionally regulated directly by *Ce*-DAF-16 during dauer development and have dauer-associated phenotypes upon RNAi knock-down of their transcripts [170]. Our previous work points to *S. stercoralis* IIS regulating L3i arrest and activation, but the genes regulated by *Ss*-DAF-16 to carry out this process are unknown. In future studies, we hope to determine which *S. stercoralis* genes are regulated by *Ss*-DAF-16 using a chromatin immunoprecipitation and deep sequencing (ChIPseq) approach by constructing a stable transgenic *S. stercoralis* line that expresses a tagged version of *Ss*-DAF-16 [98].

The role of dauer-like TGFβ signaling in *S. stercoralis* development

Previously, we identified an *S. stercoralis* TGFβ ligand similar to *Ce*-DAF-7 [76], a finding repeated in two closely related parasitic nematodes [73]. In contrast to *C. elegans*, these putative TGFβ ligand-encoding genes are up-regulated in L3i, while *Ce-daf-7* is down-regulated in the dauer stage [73]. In this study, we identified six additional *S. stercoralis* genes encoding TGFβ1 family ligands similar to *Ce*-DAF-7 (Figure 2.6A), which is the only dauer pathway TGFβ ligand in *C. elegans* [123,174]. We were not only surprised by the increase in the number of genes encoding *Ce*-DAF-7-like ligands in *S. stercoralis*, but also by their temporal regulation.

We noted that *Ss-tgh-1*, *Ss-tgh-2*, and *Ss-tgh-3* transcripts are found exclusively in L3i (Figure 2.6B-D), suggesting a similar function. As previously proposed, the *S. stercoralis* TGFβ-like ligands encoded by *Ss-tgh-1*, *Ss-tgh-2*, and *Ss-tgh-3* may play a role in L3i arrest [73] or may be stored in L3i and secreted into the host following activation for purposes of immunomodulation [75]. Recent work has shown that *H. polygyrus* excretory-secretory antigen binds and activates the host TGFβ receptor, potentially supporting an immunomodulatory role for nematode TGFβ ligands [209]. Additionally, we noted highly variable transcript abundances for these three genes, as well as several others, in the L3i developmental stage, evidenced by the large 95% confidence intervals. Since we isolated L3i incubated at 21°C or 25°C and after 7, 8, or 10 days of culture, we plotted the transcript abundances for the genes encoding both the ILP and TGH ligands over the course of post-free-living larval development, with each L3i biological replicate plotted by relative age (Figure 2.S7). We observed that the large 95% confidence intervals were not stochastic, but rather represented underlying developmental trends dependent upon the relative age of the L3i. Therefore, we concluded that L3i may not be the static population originally assumed. Instead, physiologic age of developmentally arrested L3i, which is a function of temperature and time, may influence the transcriptomic profile of a synchronous population of these infectious larvae. These observations lead us to favor the hypothesis that the up-regulation of *Ss-tgh-1*, *Ss-tgh-2*, and *Ss-tgh-3* during L3i development may play a role in L3i arrest; however, this role is not mutually exclusive with immunomodulation, given the plurality of TGH ligands in *S. stercoralis*.

In this study, we also identified four other genes encoding *Ce*-DAF-7-like ligands (Figure 2.6A). Both *Ss-tgh-4* and *Ss-tgh-5* transcripts were not detected in any developmental stage examined (Figure 2.6E-F), while *Ss-tgh-6* and *Ss-tgh-7* transcripts encoded putative peptides without a pro-peptide domain. We do not know whether *Ss-tgh-4* or *Ss-tgh-5* are ever robustly expressed during *S. stercoralis* development or are pseudo-genes; however, two important developmental stages, free-living males and auto-infective L3, were absent from this study.

Additionally, the function of the putative ligands encoded by *Ss-tgh-6* and *Ss-tgh-7* are altogether unknown. Advances in the technologies to knock down genes by RNAi in *S. stercoralis*, which to date has been intractable to this approach, would facilitate our ability to address these questions [94].

Examination of intracellular signaling components of the dauer TGFβ pathway in *S. stercoralis* also led to some perplexing observations. While we were able to identify clear *S. stercoralis* homologs of genes encoding the Type I and Type II dauer pathway TGFβ receptors, *Ss-daf-1* and *Ss-daf-4*, as well as the homolog of the *Ce*-DAF-5 transcriptional co-factor, *Ss*-DAF-5, we were unable to clearly identify homologs of the SMADs *Ce*-DAF-8, *Ce*-DAF-14, and *Ce*-DAF-3 (Figure 2.S4). The large protein sequence divergence of dauer pathway TGFβ SMADs in *S. stercoralis* and all other sequenced nematodes, evidenced by our inability to resolve them phylogenetically, indicates a high degree of evolutionary divergence and suggests the potential for rapid evolution of these genes. This is in stark contrast to the SMADs in the Sma/Mab TGFβ pathway, for which clear sequence-level relationships exist for all nematode species examined (Figure 2.S4). However, future testing of the functional consequences of this sequence-level divergence of dauer pathway TGFβ SMADs will be challenging due to the current limitations of functional genomic methods in *S. stercoralis*.

The regulation of dafachronic acid biosynthesis and DAF-12 in *S. stercoralis* development

We previously demonstrated that Δ^7-DA is a potent activator of L3i and can act as a ligand for the nuclear hormone-receptor *Ss*-DAF-12 [69]. Furthermore, Δ^7-DA can promote L3i bypass phenotypes in the post-free-living generation [69]. From these observations, we hypothesized that *S. stercoralis* synthesizes DAs *in vivo* and that the homologs of the enzymes responsible for DA biosynthesis would be up-regulated during reproductive development and down-regulated in L3i. This would also be consistent with observations in *C. elegans*, where *Ce-daf-9* and *Ce-daf-36* are up-regulated during dauer recovery [124].

Contrary to our hypothesis, we did not observe consistent developmental regulation of *S. stercoralis* homologs putatively involved in DA biosynthesis (Figure 2.7). Most puzzling was the significant decrease in *Ss-cyp-9* transcripts, which encode a putative cytochrome P450 most similar to *Ce*-DAF-9, in both free-living and parasitic females (Figure 2.7D). Although *Ss-daf-36* transcripts, which encode a putative Rieske-like oxygenase, appeared to be decreased in L3i and L3+ in comparison to other developmental stages, there was no significant difference between L3i and L3+ (Figure 2.7B). We expected both *Ss-cyp-9* and *Ss-daf-36* transcripts to be down-

regulated in the developmentally arrested L3i and up-regulated in activated L3+; however, the L3+ may not have fully initiated all programs associated with resumption of development, as discussed for the ILPs. Only *Ss-strm-1*, the homolog of which in *C. elegans* encodes a methyltransferase that decreases DA levels when active, was down-regulated from L3i to L3+ and consistent with our hypothesis (Figure 2.7F). This inconsistent regulation of putative DA biosynthetic enzymes may be a result of our misidentification of several enzymes, such as *Ss-cyp-9* and *Ss-scdh-16*, of which several closely related homologs are present in *S. stercoralis* (Figure 2.S5, Figure 2.S6). Additionally, these inconsistent results may be a result of additional layers of regulation which await discovery. In future studies, we hope to verify the role of these enzymes in a DA biosynthetic pathway.

Interestingly, we noted that unlike *Ce*-DAF-12, which is down-regulated in the dauer stage [193], *Ss-daf-12* transcripts were at their peak in L3i (Figure 2.7G) and that this up-regulation was isoform specific (Figure 2.S9). The differences in promoter usage as well as the predicted differences in the N-terminus of *Ss*-DAF-12 may represent additional layers of regulation. Until the native *Ss*-DAF-12 ligand(s) are identified and quantified for each developmental stage in future studies, the endogenous role of DAs in *S. stercoralis* development will remain difficult to assess.

Transcriptional regulation of *S. stercoralis* homologs of *Ce*-DAF-12-regulated genes was more difficult to interpret than for the *S. stercoralis* homologs of *Ce*-DAF-16-regulated genes. While some genes, including *Ss-lev-9* and *Ss-lint-1*, appeared to be regulated similarly to *Ss-cyp-9*, others, including *Ss-gck-2* and *Ss-lint-2*, did not display substantial changes in their transcript levels in the developmental stages examined (Figure 2.S13). Our inability to identify *S. stercoralis* homologs of the *Ce-let-7* miRNA family, which in *C. elegans* are directly regulated by *Ce*-DAF-12 to control development [205], further confounded our ability to interpret these results. In future studies, a ChIPseq approach using a tagged *Ss*-DAF-12 construct expressed in a stable transgenic *S. stercoralis* line would allow for the identification of native *Ss*-DAF-12-regulated genes in different developmental stages [98].

Putative mechanisms controlling *S. stercoralis* L3i development

Our data, as well as that from previous studies in other parasitic nematodes, point to several key regulatory pathways that may govern *S. stercoralis* L3i arrest and activation. The potent up-regulation of many cGMP signaling pathway components in L3i (Figure 2.4) is

striking. We hypothesize that this pathway is directly involved in sensing/transducing host cues when L3i encounter a favorable host.

Perhaps the most interesting observation in this study is the paucity of *S. stercoralis* ILPs in comparison to *C. elegans* and the fact that several of these ILP encoding genes are dramatically up-/down-regulated during the course of L3i development (Figure 2.5). These data support a role for ILPs in regulating L3i arrest by modulating IIS, in agreement with our previous findings that *Ss*-DAF-16 regulates L3i arrest [78] and that *S. stercoralis* PI3Ks play a role in L3i activation [111]. We hypothesize that both L3i arrest in the environment and activation in the host are functions of the balance between agonistic and antagonistic ILPs. Under this hypothesis, down-regulation of agonistic ILPs and up-regulation of antagonistic ILPs would drive L3i arrest, while the reciprocal balance of ILPs would stimulate L3i activation and resumption of development in the host.

We were surprised by the increased number of genes encoding *S. stercoralis* TGFβ ligands similar to the single *C. elegans* dauer TGFβ ligand and the fact that three of these are expressed solely in L3i (Figure 2.6). As previously proposed [27], we hypothesize that these *Ce*-DAF-7-like TGFβ ligands play an important role in regulating L3i arrest. It is also possible that these TGFβ ligands may modulate host immunity.

Our lab and others have demonstrated that DAs are potent activators of L3i as well as stimulators of heterogonic development [69,86]. However, the transcriptional profiles of the *S. stercoralis* DA biosynthetic enzyme homologs identified in this study do not demonstrate any coordinated regulation (Figure 2.7). Careful dissection of this pathway in future studies will be needed to determine the *in vivo* role of DA biosynthesis and *Ss*-DAF-12 regulation during L3i activation and heterogonic development. Together, these four pathways present several exciting avenues of future research in understanding the mechanisms controlling *S. stercoralis* L3i arrest and activation. Additionally, the transcriptomic data that formed the basis of this study provide a rich source of information for future unbiased global surveys of genes differentially regulated during L3i development and for many other aspects of parasitic nematode biology.

2.6 Figures

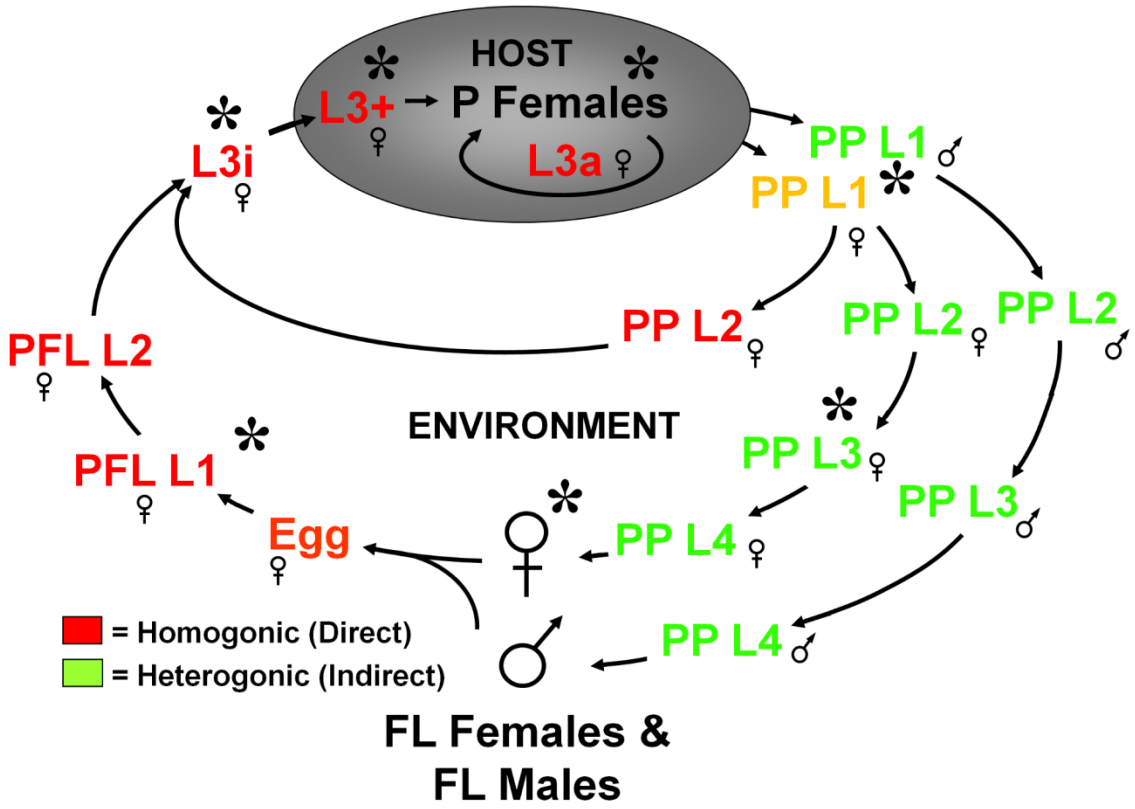

Figure 2.1. Diagram of the *Strongyloides stercoralis* life cycle.
Developmentally arrested infective third-stage larvae (L3i) can form by either a homogonic route (dark red) or a heterogonic route (light green). Female post-parasitic first-stage larvae (PP L1) passed in the feces of the infected host can develop homogonically through two larval molts directly to L3i or heterogonically through four larval molts to free-living females (FL Females). Post-parasitic L1 males invariably develop heterogonically through four molts to free-living males (FL Males). Post-free-living L1 (PFL L1), which are all female, molt twice and develop exclusively to L3i. Upon encountering and penetrating a susceptible host, activated third-stage larvae (L3+) resume feeding and development, migrate to the intestines, and molt twice into parasitic females (P Females). Post-parasitic L1 larvae can also precociously develop into auto-infective third-stage larvae (L3a) entirely within the host. Developmental stages marked with an asterisk (*) were interrogated by RNAseq. Adapted from [8].

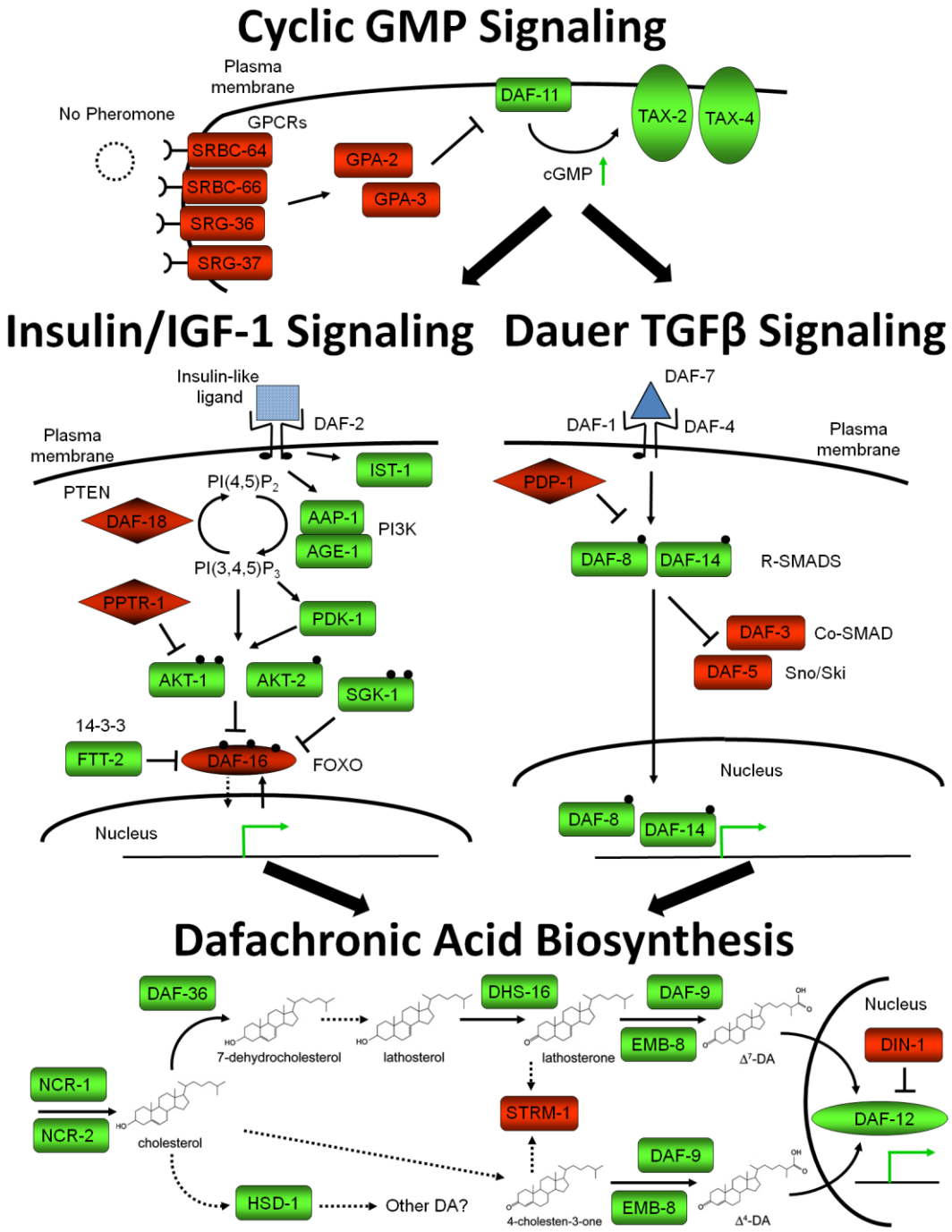

Figure 2.2. *Caenorhabditis elegans* dauer pathways during reproductive development.
Four developmental pathways regulate *C. elegans* dauer entry and exit: a cyclic guanosine monophosphate (GMP) signaling pathway, an insulin/insulin-like growth factor 1 (IGF-1) -like signaling pathway, a dauer transforming growth factor β (TGFβ) pathway, and a nuclear hormone receptor (DAF-12) regulated by a class of steroid ligands known as dafachronic acids (DAs). This simplified model depicts the four pathways under conditions favoring reproductive development and repression of dauer arrest. Proteins in

light green are “active,” while proteins in dark red are “inactive.” Black circles represent phosphorylation sites and diamond-shaped boxes represent phosphatases. Green arrows represent either increases in metabolite concentration or increases in gene transcription. Solid black lines represent well-established pathways, while dashed lines represent putative pathways. Adapted from [41,133,179,196].

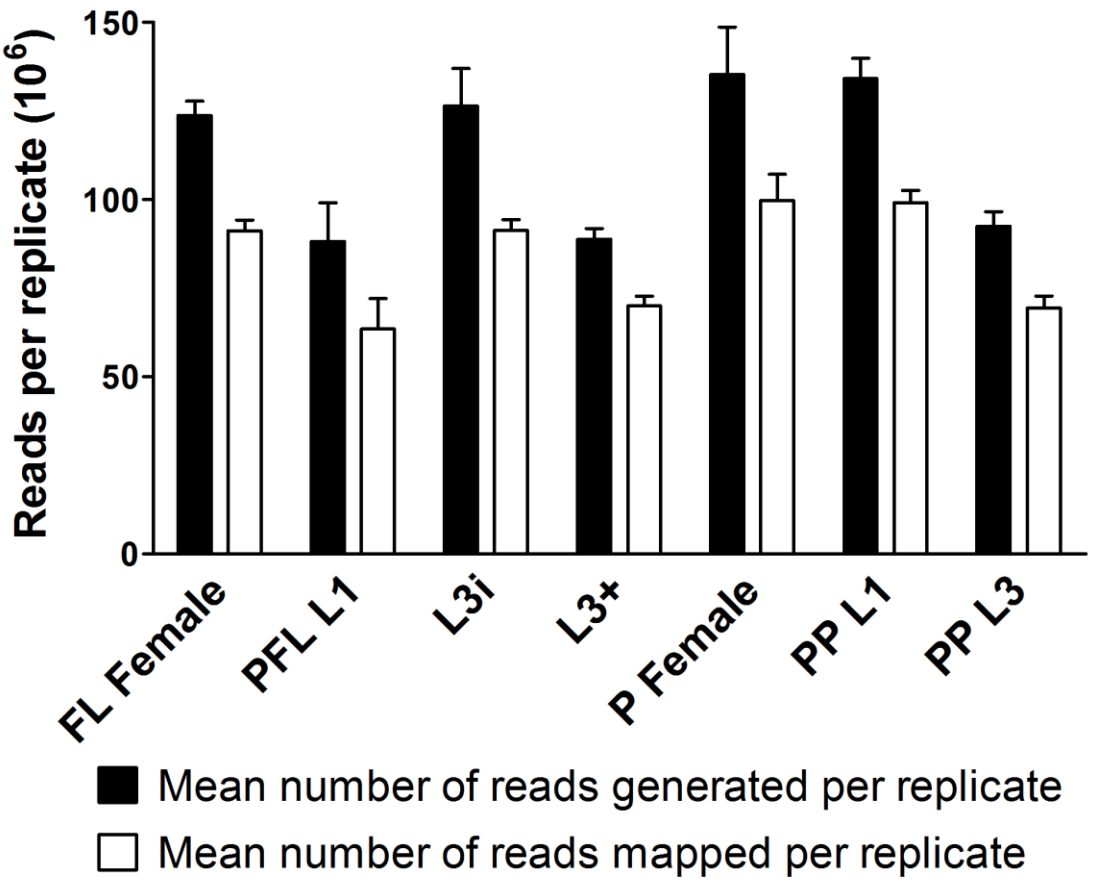

Figure 2.3. *S. stercoralis* RNAseq mean library sizes and number of reads aligning to the genome. A total of 21 libraries were derived from polyadenylated RNA and sequenced from seven developmental stages, each in biological triplicate. Paired-end 100 base-pair (bp) reads were generated from the following developmental stages: free-living females (FL Female), post-free-living first-stage larvae (PFL L1), infectious third-stage larvae (L3i), *in vivo* activated third-stage larvae (L3+), parasitic females (P Female), predominantly (>95%) heterogonically developing post-parasitic first-stage larvae (PP L1), and post-parasitic approximately third-stage larvae heterogonically developing to free-living adults and enriched for females (PP L3). The mean number of reads generated per replicate refers to the mean number of 100 bp reads sequenced (black bars) per biological replicate from each developmental stage. The mean number of mapped reads per replicate refers to the mean number of 100 bp reads aligned to *S. stercoralis* genomic contigs using TopHat (white bars) per biological replicate from each developmental stage. Error bars represent +1 standard deviation.

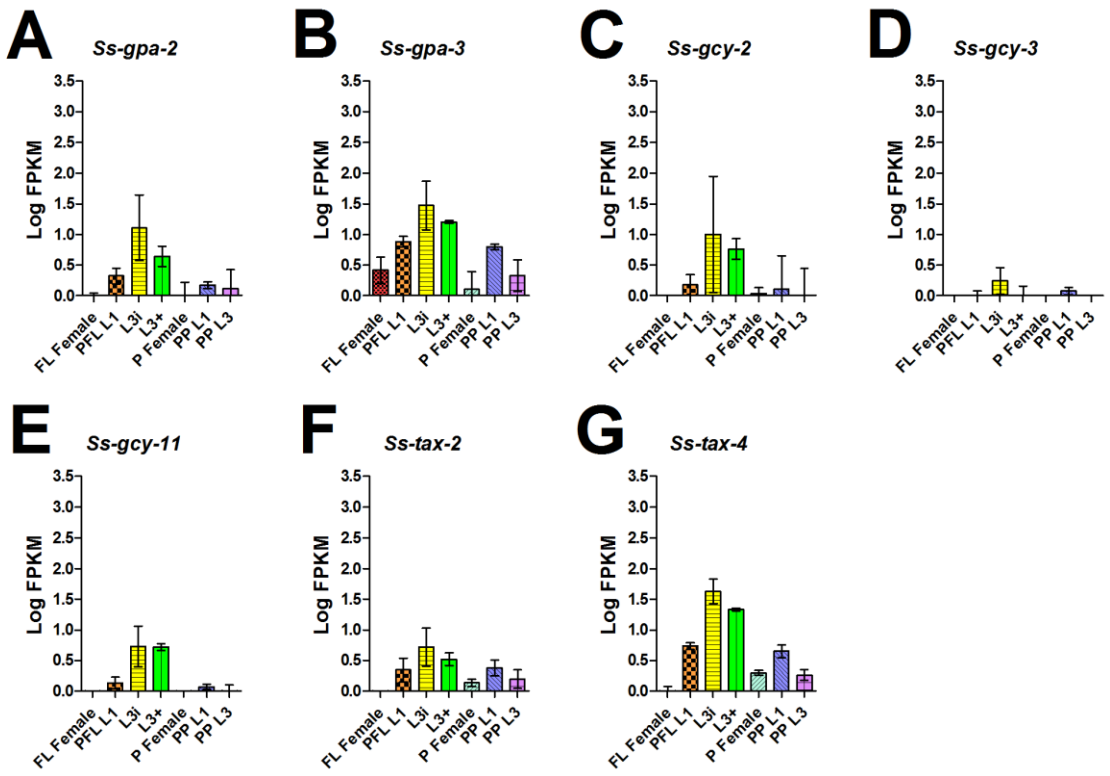

Figure 2.4. *S. stercoralis* cGMP signaling pathway homologs are coordinately up-regulated in L3i. Transcript abundances were determined for the coding region of: (A) *Ss-gpa-2* and (B) *Ss-gpa-3*, the genes encoding homologs of the G-protein α subunits *Ce*-GPA-2 and *Ce*-GPA-3, respectively; (C) *Ss-gcy-2*, (D) *Ss-gcy-3*, and (E) S*s-gcy-11*, genes which all encode guanylyl cyclase homologs, of which *Ss-gcy-11* encodes the *S. stercoralis* homolog most similar to the guanylyl cyclase *Ce*-DAF-11; (F) *Ss-tax-2* and (G) *Ss-tax-4*, genes encoding homologs of the cyclic nucleotide-gated ion channels *Ce*-TAX-2 and *Ce*-TAX-4, respectively. Transcript abundances were quantified in seven developmental stages: free-living females (FL Female), post-free-living first-stage larvae (PFL L1), infectious third-stage larvae (L3i), *in vivo* activated third-stage larvae (L3+), parasitic females (P Female), post-parasitic first-stage larvae (PP L1), and post-parasitic third-stage larvae (PP L3). Transcript abundances were calculated as fragments per kilobase of coding exon per million mapped reads (FPKM) and log transformed. Error bars represent 95% confidence intervals. The y-axes were scaled from 0 to 3.5 to aid comparison between genes.

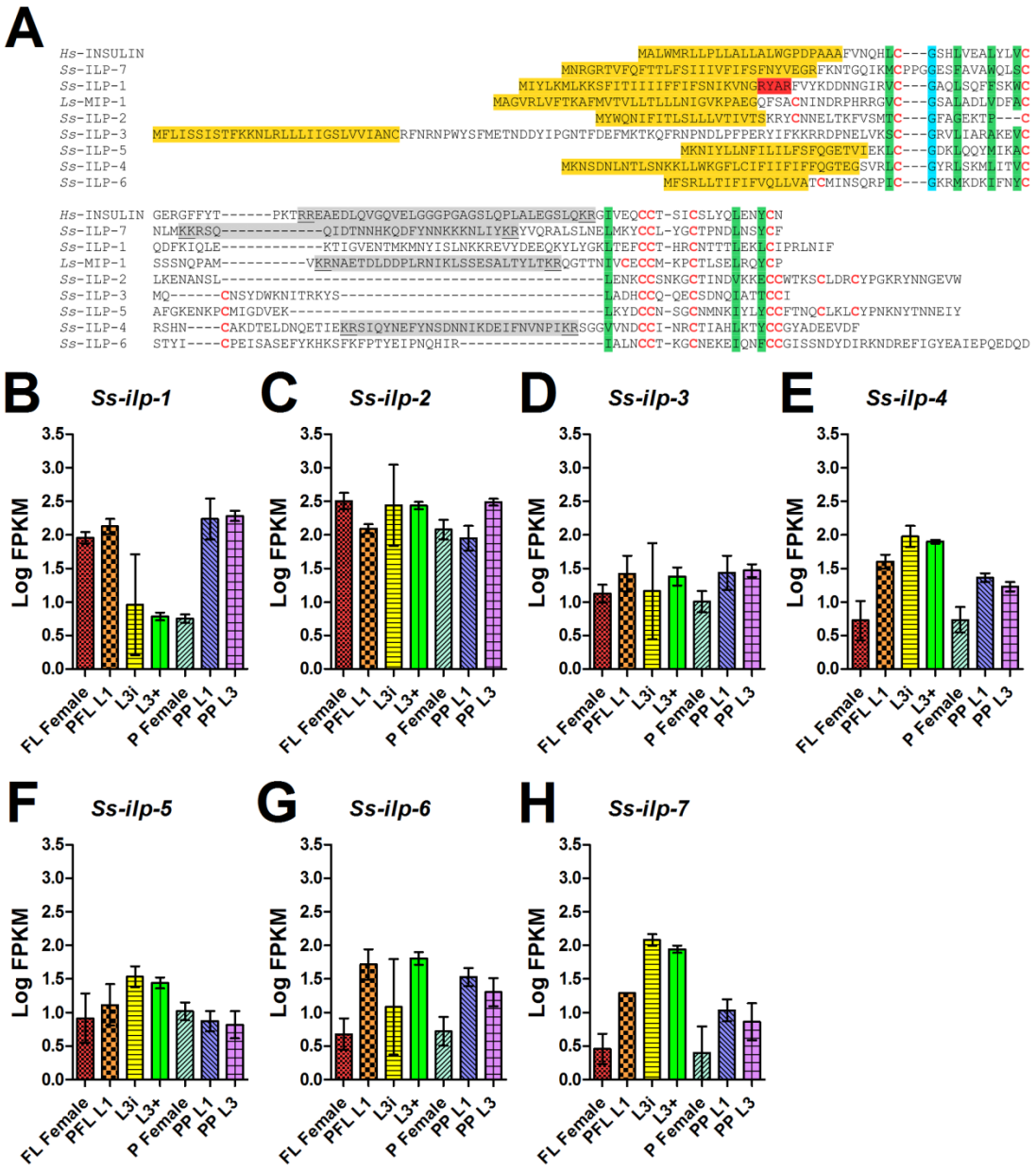

Figure 2.5. Protein sequence diversity and temporal regulation of *S. stercoralis* insulin-like peptides. (A) A predicted protein sequence alignment of seven *S. stercoralis* insulin-like peptides (ILPs), *Ss*-ILP-1 through -7, was constructed using human insulin (*Hs*-INSULIN) and *Lymnaea stagnalis* molluscan insulin-related peptide I (*Ls*-MIP-1) as the references. Cysteine residues, which are predicted to form disulfide bonds, are in red letters. Predicted signal sequences are highlighted in yellow, predicted furin recognition motifs are highlighted in red, hydrophobic residues important for helix formation are highlighted in green, and a conserved glycine is highlighted in blue. Predicted C peptides are highlighted in gray with dibasic predicted cleavage sites underlined. The B peptide is N-terminal of the C peptide, while the A peptide is C-terminal of the C peptide. (B-H) Transcript abundances were determined for the coding region of seven *S.*

stercoralis ILP-encoding genes (*Ss-ilp-1* through -*7*) in seven developmental stages: free-living females (FL Female), post-free-living first-stage larvae (PFL L1), infectious third-stage larvae (L3i), *in vivo* activated third-stage larvae (L3+), parasitic females (P Female), post-parasitic first-stage larvae (PP L1), and post-parasitic third-stage larvae (PP L3). Transcript abundances were calculated as fragments per kilobase of coding exon per million mapped reads (FPKM) and log transformed. Error bars represent 95% confidence intervals. The y-axes were scaled from 0 to 3.5 to aid comparison between genes.

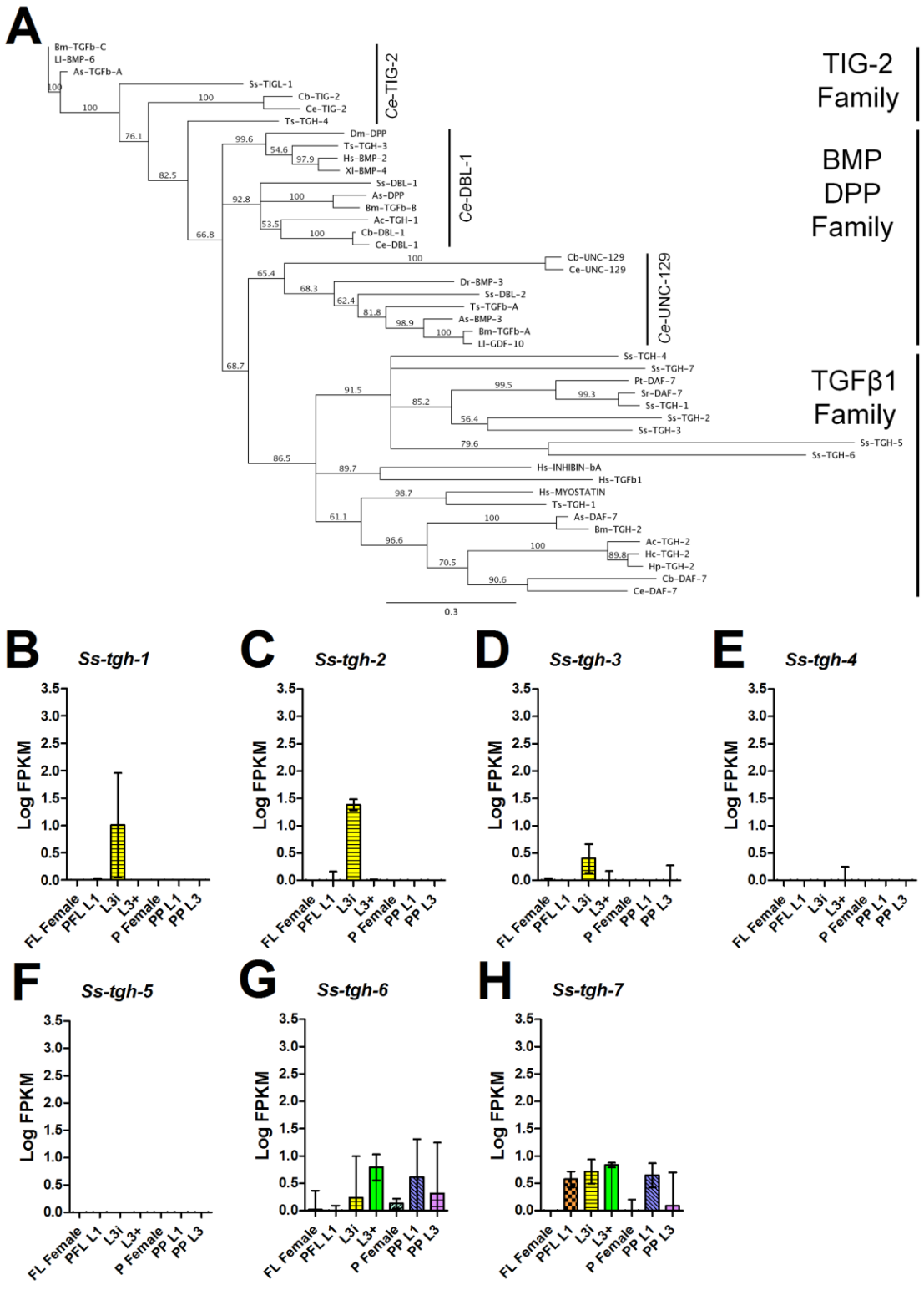
A
Bm-TGFb-C
Ll-BMP-6
As-TGFb-A
Ss-TIGL-1
Cb-TIG-2
Ce-TIG-2
Ts-TGH-4
Dm-DPP
Ts-TGH-3
Hs-BMP-2
Xl-BMP-4
Ss-DBL-1
As-DPP
Bm-TGFb-B
Ac-TGH-1
Cb-DBL-1
Ce-DBL-1
Cb-UNC-129
Ce-UNC-129
Dr-BMP-3
Ss-DBL-2
Ts-TGFb-A
As-BMP-3
Bm-TGFb-A
Ll-GDF-10
Ss-TGH-4
Ss-TGH-7
Pt-DAF-7
Sr-DAF-7
Ss-TGH-1
Ss-TGH-2
Ss-TGH-3
Ss-TGH-5
Ss-TGH-6
Hs-INHIBIN-bA
Hs-TGFb1
Hs-MYOSTATIN
Ts-TGH-1
As-DAF-7
Bm-TGH-2
Ac-TGH-2
Hc-TGH-2
Hp-TGH-2
Cb-DAF-7
Ce-DAF-7
0.3
Ce-TIG-2
Ce-DBL-1
Ce-UNC-129
TIG-2 Family
BMP DPP Family
TGFβ1 Family
B Ss-tgh-1
C Ss-tgh-2
D Ss-tgh-3
E Ss-tgh-4
F Ss-tgh-5
G Ss-tgh-6
H Ss-tgh-7
Log FPKM
FL Female
PFL L1
L3i
L3+
P Female
PP L1
PP L3

Figure 2.6. Phylogenetic analysis and temporal regulation of *S. stercoralis* TGFβ ligands.
(A) Phylogenetic analysis of the transforming growth factor β (TGFβ) super-family ligands was performed; nematode TGFβ ligands resolved into three main families that share the same cysteine architecture. *Ss*-TIGL-1 groups with the *Ce*-TIG-2-like family; *Ss*-DBL-1 and *Ss*-DBL-2 group with the *D. melanogaster* decapentaplegic (DPP) and vertebrate bone morphogenetic protein (BMP) family; and *Ss*-TGH-1 through -7 group with the human TGFβ1 family that also includes *Ce*-DAF-7. A Clustal W alignment of the TGFβ ligands truncated at the first conserved cysteine was used to construct the neighbor-joining tree with 100 iterations of boot-strapping. Abbreviations: *Ancylostoma caninum* (Ac), *Ascaris suum* (As), *Brugia malayi* (Bm), *Caenorhabditis briggsae* (Cb), *Caenorhabditis elegans* (Ce), *Danio rerio* (Dr), *Drosophila melanogaster* (Dm), *Haemonchus contortus* (Hc), *Heligmosomoides polygyrus* (Hp), *Homo sapiens* (Hs), *Loa loa* (Ll), *Parastrongyloides trichosuri* (Pt), *Strongyloides ratti* (Sr), *Strongyloides stercoralis* (Ss), *Trichinella spiralis* (Ts), and *Xenopus laevis* (Xl). The scale bar represents substitutions per position. (B-H) Transcript abundances were determined for the coding region of seven *S. stercoralis* genes, *Ss-tgh-1* through *-7*, encoding putative TGFβ ligands similar to *Ce*-DAF-7 in seven developmental stages: free-living females (FL Female), post-free-living first-stage larvae (PFL L1), infectious third-stage larvae (L3i), *in vivo* activated third-stage larvae (L3+), parasitic females (P Female), post-parasitic first-stage larvae (PP L1), and post-parasitic third-stage larvae (PP L3). Transcript abundances were calculated as fragments per kilobase of coding exon per million mapped reads (FPKM) and log transformed. Error bars represent 95% confidence intervals. The y-axes were scaled from 0 to 3.5 to aid comparison between genes.

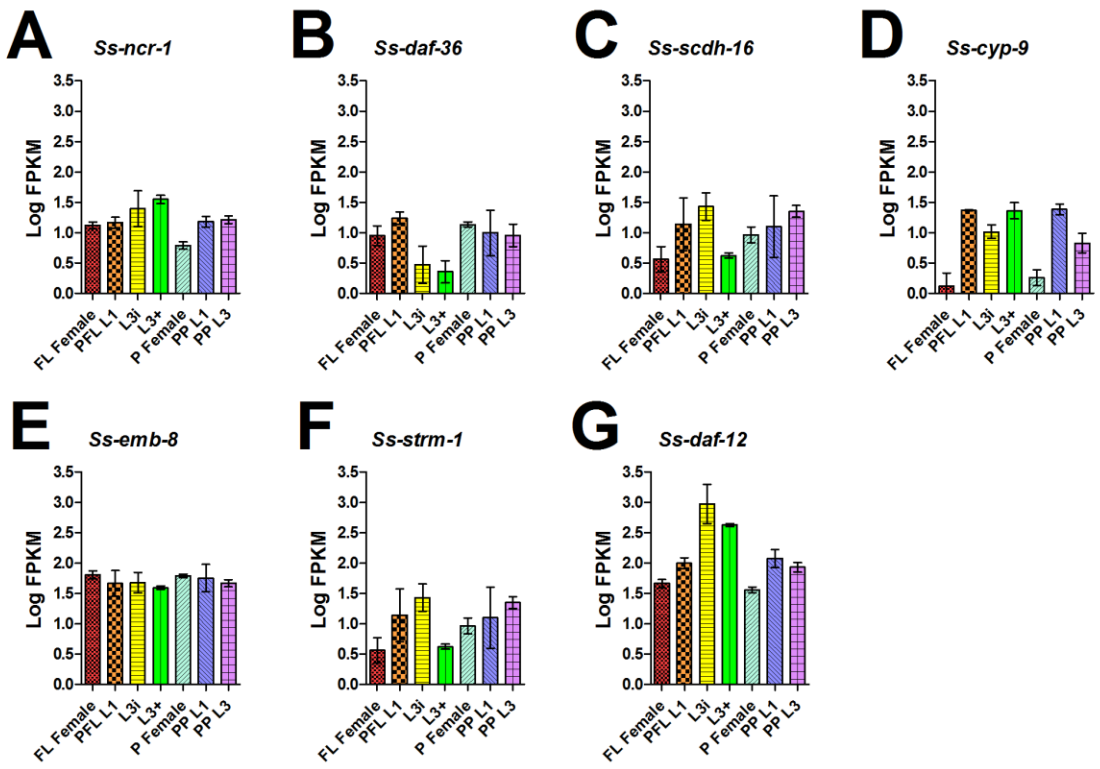

Figure 2.7. Temporal regulation of *S. stercoralis* DAF-12 and genes putatively involved in dafachronic acid synthesis.

Transcript abundances were determined for the coding region of: (A) *Ss-ncr-1*, a gene encoding a homolog of the intracellular cholesterol transporters *Ce*-NCR-1 and *Ce*-NCR-2; (B) *Ss-daf-36*, a gene encoding a homolog of the Rieske-like oxygenase *Ce*-DAF-36; (C) *Ss-scdh-16*, a gene encoding a short-chain dehydrogenase homolog most similar to *Ce*-DHS-16; (D) *Ss-cyp-9*, a gene encoding a cytochrome P450 homolog most similar to *Ce*-DAF-9; (E) *Ss-emb-8*, a gene encoding a homolog of the cytochrome P450 reductase *Ce*-EMB-8; (F) *Ss-strm-1*, a gene encoding a homolog of the methyltransferase *Ce*-STRM-1; and (G) *Ss-daf-12*, the homolog of the nuclear hormone receptor *Ce*-DAF-12. Transcript abundances were quantified in seven developmental stages: free-living females (FL Female), post-free-living first-stage larvae (PFL L1), infectious third-stage larvae (L3i), *in vivo* activated third-stage larvae (L3+), parasitic females (P Female), post-parasitic first-stage larvae (PP L1), and post-parasitic third-stage larvae (PP L3). Transcript abundances were calculated as fragments per kilobase of coding exon per million mapped reads (FPKM) and log transformed. Error bars represent 95% confidence intervals. The y-axes were scaled from 0 to 3.5 to aid comparison between genes.

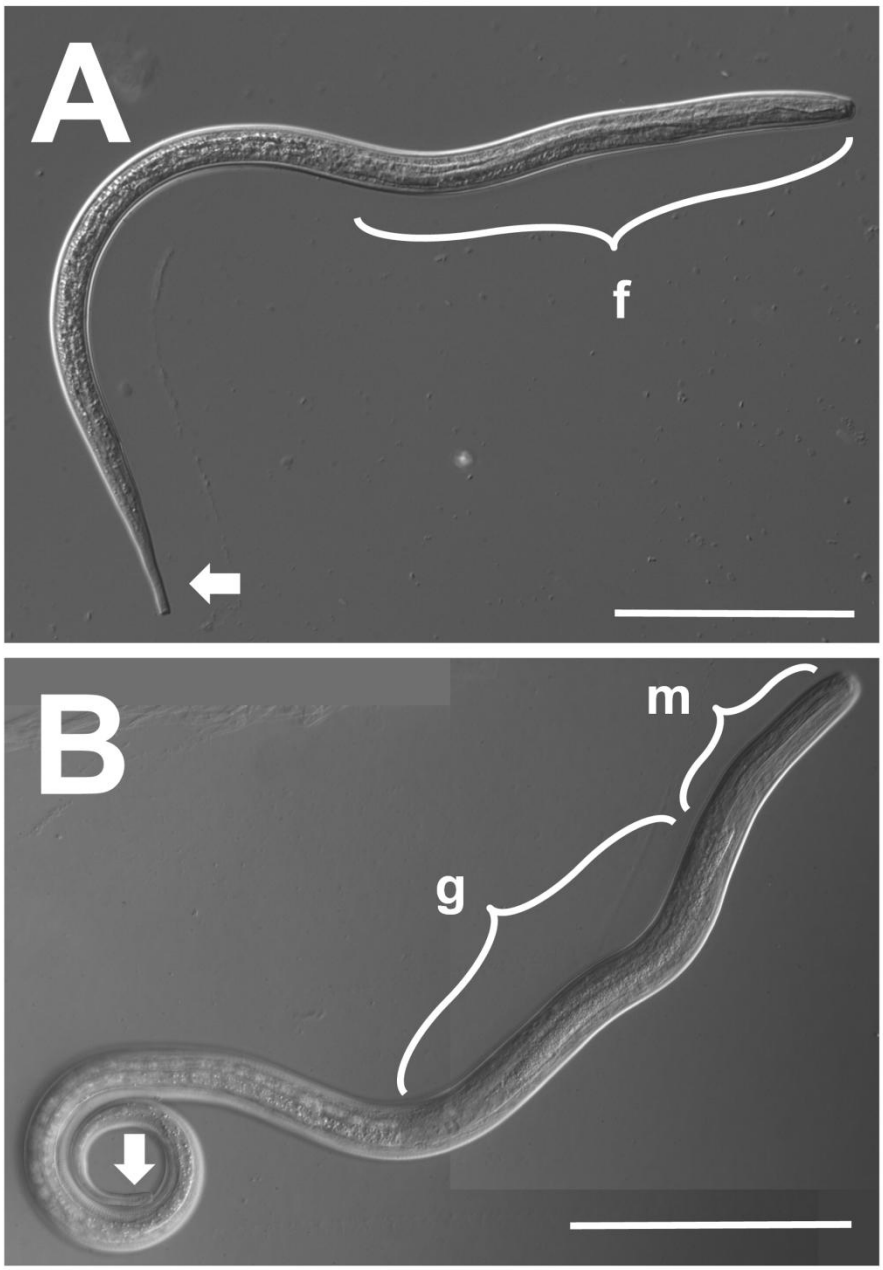

Figure 2.S1. Morphological comparison of *S. stercoralis* L3i and L3+.
S. stercoralis third-stage larvae were photographed as (A) developmentally arrested and non-feeding third-stage larvae (L3i) or (B) as feeding third-stage larvae activated *in vivo* for three days in a permissive host (L3+). Overall, the body of the (A) L3i is more radially constricted than that of the (B) L3+. Similarly, the (A) L3i has a filariform pharynx (f) that is radially constricted forming a long thin tube extending almost to the midpoint of the worm, while the (B) L3+ has a pharynx that is pumping, is not radially constricted, and has differentiated into both muscular (m) and glandular(g) segments. The fork-shaped tail (arrow) in both the (A) L3i and (B) L3+ is characteristic of third-stage larvae in *Strongyloides* species and is lost in subsequent larval stages. Scale bar represents 100 μM.

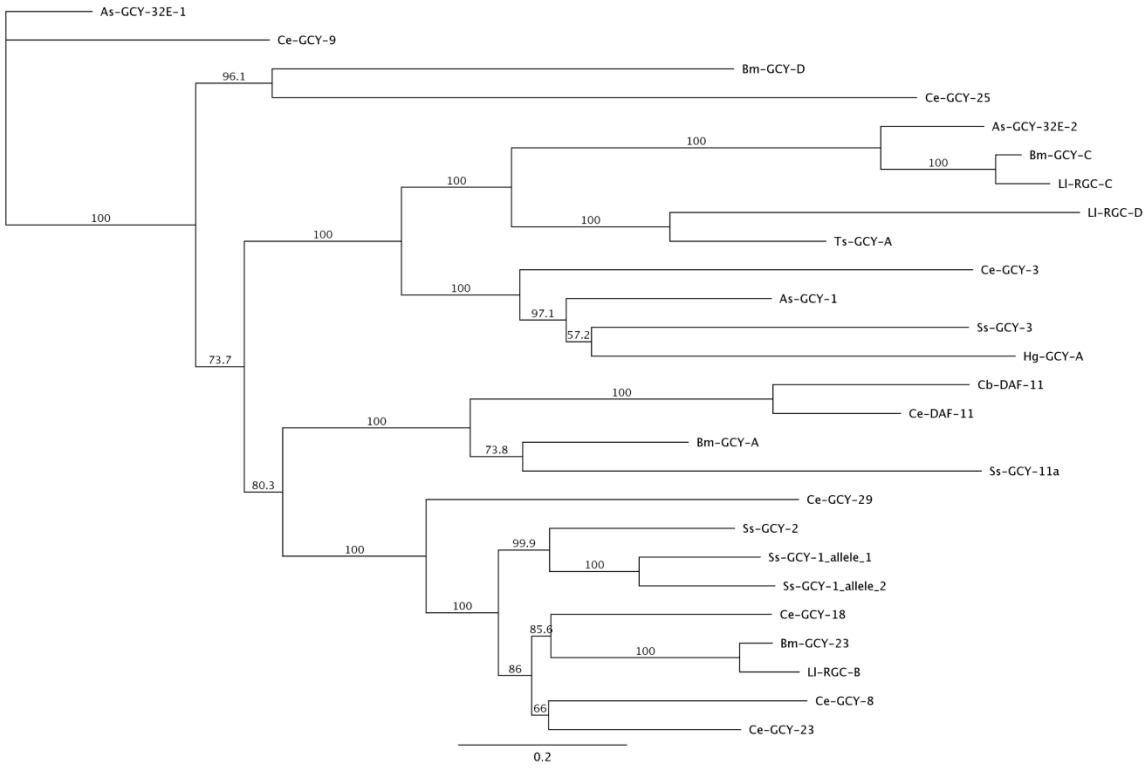

Figure 2.S2. Phylogenetic analysis of phylum Nematoda guanylyl cyclases similar to *Ce*-DAF-11. A protein alignment, generated with Clustal W, of several predicted guanylyl cyclases similar to *Ce*-DAF-11 from *S. stercoralis* and other parasitic nematodes was used to construct a neighbor-joining tree with 100 iterations of boot-strapping. The predicted *Ss*-GCY-11 protein grouped with *Ce*-DAF-11. Abbreviations: *Ascaris suum* (As), *Brugia malayi* (Bm), *Caenorhabditis briggsae* (Cb), *Caenorhabditis elegans* (Ce), *Heterodera glycines* (Hg), *Loa loa* (Ll), *Strongyloides stercoralis* (Ss), and *Trichinella spiralis* (Ts). The scale bar represents substitutions per position.

Figure 2.S3. Protein alignment of TGFβ ligand domains by cysteine architecture.
Protein sequence alignment of TGFβ ligand domains including all cysteine residues in *S. stercoralis* and other metazoans revealed three distinct sets of cysteine architecture: *Hs*-TGFβ1-like ligands, including *Ce*-DAF-7, which have nine conserved cysteine residues; *Drosophila melanogaster* decapentaplegic (DPP) and vertebrate bone morphogenetic protein (BMP) -like ligands, including *Ce*-DBL-1 and *Ce*-UNC-129 subfamilies, which have seven conserved cysteine residues; and *Ce*-TIG-2-like ligands, which have six conserved cysteine residues. The conserved cysteine residues, critical for disulfide bond formation and "cysteine knot" folding, are in red. Abbreviations: *Ancylostoma caninum* (Ac), *Ascaris suum* (As), *Brugia malayi* (Bm), *Caenorhabditis briggsae* (Cb), *Caenorhabditis elegans* (Ce), *Danio rerio* (Dr), *Drosophila melanogaster* (Dm), *Haemonchus contortus* (Hc), *Heligmosomoides polygyrus* (Hp), *Homo sapiens* (Hs), *Loa loa* (Ll), *Parastrongyloides trichosuri* (Pt), *Strongyloides ratti* (Sr), *Strongyloides stercoralis* (Ss), *Trichinella spiralis* (Ts), and *Xenopus laevis* (Xl).

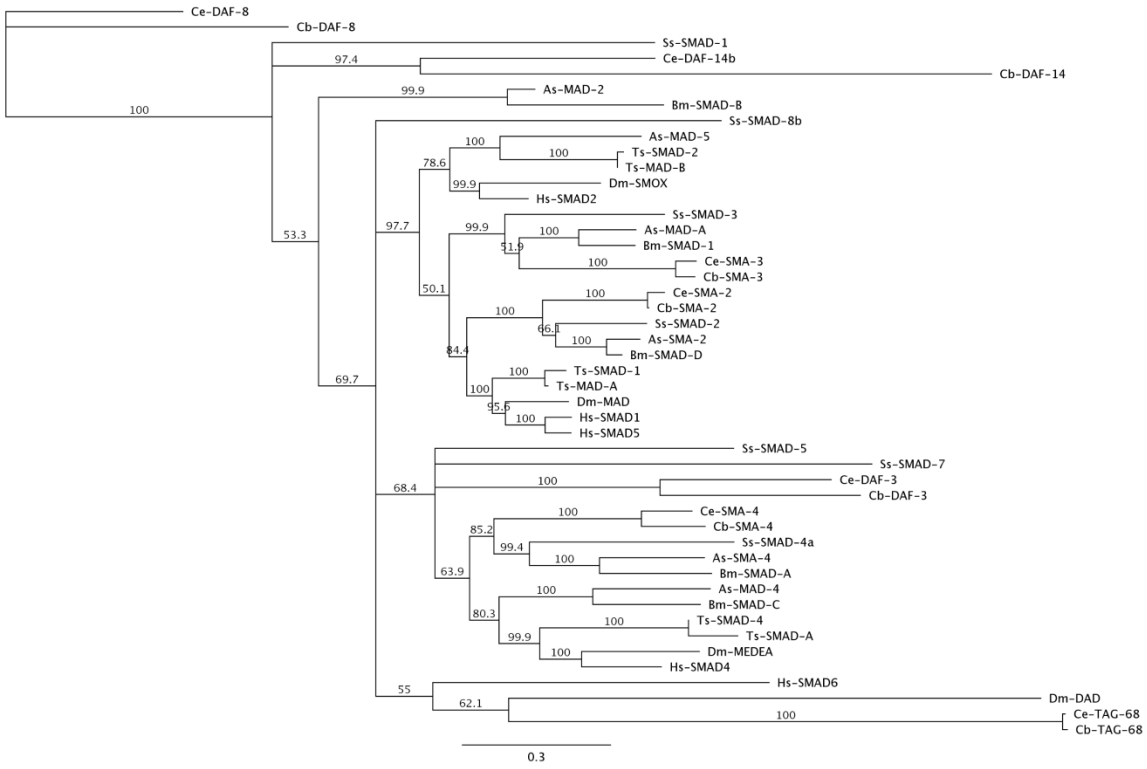

Figure 2.S4. Phylogenetic analysis of phylum Nematoda SMAD homologs.
A protein alignment, generated with Clustal W, of all publicly available phylum Nematoda SMAD homolog predicted proteins, was used to construct a neighbor-joining tree with 100 iterations of boot-strapping. The small body size and male tail abnormal (Sma/Mab) TGFβ pathway SMADs, including *Ce*-SMA-2, *Ce*-SMA-3, and *Ce*-SMA-4, resolved into distinct clades while the dauer TGFβ pathway SMADs, including *Ce*-DAF-3, *Ce*-DAF-8, and *Ce*-DAF-14, did not. Abbreviations: *Ascaris suum* (As), *Brugia malayi* (Bm), *Caenorhabditis briggsae* (Cb), *Caenorhabditis elegans* (Ce), *Drosophila melanogaster* (Dm), *Heterodera glycines* (Hg), *Homo sapiens* (Hs), *Loa loa* (Ll), *Strongyloides stercoralis* (Ss), and *Trichinella spiralis* (Ts). The scale bar represents substitutions per position.

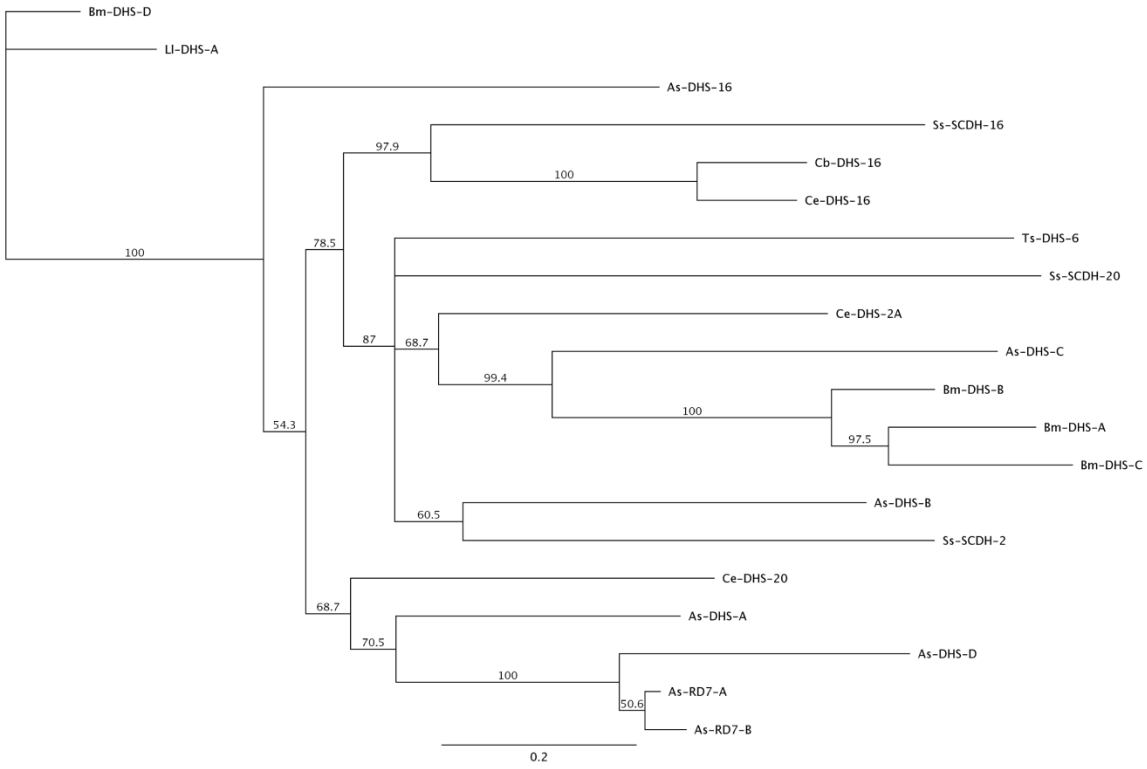

Figure 2.S5. Phylogenetic analysis of phylum Nematoda short-chain dehydrogenase homologs similar to *Ce*-DHS-16.

A protein alignment, generated with Clustal W, of phylum Nematoda short-chain dehydrogenase homologs similar to *Ce*-DHS-16 was used to construct a neighbor-joining tree with 100 iterations of boot-strapping. The predicted protein for *Ss*-SCDH-16 grouped closest to *Ce*-DHS-16. Abbreviations: *Ascaris suum* (As), *Brugia malayi* (Bm), *Caenorhabditis briggsae* (Cb), *Caenorhabditis elegans* (Ce), *Loa loa* (Ll), *Strongyloides stercoralis* (Ss), and *Trichinella spiralis* (Ts). The scale bar represents substitutions per position.

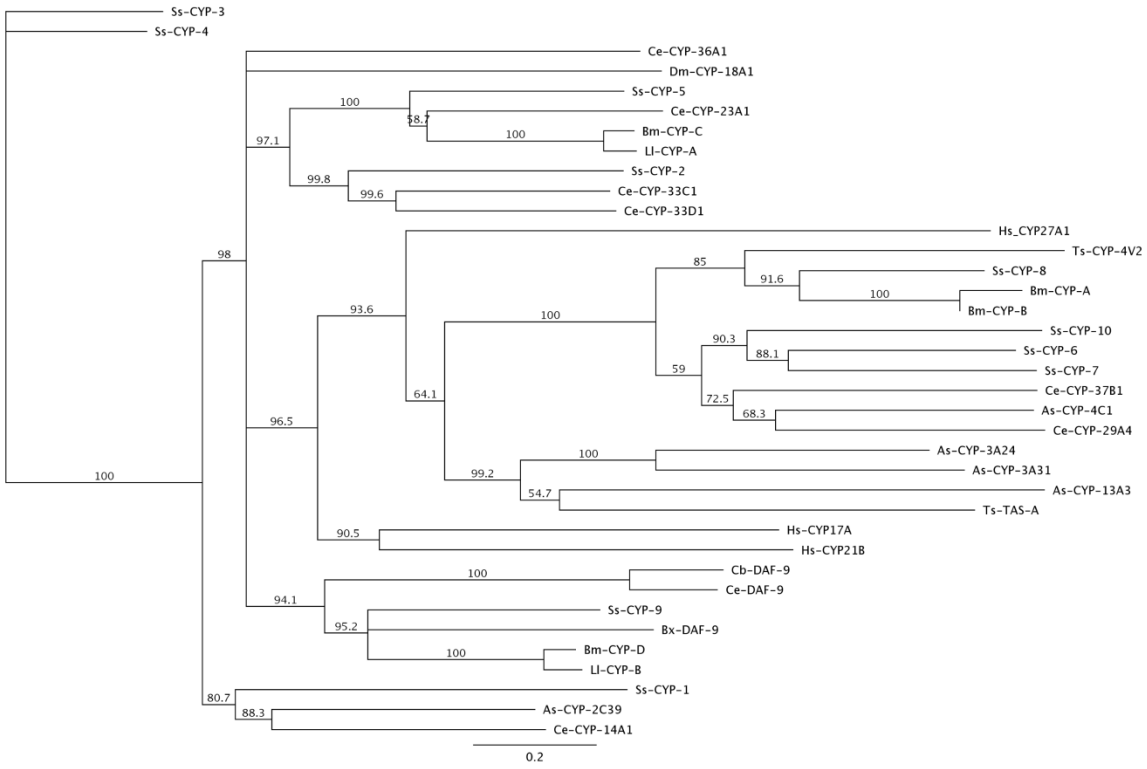

Figure 2.S6. Phylogenetic analysis of phylum Nematoda cytochrome P450 homologs similar to *Ce*-DAF-9.

A protein alignment, generated with Clustal W, of phylum Nematoda cytochrome P450 homologs similar to *Ce*-DAF-9 was used to construct a neighbor-joining tree with 100 iterations of boot-strapping. The predicted protein for *Ss*-CYP-9 grouped closest to *Ce*-DAF-9. Abbreviations: *Ascaris suum* (As), *Brugia malayi* (Bm), *Bursaphelenchus xylophilus* (Bx), *Caenorhabditis briggsae* (Cb), *Caenorhabditis elegans* (Ce), *Drosophila melanogaster* (Dm), *Homo sapiens* (Hs), *Loa loa* (Ll), *Strongyloides stercoralis* (Ss), and *Trichinella spiralis* (Ts). The scale bar represents substitutions per position.

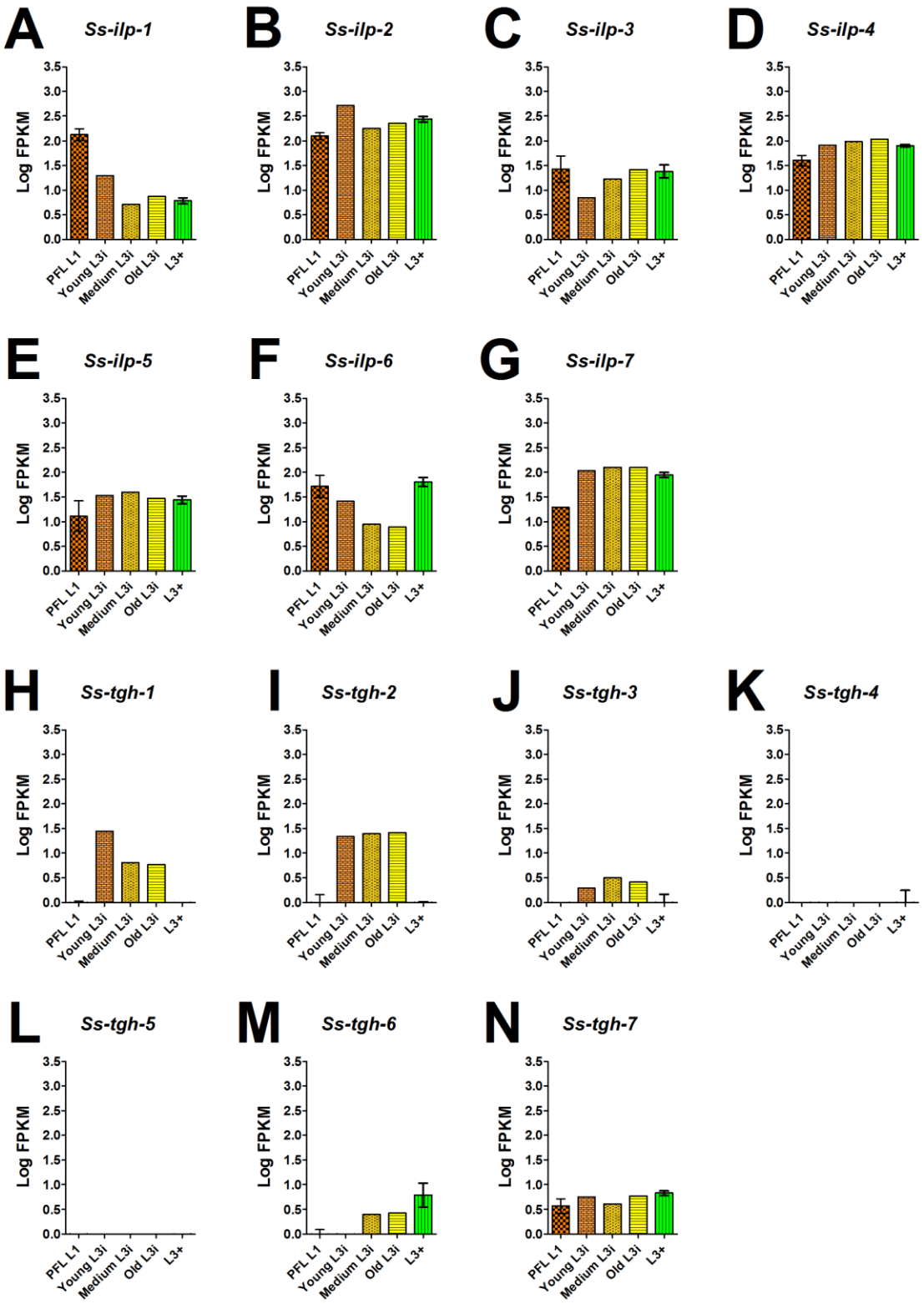
A
Ss-ilp-1
B
Ss-ilp-2
C
Ss-ilp-3
D
Ss-ilp-4
E
Ss-ilp-5
F
Ss-ilp-6
G
Ss-ilp-7
H
Ss-tgh-1
I
Ss-tgh-2
J
Ss-tgh-3
K
Ss-tgh-4
L
Ss-tgh-5
M
Ss-tgh-6
N
Ss-tgh-7
Log FPKM
0.0
0.5
1.0
1.5
2.0
2.5
3.0
3.5
PFL L1
Young L3i
Medium L3i
Old L3i
L3+

Figure 2.S7. Regulation of ILP and TGFβ ligand genes during post-free-living development. Transcript abundances were determined for the coding region of (A-G) seven *S. stercoralis* insulin-like peptide (ILP) -encoding genes (*Ss-ilp-1* through -*7*) and (H-N) seven *S. stercoralis* DAF-7-like TGFβ ligand encoding genes (*Ss-tgh-1* through -*7*) over the course of post-free living larval development. Transcript abundances were examined for post-free-living first-stage larvae (PFL L1), infectious third-stage larvae (L3i), and *in vivo* activated third-stage larvae (L3+). The mean of both PFL L1 and L3+, from the three biological replicates, was plotted along with the 95% confidence intervals. Each biological sample of L3i was plotted individually according to relative age: L3i incubated at 21°C for 8 days (young L3i), L3i incubated at 25°C for 7 days (medium L3i), and L3i incubated at 21°C for 10 days (old L3i). Transcript abundances were calculated as fragments per kilobase of coding exon per million mapped reads (FPKM) and log transformed. The y-axes were scaled from 0 to 3.5 to aid comparison between genes.

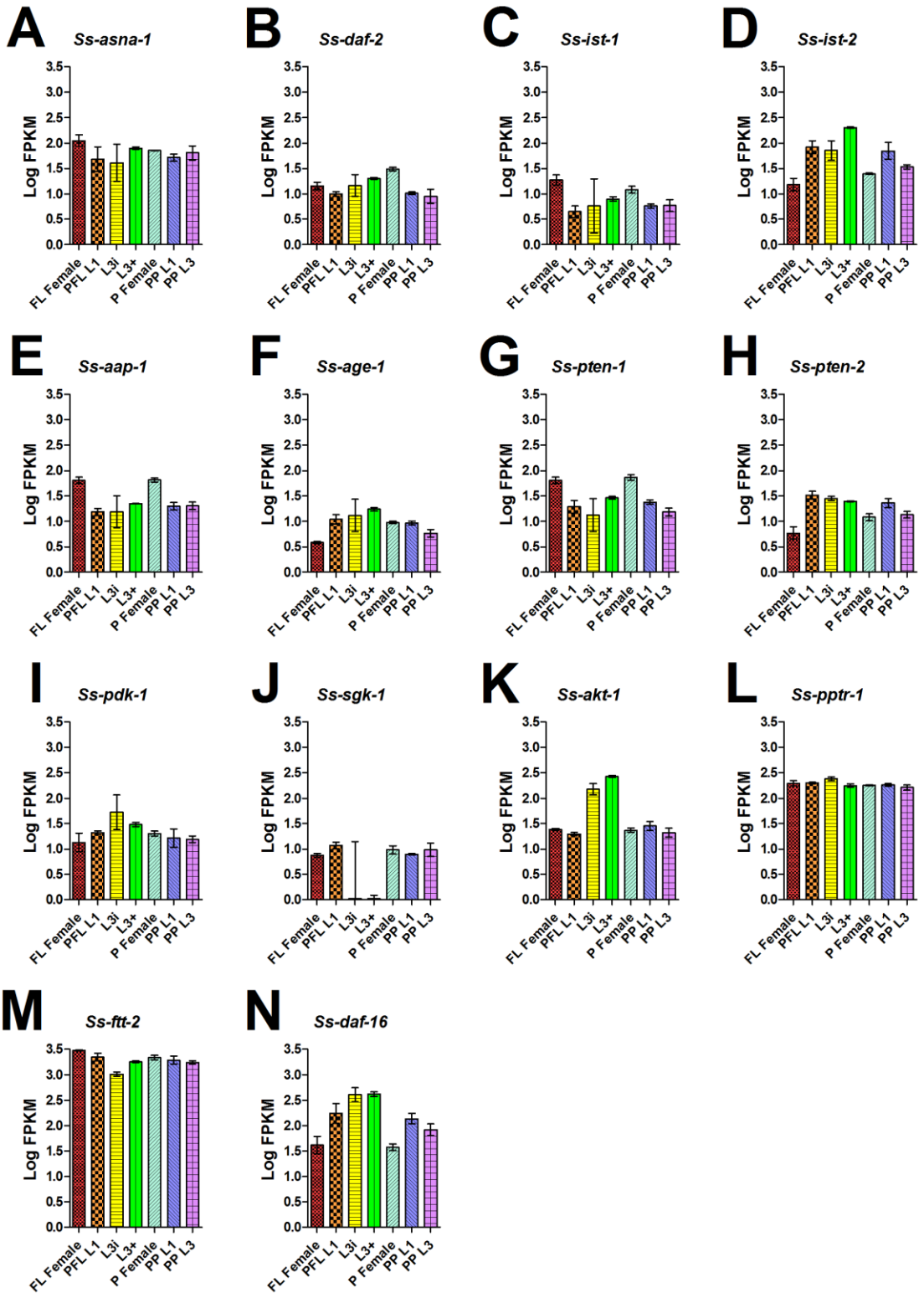
A
Ss-asna-1
B
Ss-daf-2
C
Ss-ist-1
D
Ss-ist-2
E
Ss-aap-1
F
Ss-age-1
G
Ss-pten-1
H
Ss-pten-2
I
Ss-pdk-1
J
Ss-sgk-1
K
Ss-akt-1
L
Ss-pptr-1
M
Ss-ftt-2
N
Ss-daf-16
Log FPKM
0.0
0.5
1.0
1.5
2.0
2.5
3.0
3.5
FL Female
PFL L1
L3i
L3+
P Female
PP L1
PP L3

Figure 2.S8. Developmental regulation of *S. stercoralis* homologs of intracellular IIS genes. Transcript abundances were determined for the coding region of *S. stercoralis* homologs of genes encoding insulin/IGF-1-like signaling (IIS) pathway proteins, including: (A) *Ss-asna-1*, a homolog of *Ce-asna-1*, which encodes a putative membrane transporter involved in insulin-like peptide secretion; (B) *Ss-daf-2*, a homolog of *Ce-daf-2*, which encodes an insulin-like receptor; (C) *Ss-ist-1* and (D) *Ss-ist-2*, homologs of the insulin receptor substrate encoding gene *Ce-ist-1*; (E) *Ss-aap-1*, a homolog of *Ce-aap-1*, which encodes a phosphatidylinositol-3 (PI3) kinase accessory/regulatory subunit; (F) *Ss-age-1*, a homolog of *Ce-age-1*, which encodes a PI3 kinase catalytic subunit; (G) *Ss-pten-1* and (H) *Ss-pten-2*, homologs of *Ce-daf-18*, which encodes a phosphatase opposing *Ce-age-1* function; (I) *Ss-pdk-1*, a homolog of *Ce-pdk-1*, which encodes a PTEN-like kinase; (J) *Ss-sgk-1*, a homolog of the serum- and glucocorticoid-inducible kinase *Ce-sgk-1*; (K) *Ss-akt-1*, a homolog of *Ce-akt-1* and *-2*, which encode AKT kinases; (L) *Ss-pptr-1*, a homolog of *Ce-pptr-1*, which encodes a B56 regulatory subunit of the PP2A phosphatase opposing *Ce*-AKT-1 function; (M) *Ss-ftt-2*, a homolog of the 14-3-3 encoding gene *Ce-ftt-2*; and (N) *Ss-daf-16*, a homolog of *Ce-daf-16*, which encodes a forkhead transcription factor. Transcript abundances were quantified in seven developmental stages: free-living females (FL Female), post-free-living first-stage larvae (PFL L1), infectious third-stage larvae (L3i), *in vivo* activated third-stage larvae (L3+), parasitic females (P Female), post-parasitic first-stage larvae (PP L1), and post-parasitic third-stage larvae (PP L3). Transcript abundances were calculated as fragments per kilobase of coding exon per million mapped reads (FPKM) and log transformed. Error bars represent 95% confidence intervals. The y-axes were scaled from 0 to 3.5 to aid comparison between genes.

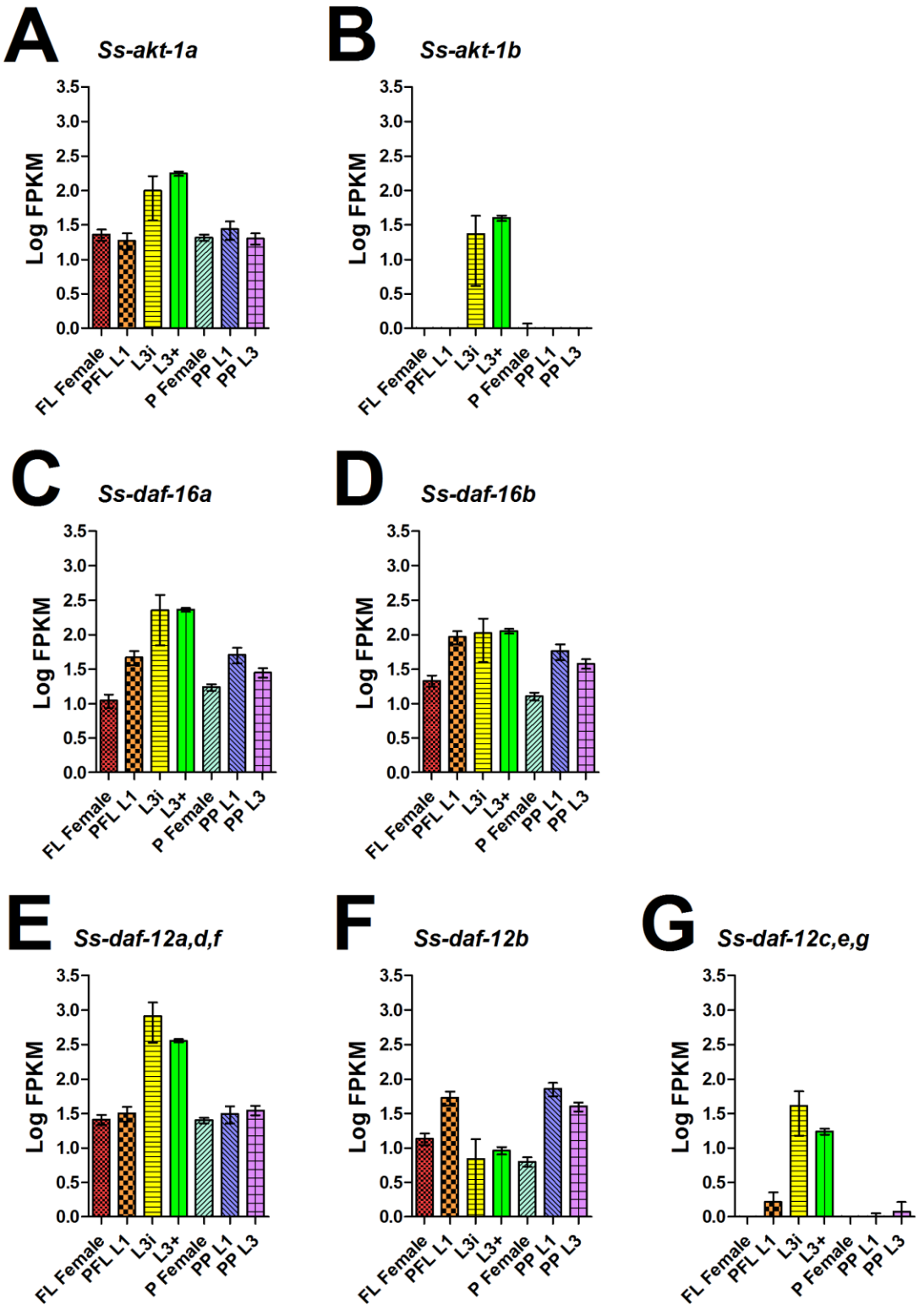
A
Ss-akt-1a
B
Ss-akt-1b
C
Ss-daf-16a
D
Ss-daf-16b
E
Ss-daf-12a,d,f
F
Ss-daf-12b
G
Ss-daf-12c,e,g
Log FPKM
0.0
0.5
1.0
1.5
2.0
2.5
3.0
3.5
FL Female
PFL L1
L3i
L3+
P Female
PP L1
PP L3

Figure 2.S9. Developmental stage-specific transcripts of *S. stercoralis akt-1, daf-16,* and *daf-12* isoforms.

(A, B) Two transcripts, each from different promoters, are generated from the *Ss-akt-1* locus: (A) *Ss-akt-1a* and (B) *Ss-akt-1b*. The *Ss-akt-1b* transcript encodes a putative 525 amino acid *Ss*-AKT-1B peptide that has 33 amino acids truncated from the conserved AKT pleckstrin homology (PH) domain at the N-terminus. The *Ss-akt-1a* transcript encodes a putative 580 amino acid *Ss*-AKT-1A protein with a conserved full-length PH domain. (C, D) The locus from which the *S. stercoralis* forkhead transcription factor *Ss-daf-16* is transcribed also produces two transcripts, (C) *Ss-daf-16a* and (D) *Ss-daf-16b*, each from a different promoter. These transcripts encode a 741 amino acid *Ss*-DAF-16A predicted protein and a 566 amino acid *Ss*-DAF-16B predicted protein, which differ at the N-terminus. (E-G) The genomic locus encoding the *S. stercoralis* nuclear hormone receptor homolog *Ss*-DAF-12 expresses at least seven different transcripts, which we termed *Ss-daf-12a-g*, from several promoters. These seven transcripts encode a total of three predicted proteins, each differing at the N-terminus before the DNA-binding domain, with transcripts (E) *Ss-daf-12a,d,f* encoding a putative 752 amino acid *Ss*-DAF-12A protein, (F) *Ss-daf-12b* encoding a putative 947 amino acid *Ss*-DAF-12B protein, and (G) *Ss-daf-12c,e,g* encoding a putative 722 amino acid *Ss*-DAF-12C protein. Transcript abundances were quantified in seven developmental stages: free-living females (FL Female), post-free-living first-stage larvae (PFL L1), infectious third-stage larvae (L3i), *in vivo* activated third-stage larvae (L3+), parasitic females (P Female), post-parasitic first-stage larvae (PP L1), and post-parasitic third-stage larvae (PP L3). Transcript abundances were calculated as fragments per kilobase of transcript exon per million mapped reads (FPKM) and log transformed. Error bars represent 95% confidence intervals. The y-axes were scaled from 0 to 3.5 to aid comparison between genes.

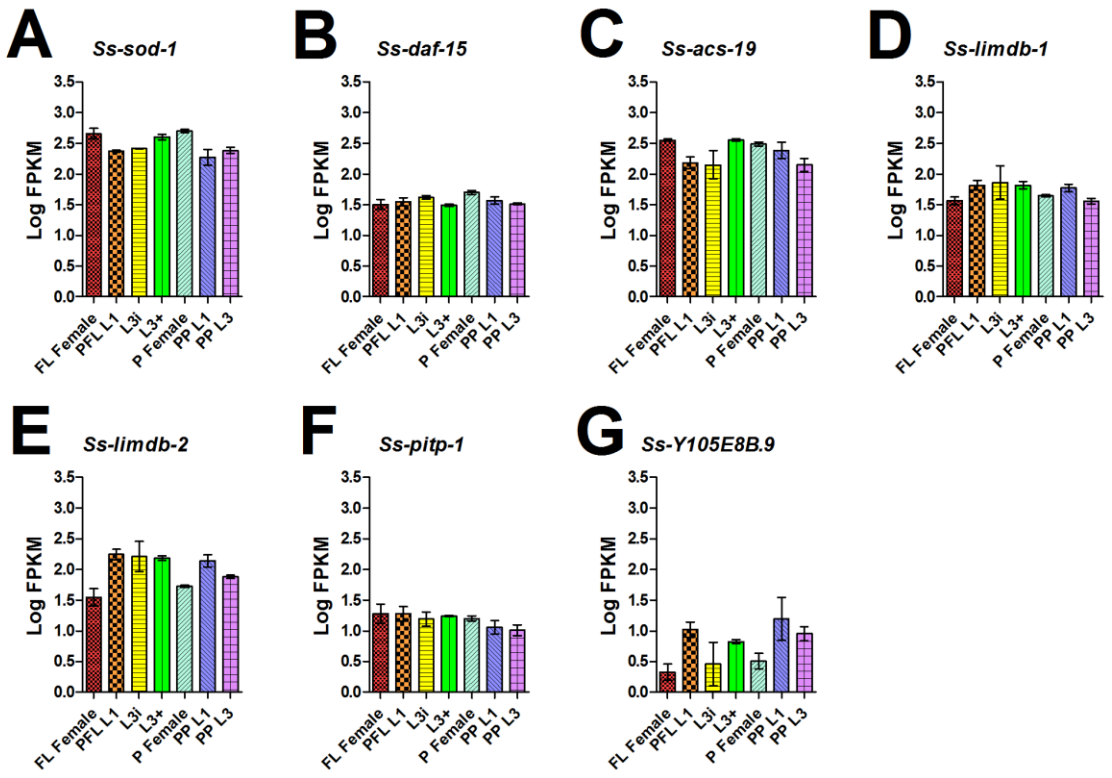

Figure 2.S10. Lack of developmental regulation of *S. stercoralis* homologs of *Ce*-DAF-16-regulated genes.

Transcript abundances were examined for *S. stercoralis* homologs of *C. elegans* genes that are transcriptionally regulated directly by *Ce*-DAF-16 and have a phenotype associated with RNAi knock-down. (A) *Ss-sod-1* is the sole *S. stercoralis* superoxide dismutase and is a homolog of *Ce-sod-3*. (B) *Ss-daf-15* and (C) *Ss-acs-19* are homologs of *Ce-daf-15* and *Ce-acs-19*, respectively. Both (D) *Ss-limdb-1* and (E) *Ss-limdb-2* are homologs of *Ce-lim-1*, while (F) *Ss-pitp-1* and (G) *Ss-Y105E8B.9* are homologs of *Ce-pitp-1* and *Ce-Y105E8B.9*, respectively. Transcript abundances were quantified in seven developmental stages: free-living females (FL Female), post-free-living first-stage larvae (PFL L1), infectious third-stage larvae (L3i), *in vivo* activated third-stage larvae (L3+), parasitic females (P Female), post-parasitic first-stage larvae (PP L1), and post-parasitic third-stage larvae (PP L3). Transcript abundances were calculated as fragments per kilobase of coding exon per million mapped reads (FPKM) and log transformed. Error bars represent 95% confidence intervals. The y-axes were scaled from 0 to 3.5 to aid comparison between genes.

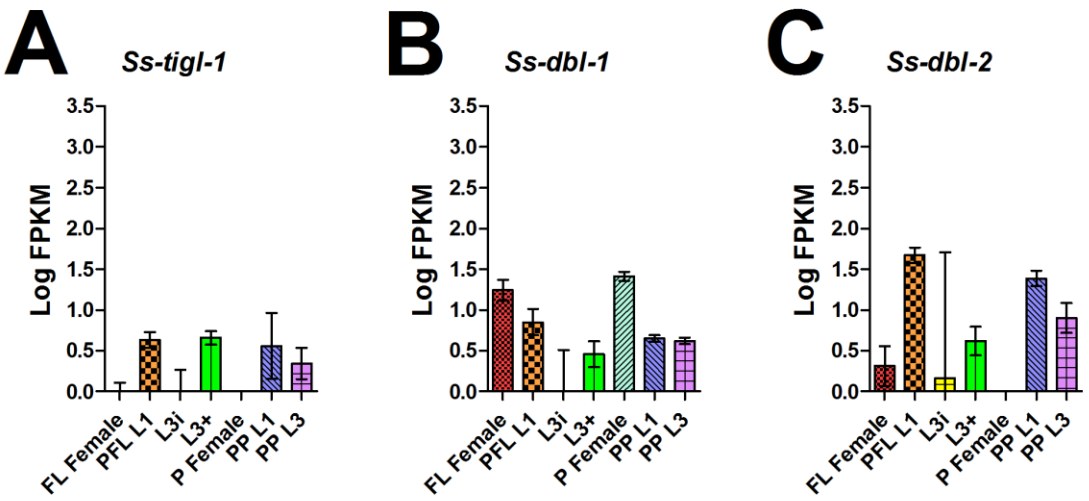

Figure 2.S11. Developmental regulation of additional *S. stercoralis* TGFβ ligand transcripts. The *S. stercoralis* genome contains three TGFβ super-family ligands that do not group with the human TGFβ1 and *Ce*-DAF-7 family: (A) *Ss-tigl-1*, a gene encoding a homolog of *Ce*-TIG-2, a TGFβ ligand that does not have any known biological function or receptor; (B) *Ss-dbl-1*, a gene encoding a homolog of *Ce*-DBL-1, a TGFβ ligand homolog of *D. melanogaster* decapentaplegic (DPP) and vertebrate bone morphogenetic protein (BMP), which signals through the small body size and male tail abnormal (Sma/Mab) pathway; and (C) *Ss-dbl-2*, a gene encoding a homolog of the *Ce*-UNC-129 TGFβ ligand that regulates cell migration and axon guidance and acts independently of type I or type II receptors. Transcript abundances were quantified in seven developmental stages: free-living females (FL Female), post-free-living first-stage larvae (PFL L1), infectious third-stage larvae (L3i), *in vivo* activated third-stage larvae (L3+), parasitic females (P Female), post-parasitic first-stage larvae (PP L1), and post-parasitic third-stage larvae (PP L3). Transcript abundances were calculated as fragments per kilobase of coding exon per million mapped reads (FPKM) and log transformed. Error bars represent 95% confidence intervals. The y-axes were scaled from 0 to 3.5 to aid comparison between genes.

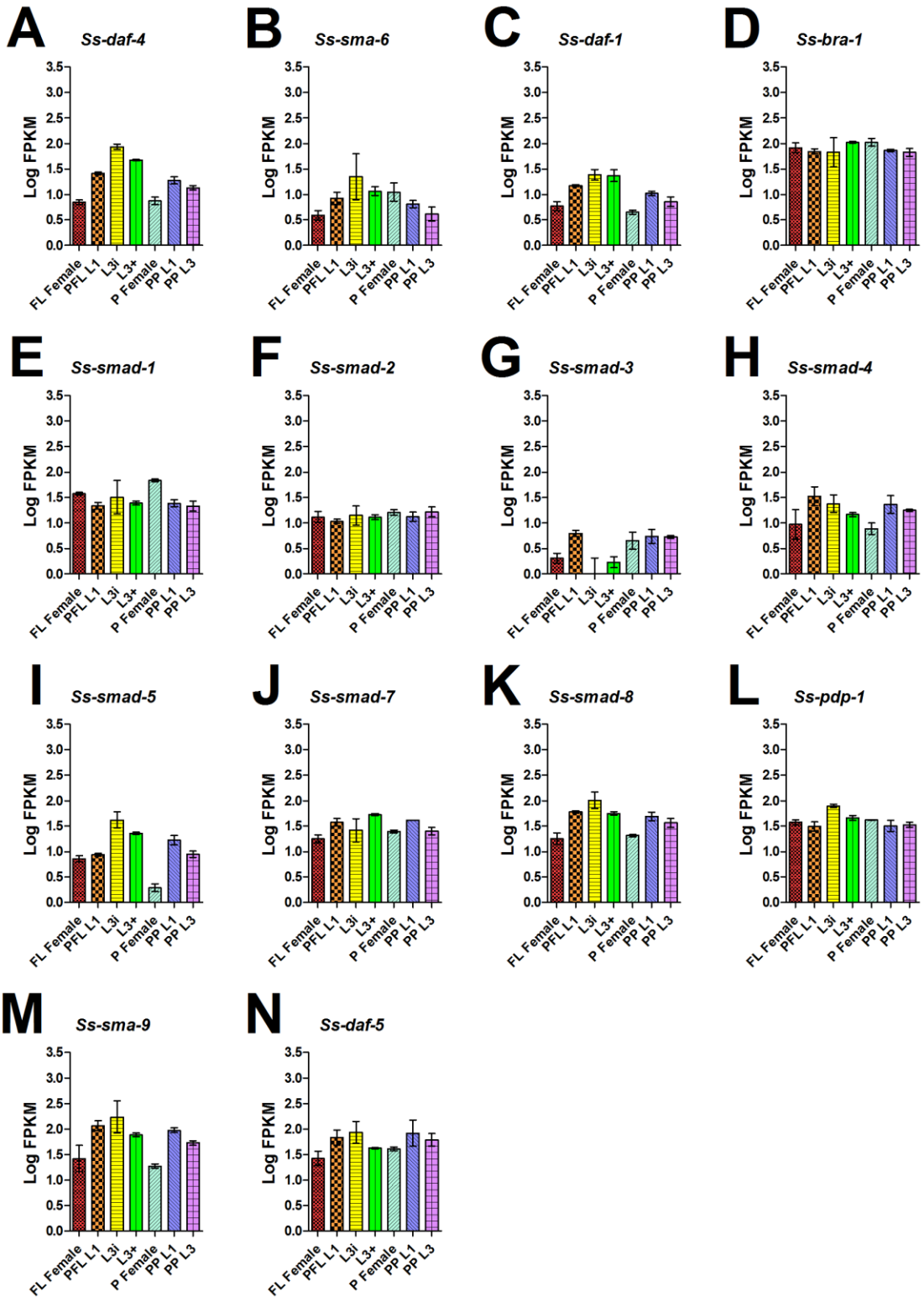
A
Ss-daf-4
B
Ss-sma-6
C
Ss-daf-1
D
Ss-bra-1
E
Ss-smad-1
F
Ss-smad-2
G
Ss-smad-3
H
Ss-smad-4
I
Ss-smad-5
J
Ss-smad-7
K
Ss-smad-8
L
Ss-pdp-1
M
Ss-sma-9
N
Ss-daf-5
Log FPKM
0.0
0.5
1.0
1.5
2.0
2.5
3.0
3.5
FL Female
PFL L1
L3i
L3+
P Female
PP L1
PP L3

Figure 2.S12. Developmental regulation of TGFβ signaling homologs in *S. stercoralis*.
Developmental expression patterns were assessed for members of both the dauer and small body size and male tail abnormal (Sma/Mab) TGFβ pathways: (A) *Ss-daf-4*, a gene encoding a homolog of the type II receptor *Ce*-DAF-4; (B) *Ss-sma-6*, a gene encoding a homolog of the Sma/Mab type I receptor *Ce*-SMA-6; (C) *Ss-daf-1*, a gene encoding a homolog of the dauer type I receptor *Ce*-DAF-1; (D) *Ss-bra-1*, a gene encoding a homolog of the *Ce*-DAF-1 negative regulator *Ce*-BRA-1; (E) *Ss-smad-1*, a gene encoding a SMAD similar to *Ce*-DAF-14; (F) *Ss-smad-2*, (G) *Ss-smad-3*, and (H) *Ss-smad-4*, genes encoding SMAD homologs similar to *Ce*-SMA-2, *Ce*-SMA-3, and *Ce*-SMA-4, respectively; (I) *Ss-smad-5*, (J) *Ss-smad-7*, and (K) *Ss-smad-8*, genes encoding SMAD homologs similar to *Ce*-DAF-3 and *Ce*-DAF-8; (L) *Ss-pdp-1*, a gene encoding a homolog of the phosphatase *Ce*-PDP-1; (M) *Ss-sma-9*, a gene encoding a homolog of the Sma/Mab transcriptional co-factor *Ce*-SMA-9; and (N) *Ss-daf-5*, a gene encoding a Sno/Ski transcription factor homolog similar to *Ce*-DAF-5. Transcript abundances were quantified in seven developmental stages: free-living females (FL Female), post-free-living first-stage larvae (PFL L1), infectious third-stage larvae (L3i), *in vivo* activated third-stage larvae (L3+), parasitic females (P Female), post-parasitic first-stage larvae (PP L1), and post-parasitic third-stage larvae (PP L3). Transcript abundances were calculated as fragments per kilobase of coding exon per million mapped reads (FPKM) and log transformed. Error bars represent 95% confidence intervals. The y-axes were scaled from 0 to 3.5 to aid comparison between genes.

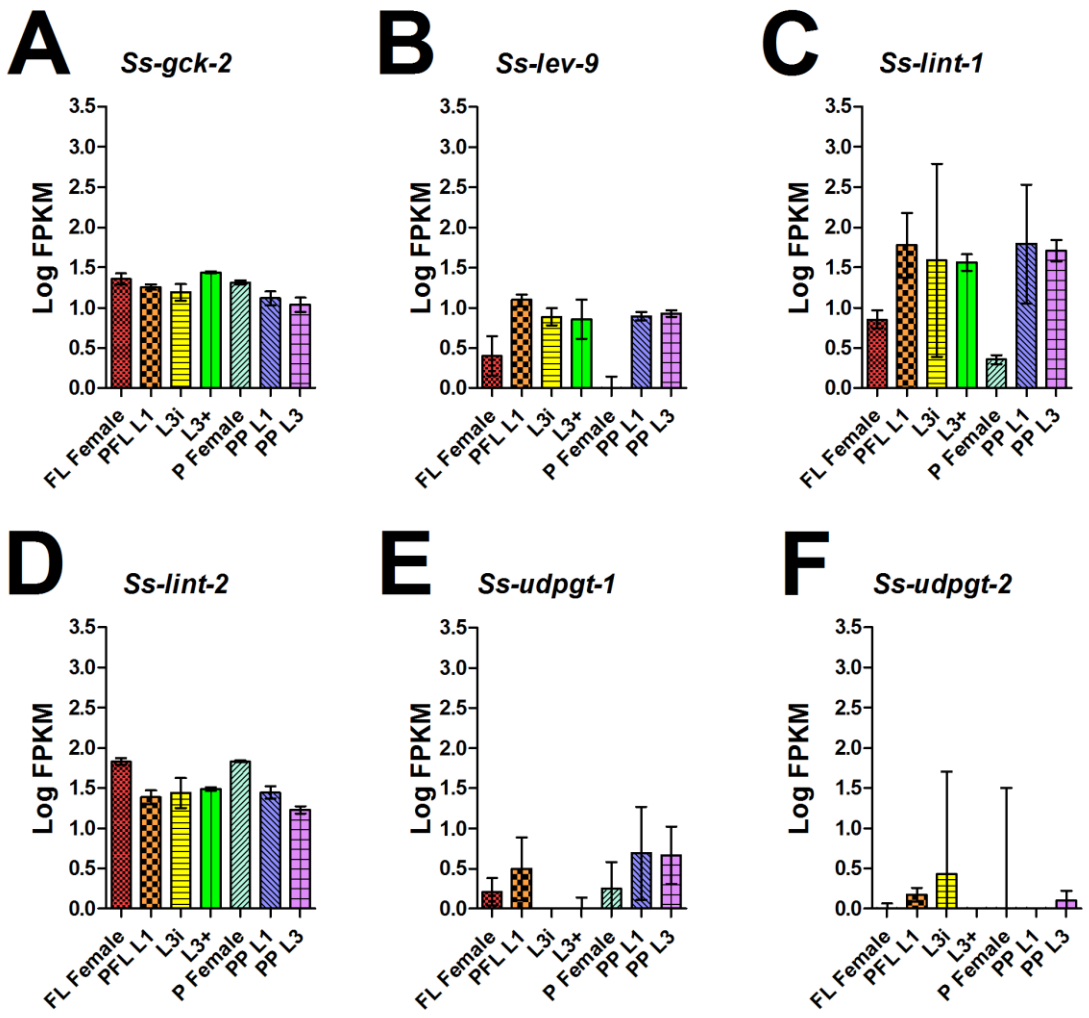

Figure 2.S13. Developmental regulation of *S. stercoralis* homologs of *Ce*-DAF-12-regulated genes. Transcript abundances of *S. stercoralis* homologs of *C. elegans* genes transcriptionally regulated directly by *Ce*-DAF-12 during dauer development were examined: (A) *Ss-gck-2*, a gene encoding a homolog of *Ce*-GCK-2; (B) *Ss-lev-9*, a gene encoding a homolog of *Ce*-LEV-9; (C) *Ss-lint-1* and (D) *Ss-lint-2*, genes encoding homologs of *Ce*-LIT-1; and (E) *Ss-udpgt-1* and (F) *Ss-udpgt-2*, genes encoding homologs of *Ce*-UGT-65. Transcript abundances were quantified in seven developmental stages: free-living females (FL Female), post-free-living first-stage larvae (PFL L1), infectious third-stage larvae (L3i), *in vivo* activated third-stage larvae (L3+), parasitic females (P Female), post-parasitic first-stage larvae (PP L1), and post-parasitic third-stage larvae (PP L3). Transcript abundances were calculated as fragments per kilobase of coding exon per million mapped reads (FPKM) and log transformed. Error bars represent 95% confidence intervals. The y-axes were scaled from 0 to 3.5 to aid comparison between genes.

2.7 Tables

Table 2.1. Comparison of cGMP signaling pathway homologs and transcript abundances in *S. stercoralis* and *C. elegans*.

C. elegans gene(s)	*S. stercoralis* homolog(s)	*S. stercoralis* transcript abundance profile	Regulation consistent with *C. elegans* (+, +/-, -)[1]
Ce-gpa-2 & -3	*Ss-gpa-2* & *-3*	peak in L3i	+
Ce-daf-11	*Ss-gcy-11*[2]	peak in L3i and L3+	+
Ce-tax-2	*Ss-tax-2*	peak in L3i	+
Ce-tax-4	*Ss-tax-4*	peak in L3i	+

[1] (+) similar, (+/-) unclear, and (-) dissimilar transcript abundance patterns.
[2] Homology is by phylogenetic similarity only.

Table 2.2. Comparison of IIS pathway homologs and transcript abundances in *S. stercoralis* and *C. elegans*.

C. elegans gene(s)	*S. stercoralis* homolog(s)	*S. stercoralis* transcript abundance profile	Regulation consistent with *C. elegans* (+, +/-, -)[1]
Insulin-like Peptides			
Type α: *Ce-ins -20* to *-30*, and *-33* to *-36*	None identified		
Type β: *Ce-daf-28*, and *Ce-ins -1* to *-10*	*Ss-ilp-3*	present in all stages examined	+/-
	Ss-ilp-4	decreased in FL and P Females	+/-
	Ss-ilp-6	increased from L3i to L3+	+
Type γ: *Ce-ins-11* to *-19, -31, -32,* and *-37*	*Ss-ilp-1*	decreased in PFL generation	+
	Ss-ilp-7	increased in L3i and L3+	+
Type δ: None	*Ss-ilp-2* & *-5*	present in all stages examined	+/-
Intracellular signaling components			
Ce-asna-1	*Ss-asna-1*	present in all stages examined	+
Ce-daf-2	*Ss-daf-2*	increased in PFL generation	+
Ce-ist-1	*Ss-ist-1* & *-2*	present in all stages examined	+
Ce-aap-1	*Ss-aap-1*	increased in FL and P Females	+
Ce-age-1	*Ss-age-1*	increased in L3+	+
Ce-daf-18	*Ss-pten-1* & *-2*	present in all stages examined	+
Ce-pdk-1	*Ss-pdk-1*	increased in L3i	+
Ce-sgk-1	*Ss-sgk-1*	absent in L3i and L3+	-
Ce-akt-1* and *-2	*Ss-akt-1*	increased in L3i and L3+	+/-
***Ce-pptr-1*[2]**	*Ss-pptr-1*	present in all stages examined	+
Ce-ftt-2	*Ss-ftt-2*	present in all stages examined	+
Ce-daf-16	*Ss-daf-16*	decreased in FL and P Females	+/-
Ce-DAF-16 regulated genes			
***Ce-sod-3*[3]**	*Ss-sod-1*	present in all stages examined	-
Ce-daf-15	*Ss-daf-15*	present in all stages examined	-
Ce-acs-19	*Ss-acs-19*	present in all stages examined	-
Ce-ldb-1	*Ss-limdb-1* & *-2*	present in all stages examined	-
Ce-pitp-1	*Ss-pitp-1*	present in all stages examined	-
Ce-Y105E8B.9	*Ss- Y105E8B.9*	increased in developing larvae	+/-

[1] (+) similar, (+/-) unclear, and (-) dissimilar transcript abundance patterns.

[2] A homolog for the closely related gene *Ce-pptr-2* was identified and termed *Ss-pptr-2*.

[3] The closely related gene *Ce-sod-2* was accounted for; only one *sod* gene was identified in *S. stercoralis*.

Table 2.3. Comparison of dauer TGFβ signaling pathway homologs and transcript abundances in *S. stercoralis* and *C. elegans*.

C. elegans gene(s)	*S. stercoralis* homolog(s)	*S. stercoralis* transcript abundance profile	Regulation consistent with *C. elegans* (+, +/-, -)[1]
Ce-daf-7[2]	*Ss-tgh-1* to *-3*	L3i only	-
	Ss-tgh-4 & *-5*	not present in stages examined	+/-
	Ss-tgh-6	increased from PFL L1 to L3+	-
	Ss-tgh-7	not present in FL or P Females	+/-
Ce-daf-1	*Ss-daf-1*	increased in L3i and L3+	-
Ce-daf-4[3]	*Ss-daf-4*	increased in L3i	-
Ce-bra-1	*Ss-bra-1*	present in all stages examined	+/-
Ce-daf-3, -8, & -14[4]	*Ss-smad-1*	present in all stages examined	+/-
	Ss-smad-5	decreased in P Females	+/-
	Ss-smad-7	present in all stages examined	+/-
	Ss-smad-8	decreased in FL and P Females	+/-
Ce-pdp-1	*Ss-pdp-1*	present in all stages examined	+/-
Ce-daf-5[5]	*Ss-daf-5*	present in all stages examined	+/-

[1] (+) similar, (+/-) unclear, and (-) dissimilar transcript abundance patterns.

[2] Homologs for the *Ce-dbl-1*, *Ce-unc-129*, and *Ce-tig-2* were identified and termed *Ss-dbl-1*, *Ss-dbl-2*, and *Ss-tigl-1*, respectively.

[3] A homolog for the related gene *Ce-sma-6* was identified and termed *Ss-sma-6*.

[4] Homologs for *Ce-sma-2*, *Ce-sma-3*, and *Ce-sma-4* were identified and termed *Ss-smad-2*, *Ss-smad-3*, and *Ss-smad-4*, respectively.

[5] A homolog for *Ce-sma-9* was identified and termed *Ss-sma-9*.

Table 2.4. Comparison of NHR pathway homologs and transcript abundances in *S. stercoralis* and *C. elegans*.

C. elegans gene(s)	*S. stercoralis* homolog(s)	*S. stercoralis* transcript abundance profile	Regulation consistent with *C. elegans* (+, +/-, -)[1]
Dafachronic acid biosynthesis			
Ce-ncr-1 & -2	*Ss-ncr-1*	decreased in P Females	+/-
Ce-daf-36	*Ss-daf-36*	decreased in L3i and L3+	+/-
Ce-dhs-16	*Ss-scdh-16*[2]	decreased from L3i to L3+	-
Ce-daf-9	*Ss-cyp-9*[2]	decreased in FL and P Females	-
Ce-emb-8	*Ss-emb-8*	present in all stages examined	+/-
Ce-strm-1	*Ss-strm-1*	decreased from L3i to L3+	+
Nuclear hormone receptor			
Ce-daf-12	*Ss-daf-12*	peak in L3i	+
Ce-din-1	Not identified		
Ce-DAF-12 regulated genes			
Ce-gck-2	*Ss-gck-2*	present in all stages examined	-
Ce-lev-9	*Ss-lev-9*	decreased in FL and P Females	-
Ce-lit-1	*Ss-lint-1*	decreased in FL and P Females	-
	Ss-lint-2	present in all stages examined	-
Ce-ugt-65	*Ss-udpgt-1*	not present in L3i or L3+	+
	Ss-udpgt-2	low expression, peak in L3i	-

[1] (+) similar, (+/-) unclear, and (-) dissimilar transcript abundance patterns.

[2] Homology is by phylogenetic similarity only.

CHAPTER 3 - *Strongyloides stercoralis age-1*: A Potential Regulator of Infective Larval Development in a Parasitic Nematode

The contents of this chapter has been published as:

Stoltzfus JD, Massey HC, Jr., Nolan TJ, Griffith SD, Lok JB (2012) *Strongyloides stercoralis age-1*: a potential regulator of infective larval development in a parasitic nematode. PLoS ONE 7(6): e38587. doi:10.1371/journal.pone.0038587

3.1 Abstract

Infective third-stage larvae (L3i) of the human parasite *Strongyloides stercoralis* share many morphological, developmental, and behavioral attributes with *Caenorhabditis elegans* dauer larvae. The 'dauer hypothesis' predicts that the same molecular genetic mechanisms control both dauer larval development in *C. elegans* and L3i morphogenesis in *S. stercoralis*. In *C. elegans*, the phosphatidylinositol-3 (PI3) kinase catalytic subunit AGE-1 functions in the insulin/IGF-1 signaling (IIS) pathway to regulate formation of dauer larvae. Here we identify and characterize *Ss-age-1*, the *S. stercoralis* homolog of the gene encoding *C. elegans* AGE-1. Our analysis of the *Ss-age-1* genomic region revealed three exons encoding a predicted protein of 1,209 amino acids, which clustered with *C. elegans* AGE-1 in phylogenetic analysis. We examined temporal patterns of expression in the *S. stercoralis* life cycle by reverse transcription quantitative PCR and observed low levels of *Ss-age-1* transcripts in all stages. To compare anatomical patterns of expression between the two species, we used *Ss-age-1* or *Ce-age-1* promoter*::enhanced green fluorescent protein* reporter constructs expressed in transgenic animals for each species. We observed conservation of expression in amphidial neurons, which play a critical role in developmental regulation of both dauer larvae and L3i. Application of the PI3 kinase inhibitor LY294002 suppressed L3i *in vitro* activation in a dose-dependent fashion, with 100 μM resulting in a 90% decrease (odds ratio: 0.10, 95% confidence interval: 0.08-0.13) in the odds of resumption of feeding for treated L3i in comparison to the control. Together, these data support the hypothesis that *Ss-age-1* regulates the development of *S. stercoralis* L3i via an IIS pathway in a manner similar to that observed in *C. elegans* dauer larvae. Understanding the mechanisms by which infective larvae are formed and activated may lead to novel control measures and treatments for strongyloidiasis and other soil-transmitted helminthiases.

3.2 Introduction

Helminth infections represent a vast global burden of disease, with parasitic nematodes infecting more than one billion people [5,210]. The infectious form of many parasitic nematodes, including the medically relevant species which cause strongyloidiasis, filariasis, and hookworm disease [2], is the third-stage larva (L3i). L3i developmentally arrest, sometimes for months, before resuming development upon encountering a host [1,2]. Despite their potential as new therapeutic targets, the signaling proteins and pathways controlling developmental arrest and activation of L3i are unknown.

Our lab has employed *Strongyloides stercoralis*, a parasitic nematode infecting nearly 100 million people [5,211], as a model to study molecular mechanisms in parasitic nematodes, and we have developed methods for transgenesis that are unavailable in other species [10,78,90]. Study of *S. stercoralis* is facilitated by a life cycle that includes both parasitic and free-living generations, allowing us to probe factors driving L3i development in an otherwise "obligately parasitic" group of organisms [10,208]. In *S. stercoralis*, L3i form conditionally in the post-parasitic generation (homogonic development), along with free-living males and females (heterogonic development), and constitutively in the post-free-living generation [8]. This life cycle provides a unique opportunity to interrogate the mechanisms governing L3i formation and activation.

A similar developmentally arrested stage, the dauer larva, is formed by the free-living nematode *Caenorhabditis elegans* in response to unfavorable conditions [13,23]. Interestingly, *C. elegans* dauer larvae and *S. stercoralis* L3i arrest at the same third larval stage and share similar characteristics of morphology, extended lifespan, stress-resistance, and cessation of feeding [25,108]. Dauer larvae and L3i resume development soon after encountering favorable environmental conditions or the definitive host, respectively [8,30]. The "dauer hypothesis" proposes that the molecular mechanisms governing L3i developmental arrest and recovery in *S. stercoralis* and other parasitic nematodes are similar to those regulating dauer formation and recovery in *C. elegans* [13,24,212].

In *C. elegans*, the insulin/IGF-1 signaling (IIS) pathway plays a critical role in dauer formation and recovery. When environmental conditions are limiting, IIS signaling is suppressed, resulting in dauer arrest [213]. In response to favorable environmental cues [28,130], the IIS pathway is activated and promotes continuous growth and development. When IIS is activated via a muscarinic agonist [67], insulin-like peptides are secreted [138,144] and bind the insulin-like receptor DAF-2 [213]. DAF-2 agonists [138,144,147,149] activate the

phosphatidylinositol-3 (PI3) kinase [214], a heterodimer composed of an AGE-1 catalytic subunit [215] and an AAP-1 accessory/regulatory subunit [156]. PI3 kinase activation triggers a signaling cascade resulting in phosphorylation of the forkhead transcription factor DAF-16, which ultimately causes its removal from the nucleus [85,216]. Loss-of-function alleles for both *daf-2* and *age-1* result in a constitutive dauer arrest phenotype, while *daf-16* mutations result in a dauer defective phenotype, demonstrating the importance of IIS for regulating dauer development [217].

Members of the IIS pathway have been cloned from several parasitic nematodes [80,81,83], including *S. stercoralis*, but it remains unclear whether they comprise a pathway controlling the developmental arrest and activation of L3i. Recent studies in our lab have demonstrated that the *S. stercoralis* DAF-16 homolog is required for normal arrest of L3i under conditions of decreased IIS [78]; however, it is unknown whether the IIS pathway also regulates developmental activation of L3i in the host through increased IIS. Since *Ce-age-1* is the main mediator of increased IIS signaling from the *Ce-daf-2* insulin-like receptor to the downstream *Ce-daf-16* forkhead transcription factor [218], we endeavored to clone and characterize the *S. stercoralis* homolog of *Ce-age-1*. Here we present striking similarities between *Ce-age-1* and *Ss-age-1* as well as the first evidence of IIS regulating L3i activation in *S. stercoralis*.

3.3 Materials and Methods

Ethics statement

No human subjects were used in these studies. The *S. stercoralis* UPD strain and PV001 line were maintained in prednisolone-treated beagles in accordance with protocols 702342, 801905, and 802593 approved by the University of Pennsylvania Institutional Animal Care and Use Committee (IACUC). Experimental infections of *S. stercoralis* were conducted in Mongolian gerbils under the same IACUC-approved protocols, and animals were sacrificed by CO_2 asphyxia in accordance with standards established by the American Veterinary Medical Association. All IACUC protocols, as well as routine husbandry care of the animals, were carried out in strict accordance with the *Guide for the Care and Use of Laboratory Animals of the National Institutes of Health*.

S. stercoralis and *C. elegans* strains and maintenance

The *S. stercoralis* UPD strain was maintained and cultured as previously described [9,10,114]. UPD strain free-living adults for DNA transformation and RNA extraction were isolated via the Baermann technique from two-day-old charcoal coprocultures incubated at 22°C. UPD strain L3i for genomic DNA and *in vitro* activation were isolated via the Baermann technique from seven-day-old charcoal coprocultures incubated at 25°C.

The *S. stercoralis* isofemale line PV001 was derived from the UPD strain as a line with limited genetic variability. To derive this line, virgin free-living females were prepared by placing one first-stage larva, freshly isolated from the feces of a dog infected with the UPD strain, into each well of a 96 well tissue culture plate. The plate had been prepared by placing 50 µl of 1% agar (Lonza, Basel, Switzerland) into each well and then adding a small (several mg) piece of normal dog feces to the surface. After three days, two of the 96 wells contained an adult female and larval progeny. The mechanism by which progeny arise in the absence of mating in the free living generation is unknown. However, *S. stercoralis* parasitic females are presumed to reproduce by mitotic parthenogenesis [219,220], and it is possible that this phenomenon occurs at a low frequency among free-living females as well. At six days post plating, 34 L3i were removed from one of the positive wells and used to infect a gerbil. The gerbil was given 2 mg methylprednisolone acetate (SQ) at the time of infection and weekly thereafter [114]. L3i recovered from coprocultures made from this gerbil's feces were used to infect another gerbil and the L3i recovered from coprocultures of this second gerbil's feces were used to infect the dog from which feces were isolated for use in the RT-qPCR study.

C. elegans N2 worms were maintained by standard methods [116]. The CY246 strain, *age-1(mg44); sqt-1(sc13) / mnC1 dpy-10(e128); unc-52(e444)* II, a gift from Catherine Wolkow, was maintained by picking phenotypically wild-type (WT) worms. The *age-1*$^{-/-}$ F1 progeny in this strain, which are marked in *cis* with the *sqt-1* roller phenotype and exhibit maternal rescue, produce F2 progeny that constitutively form roller dauers. The BC10837 strain [143], *dpy-5(e907)* I, sEx10837 [rCesB0334.8::GFP + pCeh361], was obtained from the *Caenorhabditis* Genetics Center (University of Minnesota, Minneapolis, Minnesota, USA) and maintained by picking GFP-positive phenotypically WT worms.

DNA and cDNA preparation

Genomic DNA from the *S. stercoralis* UPD strain was isolated from L3i by phenol/chloroform extraction [90]. UPD strain RNA for cDNA synthesis was isolated from free-living adults by TRIzol reagent extraction (Life Technologies, Grand Island, New York, USA);

total cDNA was synthesized using SuperScript III reverse transcriptase and an oligo dT primer (Life Technologies) following the manufacturer's protocol. cDNA with ligated adapters for 5' and 3' RACE was prepared using the GeneRacer kit (Life Technologies).

For *C. elegans* genomic DNA preparations, starved plates of N2 worms were washed and DNA extracted using the DNeasy Blood and Tissue kit (Qiagen, Valencia, California, USA). RNA for cDNA synthesis was isolated from mixed-stage plates of N2 worms and cDNA synthesized by the same methods as for *S. stercoralis*.

Cloning of *S. stercoralis* genes

The genomic sequence of *Ss-age-1* was determined using degenerate primers to amplify a coding sequence homologous to a *Parastrongyloides trichosuri* EST (GenBank: BI742945), which was identified by BLAST searches of the nematode EST database (http://nematode.net/NN3_frontpage.cgi?navbar_selection=nemagene&subnav_selection=nemablast) with the *Ce*-AGE-1 sequence (GenBank: AAC47459). Repeated cycles of inverse PCR and established methods were used to determine the complete coding sequence as well as sequences of the 5' and 3' regions of *Ss-age-1* (GenBank: JQ772018) [76,80,88]. Both 5' and 3' RACE were performed using the GeneRacer protocol (Life Technologies) and Phusion polymerase (New England BioLabs, Ipswich, Massachusetts, USA). 5' RACE used the Ss-age-1-17R outer primer and Ss-age-1-20R nested primer; 3' RACE used the Ss-age-1-20F outer primer and Ss-age-1-11F nested primer. Genomic DNA and RACE PCR products were cloned using the Zero Blunt TOPO PCR cloning kit (Life Technologies) and sequenced in triplicate. The full-length *Ss-age-1* cDNA was amplified from total cDNA with Phusion polymerase (New England BioLabs) using the Ss-age-1-24FattB1 and Ss-age-1-24RstopattB2 primers, while 1.3 kb of 5' region was amplified using the Ss-age-1-23FattB4 and Ss-age-1-23RattB1r primers. The 1,327 bp 5' region (pPV450) and 3,630 bp *Ss-age-1* cDNA (pPV451) were cloned into pDONR P4-P1R and pDONR221, respectively, using Gataway recombination (Life Technologies).

The genomic sequence of *Ss-aap-1* (GenBank: JQ781500) was PCR amplified using degenerate primers for the *Strongyloides ratti* sequence, identified by BLAST searches of the *S. ratti* genome database (http://www.sanger.ac.uk/resources/downloads/helminths/strongyloides-ratti.html) with the *Ce*-AAP-1 (NCBI: NM_059121) sequence. This PCR product was cloned into pCR-Blunt II-TOPO and sequenced. Similar to *Ss-age-1*, 5' RACE of *Ss-aap-1* was performed using the Ssaap1-2R outer primer and Ssaap1-3R nested primer, with the product cloned into pCR-Blunt II-TOPO and sequenced in triplicate.

For both *Ss*-AGE-1 and *Ss*-AAP-1, protein domains were determined using BLASTp searches through NCBI's Conserved Domain Database service (http://blast.ncbi.nlm.nih.gov/Blast.cgi) [118]. Protein coding sequences for *S. ratti age-1* and *aap-1* homologs were identified by manual annotation of the respective *S. ratti* contigs. The close homology of the predicted peptides and conservation of introns between *S. ratti* and *S. stercoralis* aided this process.

Phylogenetic analysis

A protein alignment of PI3 kinase catalytic subunits was generated using Clustal X2 [221] and a BLOSUM62 matrix. A neighbor-joining tree was constructed using MEGA version 4.0 [222] with bootstrapping scores (1000 iterations) shown for robust clades (>50% cutoff). A global protein alignment between *Ce*-AGE-1 and *Ss*-AGE-1 was performed using EMBOSS Needle and a BLOSUM62 matrix [223] and was annotated for coding exons to determine conservation of introns between *Ss-age-1* and *Ce-age-1*. Accession numbers were: *Strongyloides stercoralis* (GenBank: JQ772018), *Strongyloides ratti*, *Parastrongyloides trichosuri* AGE-1 (GenBank: ADN44511), *Brugia malayi* PI3K (NCBI: XP_001902593), *Caenorhabditis briggsae* AGE-1 (NCBI: XP_002631094), *Caenorhabditis elegans* AGE-1 (GenBank: AAC47459), *Homo sapiens* PI3KCA (GenBank: AAI13604), *Drosophila melanogaster* Pi3K92E (NCBI: NP_650902), *Drosophila melanogaster* Pi3K59F (NCBI: NP_477133), *Homo sapiens* PI3KC3 (NCBI: NP_002638), *Caenorhabditis elegans* VPS-34 (NCBI: NP_491741), *Saccharomyces cerevisiae* VPS34 (NCBI: NP_013341), *Drosophila melanogaster* Pi3K68D (NCBI: NP_524028), *Caenorhabditis elegans* F39B1.1 (NCBI: NP_510529), and *Homo sapiens* PI3KC2A (NCBI: NP_002636).

A protein alignment of PI3 kinase accessory/regulatory subunits using Clustal W and a BLOSUM matrix was generated using Geneious version 5.5.6 [117] and was annotated for coding exons to determine conservation of introns between *Ss-aap-1* and *Ce-aap-1*. A global protein alignment between *Ce*-AAP-1 and *Ss*-AAP-1 was performed using EMBOSS Needle and a BLOSUM62 matrix [223]. Accession numbers were: *Strongyloides stercoralis* AAP-1 (GenBank: JQ781500), *Strongyloides ratti* AAP-1, *Caenorhabditis elegans* AAP-1 (NCBI: NM_059121), *Trichinella spiralis* AAP-1 (GenBank: EFV56516), *Brugia malayi* AAP-1 (GenBank: EDP31759), *Ascaris suum* AAP-1 (GenBank: ADY45992), *Drosophila melanogaster* PI3K-21b (GenBank: CAA73100), and *Homo sapiens* PI3K-p85a (UniProtKB: P27986).

RT-qPCR

Developmental stages of *S. stercoralis* line PV001 were isolated for RT-qPCR as previously described [80], washed, and rendered free of fine particle debris by migration through agarose [115] into BU buffer [116]. Worms were snap-frozen in TRIzol reagent (Life Technologies) in liquid nitrogen; total RNA was extracted using the manufacturer's protocol. Purified RNA was quantified using the Bioanalyzer 2100 (Agilent Technologies, Inc., Santa Clara, California, USA) and only samples with an RNA integrity number greater than 8.0 were used.

Gene specific primer sets, which only amplified spliced cDNA, included Ss-age-1RT-3F and -R, Ss-act2RT-2F and -R, and Ss-gapdhRT-2F and -R [90,99,224]. Primer sets were calibrated using a five dilution series of total RNA and efficiencies calculated using standard methods [225]. Gene specific RT-qPCR was performed on three biological replicates, each in duplicate, using the Brilliant II SYBR Green QRT-PCR kit (Agilent Technologies) with 50 ng of total RNA on an Applied Biosystems 7500 (Life Technologies) instrument with the following parameters: RT step of 30 min at 50°C; 10 min at 95°C; and 40 cycles of 30 sec at 95°C and 60 sec at 60°C (detection step); followed by a melting temperature curve. Controls omitting template or reverse transcriptase were also included.

Results were analyzed by computing the mean Ct value for each replicate. Abundances were calculated using the slope of the calibration curve and normalizing to an arbitrarily determined mean of 10 copies of *Ss-age-1* in free-living females [224,225]. Log transformed values, + 1 SEM, were plotted in Prism version 5.03 (GraphPad Software, Inc., La Jolla, California, USA).

Plasmid construction

Plasmids containing *Ce-age-1* promoter and *egfp* reporter constructs were assembled by overlap extension PCR. The construct *Ce-age-1p::egfp::Ce-tbb-2t*, contained in plasmid pPV452, was assembled in two steps. The 866 bp of *Ce-age-1* 5' region was PCR amplified using *C. elegans* genomic DNA as a template. The 870 bp *egpf* coding region, including introns, and 333 bp of the *Ce-tbb-2* 3' region (terminator) were amplified using pJA257 as template (Addgene, Cambridge, Massachusetts, USA). These PCR products were fused by overlap extension PCR using the overlapping primers Ce-age-1-EGFP-F and -R. The product was cloned into pUC19 (New England Biolabs) and the insert fully sequenced.

The construct *Ce-age-1p::Ce-age-1(102bp)::egfp::Ce-age-1t*, contained in plasmid pPV455, was assembled by a similar scheme. The 919 bp segment of *Ce-age-1* 5' region, including the first 102 bp of the *Ce-age-1* coding sequence, was PCR amplified using *C. elegans* genomic DNA as a template. The 870 bp *egfp* coding sequence, with introns, was PCR amplified using pJA257 as a template. A 1,071 bp segment of *Ce-age-1* 3' region (terminator) was PCR amplified using genomic DNA as a template. These three segments were joined using the overlapping primers Ex10837-EGFP-F and -R and EGFP-Ceage1t-F and -R, the product T/A cloned into the pCR-TOPO-XL vector (Life Technologies), and the insert fully sequenced.

The construct *Ce-age-1p::Ce-age-1(3,549bp)::Ce-unc-54t*, contained in plasmid pPV454, was assembled by a similar process. An 873 bp segment of *Ce-age-1* 5' region was amplified from genomic DNA and fused to 2,376 bp of the 5' region of *Ce-age-1*, amplified from cDNA, using the overlapping primers Ceage1p-cDNA-F and -R. This was subsequently fused to the remainder of the *Ce-age-1* cDNA with the plasmid Pdpy-30-age-1, a gift from Yuichi Iino [150], as template and using the overlapping primers Ceage1-Cat-F and -R. Finally, the promoter and full-length 3,549 bp *Ce-age-1* cDNA were fused to 765 bp of the *Ce-unc-54* 3' region (terminator), amplified from Pdpy-30-age-1 template, using the overlapping primers Ceage1-unc54-F and -R. The PCR product was T/A cloned into the pCR4-TOPO vector (Life Technologies) and the insert fully sequenced.

The construct *Ss-age-1p::egfp::Ss-era-1t*, contained in plasmid pPV453, was assembled by a similar process. A 1,326 bp segment of *Ss-age-1* 5' region was amplified from genomic DNA. The 870 bp *egfp* coding sequence, including introns, was amplified from pJA257. A 603 bp segment of *Ss-era-1* 3' region (terminator) was amplified from pAJ04 (Addgene). These three segments were fused using the overlapping primers Ss-age-1-EGFP-F and -R and EGFP-Ss-era-1-F and -R and cloned into pCR-Blunt II-TOPO with the insert fully sequenced.

Transformation of *C. elegans* and *S. stercoralis*

C. elegans N2 (WT) or CY246 (phenotypically WT) adult hermaphrodites were transformed by gonadal microinjection using standard techniques [226]. Plasmids were injected at a concentration of 20 ng/µl for *Ce-age-1p::egfp::Ce-tbb-2t* (pPV452) and *Ce-age-1p::Ce-age-1(102bp)::egfp::Ce-age-1t* (pPV455) along with 80 ng/µl non-coding pUC19 DNA. Transformations with *Ce-age-1p::Ce-age-1(3,549bp)::Ce-unc-54t* (pPV454) at 20 ng/µl included the *Ce-myo-2p::mCherry::Ce-unc-54t* (pCFJ90) (Addgene) co-injection marker at 2 ng/µl and 78 ng/µl pUC19. Injected hermaphrodites were transferred to NGM+OP50 plates and progeny

screened for fluorescence. Lines were established from single transformed F2 worms. The CY246+pPV454+pCFJ90 lines were assessed for dauer rescue by presence/absence of progeny from F1 rollers. The F2 roller progeny were subsequently passaged for more than 10 generations. Two lines of CY246 transformed with the co-injection marker pCFJ90, injected at 2 ng/µl and 98 ng/µl of pUC19, were used as a control.

S. stercoralis was transformed by gonadal micro-injection of adult free-living females as previously described [10]. A mix of 40 ng/µl *Ss-age-1p::egfp::Ss-era-1t* (pPV453) and 20 ng/µl *Ss-act-2::mRFPmars::Ss-era-1t* (pAJ50; Addgene) [90] was injected in females, which were then paired with an excess of adult males on an NGM+OP50 plate and incubated at 22°C. The F1 progeny were screened for fluorescence 48 and 72 hours after micro-injection.

C. elegans and *S. stercoralis* larvae were screened for expression of fluorescent reporter transgenes using an Olympus SZX12 stereomicroscope with coaxial epifluorescence. Transgenic *C. elegans* and *S. stercoralis* worms were examined in detail using an Olympus BX60 compound microscope equipped with Nomarski Differential Interference Contrast (DIC) optics and epifluorescence (Olympus America Inc., Center Valley, Pennsylvania, USA). Specimens were immobilized on a 2% agarose pad (Lonza), anesthetized using 10 mM levamisole (Sigma-Aldrich), and imaged with a Spot RT Color digital camera and Spot Advanced image analysis software (Diagnostic Instruments, Inc., Sterling Heights, Michigan, USA). Captured images were processed using GIMP version 2.6 (www.gimp.org).

***S. stercoralis* L3i *in vitro* activation**

In vitro activation of *S. stercoralis* L3i was performed as previously described [57,69] with the following adaptations. All conditions were supplemented with antibiotics (final concentration: 100 U/ml penicillin, 10 µg/ml streptomycin, and 12.5 µg/ml tetracycline). M9 buffer was used as the medium for the negative control [116].

DMEM (supplemented with L-glutamine, 4.5 g/L glucose, and sodium pyruvate) was used as the basal medium for the positive control and experimental conditions. The dimethyl sulfoxide (DMSO) (carrier) positive control and all experimental conditions had a final concentration of 10% naïve canine serum, 12.5 mM reduced glutathione (Sigma-Aldrich, St. Louis, Missouri, USA), and 1.3% DMSO (Sigma-Aldrich). Four concentrations of LY294002 (CAS registry number: 154447-36-6) (LC Laboratories, Woburn, Massachusetts, USA) were assessed: 500 µM, 100 µM, 50 µM, and 10 µM.

For the *in vitro* activation assay, L3i were isolated from seven-day-old charcoal coprocultures by the Baermann technique at 26°C. L3i were incubated in 100 µl aliquots of culture media at 37°C and 5% CO_2 for 21 hours, with three replicates for each condition. Cultures were then spiked with 2.5 µl fluorescein isothiocyanate (FITC) (20 mg/ml in dimethylformamide) and incubated an additional three hours for a total of 24 hours. L3i for each condition were pooled and washed five times in M9 buffer with low speed centrifugation. L3i were then mounted on glass slides with grease edged cover-slips, immobilized by a 15 second heat-shock at 60°C, and viewed by fluorescence microscopy. Only L3i with FITC in the pharynx were scored as "positive" for feeding.

Due to toxicity at 500 µM LY294002, resulting in greater than 50% death of L3i, this condition was discarded from the analysis. For all other conditions, greater than 90% of L3i were active at 24 hours. Data for five experiments were plotted, + 1 SEM, in Prism version 5.03 (GraphPad Software, Inc.). The relationship between condition and resumption of feeding was modeled using a generalized linear mixed-effects model and a logistic regression model, with condition as either a categorical predictor or a linear predictor. A logistic regression model with condition as a categorical predictor best described the data and was used to calculate the odds ratios, 95% confidence intervals, and p-values for each condition with respect to the DMSO control. All statistical models were fit using R version 2.14.1 [227].

3.4 Results and Discussion

Identification of *S. stercoralis age-1*

To identify the *S. stercoralis* homolog of *Ce-age-1*, we performed BLAST searches of the nematode expressed sequence tag (EST) database and found an EST with homology to *Ce-age-1* in *Parastrongyloides trichosuri*, a closely related parasitic nematode. We designed degenerate primers and amplified an *S. stercoralis* sequence from genomic DNA. Using successive rounds of inverse PCR, we elucidated the 3,999 base-pair (bp) genomic coding region for *Ss-age-1* along with 1.3 kilobase (kb) of the upstream sequence and 1.8 kb of the downstream sequence (GenBank: JQ772018). To determine the 5' and 3' ends of the *Ss-age-1* coding sequence, we performed rapid amplification of cDNA ends (RACE) using adapter-ligated cDNA. Subsequently, we cloned the 3,630 bp *Ss-age-1* coding sequence from cDNA derived from free-living adults (Figure 3.1A) and inferred a predicted peptide of 1,209 amino acids (Figure 3.1B). The locations of the three introns in *Ss-age-1* were not conserved in *Ce-age-1*.

Since *S. stercoralis* and *C. elegans* are members of nematode clades IV and V, respectively, their common ancestry is much more distant than their morphologic similarity suggests [109]. Therefore, we performed phylogenetic analysis to determine whether the predicted *Ss*-AGE-1 protein grouped with *Ce*-AGE-1. We obtained catalytic subunit sequences from public databases for class I, II, and III PI3 kinases found in a variety of metazoan organisms [228]. The predicted proteins were aligned, and a neighbor-joining phylogenetic tree was constructed (Figure 3.1C). In this analysis, *Ss*-AGE-1 grouped with other class I PI3 kinase catalytic subunits, including *Ce*-AGE-1. A global protein alignment of *Ss*-AGE-1 and *Ce*-AGE-1 demonstrated an overall 30.6% amino acid identity and 49.6% similarity. A search of the conserved domain database also revealed conservation of the five PI3 kinase catalytic subunit domains in *Ss*-AGE-1 [118,228]. Therefore, we conclude that *Ss-age-1* is indeed the homolog of *Ce-age-1*.

Identification of *S. stercoralis aap-1*

Functional PI3 kinases include both a catalytic subunit as well as an accessory/regulatory subunit, each encoded by a separate gene [228]. The PI3 kinase accessory/regulatory subunit in *C. elegans* has been identified as *Ce*-AAP-1 [156]. To identify the accessory/regulatory subunit for *Ss*-AGE-1, we BLAST-searched the *Strongyloides ratti* genome database for the homolog of *Ce*-AAP-1. We identified a putative *S. ratti* AAP-1 homolog and used degenerate primers to amplify a genomic region encoding *Ss*-AAP-1 from *S. stercoralis* genomic DNA.

Using the same protocol as for *Ss-age-1*, we performed 5' RACE and identified the coding sequence of *Ss-aap-1* (GenBank: JQ781500). The location of the single intron in *Ss-aap-1* was not conserved in *Ce-aap-1*. Protein alignment with other PI3 kinase accessory/regulatory subunits revealed close similarity to *Ce*-AAP-1 as well as conservation of both SH2 domains, which mediate binding to phosphorylated tyrosine residues on the activated insulin-like receptor [156,229] (Figure 3.S1). A global protein alignment of *Ss*-AAP-1 and *Ce*-AAP-1 demonstrated an overall 14.9% amino acid identity and 28.9% similarity. This analysis led us to conclude that the components of a functional PI3 kinase, consisting of an *Ss*-AGE-1 catalytic subunit and an *Ss*-AAP-1 accessory/regulatory subunit, are present in *S. stercoralis*.

***Ss-age-1* is expressed throughout the *S. stercoralis* life cycle**

In *C. elegans*, it is hypothesized that regulation of IIS is controlled transcriptionally at the level of the insulin-like peptides, while the cytoplasmic signaling components, including AGE-1,

are constitutively expressed. Low, but constitutive, expression of *Ce-age-1* has been noted in microarray analyses in both the various *C. elegans* developmental stages [143] and dauer recovery [124]. A recent study confirmed these findings through a careful quantitative examination of all *C. elegans* insulin-like peptides, *daf-2*, *age-1*, and *daf-16* transcripts in a variety of developmentally arrested and reproductively developing stages [122].

To determine whether *Ss-age-1* is transcriptionally regulated or constitutively expressed over the course of the *S. stercoralis* life cycle, we performed reverse transcription quantitative PCR (RT-qPCR) for six developmental stages. Transcript abundance was calculated for *Ss-age-1*, as well as two reference genes, *actin-2* (*Ss-act-2*) and *glyceraldehyde 3-phosphate dehydrogenase* (*Ss-gapdh*), using 50 ng of total RNA isolated from three biological replicates of each developmental stage. We calculated transcript abundances, which were normalized to an arbitrarily determined mean of 10 copies of *Ss-age-1* in free-living females and log transformed. We observed *Ss-age-1* expression at low, but consistent, levels in comparison to both *Ss-act-2* and *Ss-gapdh* for all life stages examined (Figure 3.2). Although expression of *Ss-age-1* was at its nadir in free-living females, the biological relevance of this difference is questionable, since similar levels of variability between developmental stages were also observed for *Ss-act-2* and *Ss-gapdh*. Overall, these data suggest that, like *Ce-age-1*, *Ss-age-1* is expressed at a low level throughout the course of the *S. stercoralis* life cycle. This is consistent with the hypothesis that IIS signaling through AGE-1 is regulated post-translationally and not at the transcriptional level.

Ce-age-1 and *Ss-age-1* have similar anatomical expression patterns

In *C. elegans*, expression of a *Ce-age-1* cDNA from either a pan-neuronal or intestinal promoter is sufficient to rescue the constitutive dauer arrest phenotype of strong *Ce-age-1* mutant alleles [230]. Thus, it is thought that IIS signaling in amphidial neurons and/or intestinal cells is important for regulating dauer arrest and activation. To determine whether anatomical expression of *Ss-age-1* was similarly regulated, we compared expression of transcriptional reporters under the control of putative promoters for *Ce-age-1* and *Ss-age-1*.

We first sought to determine the tissues in which *Ce-age-1* is expressed to serve as a basis for comparison to *Ss-age-1*. Previous work has reported expression of a *Ce-age-1* transcriptional reporter in amphidial neurons and the intestine, although the sole publicly available image of the BC10837 strain is limited to the head region of the worm [143,231]. To corroborate and expand these findings, we obtained the BC10837 strain and imaged first-stage larvae (L1) and adult hermaphrodites. In order to replicate the findings from the BC10837 strain,

we constructed two transgenic *C. elegans* lines, in the wild-type N2 background, that expressed enhanced green fluorescent protein (EGFP) driven by a *Ce-age-1* promoter with a *Ce-tbb-2* 3' sequence from extra-chromosomal arrays. To determine whether regulatory sequences for *Ce-age-1* expression were present in the first part of the coding sequence or the 3' region, three additional lines were transformed with a construct that fused the first 102 bp of *Ce-age-1* coding sequence to *egfp*, driven by the *Ce-age-1* promoter and using the native *Ce-age-1* 3' sequence.

In all six lines, we observed strong EGFP fluorescence in two pairs of amphidial neurons and their dendritic processes, a pair of inter-neurons or support cells anterior to the nerve ring, and the sphincter connecting the pharynx to the intestine (Figure 3.3A-D). We also noted variable expression in the hypodermis and the intestine between lines, with some lines having moderate expression in these tissues and others having little or no expression. Weak expression in a phasmidial neuron was observed in a minority of worms in each line. This led us to conclude that the main regulatory elements controlling anatomical expression of *Ce-age-1* are located in the putative promoter region and not in the 5' coding sequence or 3' region.

Intestinal fluorescence was often weak and punctate in all transgenic lines except BC10837, an observation consistent with auto-florescence or limited expression. Since intestinal expression in *C. elegans* is controlled by the ELT-2 transcription factor [232,233], we searched for extended TGATAA motifs in the 5' region of *Ce-age-1*. A single non-consensus motif at -289 bp was identified within 2 kb upstream of the *Ce-age-1* translation start site, potentially supporting our observation of weak intestinal expression. However, this observation does not preclude the possibility of distant enhancer regions that result in strong intestinal expression of *Ce-age-1* from its native locus *in vivo*.

To test the functionality of the *Ce-age-1* promoter region, we made a construct fusing the *Ce-age-1* promoter to a full-length *Ce-age-1* cDNA. We found that this construct was sufficient to fully rescue constitutive dauer arrest in two lines derived from the CY246 strain that carries the *Ce-age-1(mg44)* putative null allele. We were able to maintain these transgenic lines for more than 10 generations, indicating complete complementation. Thus, we concluded that we had identified the major tissues in which *Ce-age-1* is expressed, providing a consistent basis for comparison with *Ss-age-1*.

To determine the anatomical expression pattern of *Ss-age-1*, we transformed parental free-living *S. stercoralis* females with a construct fusing 1.3 kb of *Ss-age-1* 5' region to *egfp*, along with an *Ss-act-2p*::*mRFPmars* co-injection marker, as previously described [90]. Injected females were paired with *S. stercoralis* males, and their post-free-living L1 progeny were

screened for fluorescence. Of the more than 1,000 F1 larvae screened, 55 transgenic larvae expressing EGFP were observed. Each transgenic L1 was imaged at 400x magnification and scored for fluorescence in several tissues (Table 3.1). Strong EGFP expression was most frequently observed in the anterior intestine, gonadal primordium, amphidial/head neurons, and phasmidial/tail neurons (Figure 3.4A-D). Consistent with the observed strong intestinal expression, a search of the 1.3 kb region upstream of the *Ss-age-1* translational start site for ELT-2 recognition motifs [233] revealed two consensus TGATAA motifs 136 bp and 630 bp upstream of the start site.

Since specific amphidial neurons are important in the arrest and recovery of both *C. elegans* dauer larvae [32,34] and *S. stercoralis* L3i [43,54,57], we sought to identify the amphidial neurons in which *Ce-age-1* and *Ss-age-1* are expressed. Examination of transgenic *C. elegans* L1 and adult hermaphrodites revealed expression of *Ce-age-1* in the AWC and ASJ amphidial neuron pairs (Figure 3.3C-D). AWC neurons are important in thermotaxis [234] as well as chemotaxis to volatile odorants [40,235]. ASJ neurons play an important role in regulating dauer formation [34] as well as dauer recovery [32,147]. Additionally, ASJ neurons are sites of expression of *daf-28* [138] and *ins-6* [147], both encoding agonistic insulin-like peptides.

A similar examination of transgenic *S. stercoralis* post-free-living L1 was limited by the number of worms expressing the construct in amphidial neurons. However, using neuronal maps for both *Caenorhabditis spp.* [58] and *P. trichosuri* [236], we were able to locate expression in an amphidial neuron pair that we regard as the positional homolog of the AWC amphidial neuron pair in *C. elegans* (Figure 3.4C-D). This does not preclude the possibility of *Ss-age-1* expression in other amphidial neurons, including ASJ; however, the current limitations of transgenesis in *S. stercoralis* prevented us from pursuing this in the present study.

We conclude that although the anatomical expression patterns of *Ce-age-1* and *Ss-age-1* are not completely consistent, expression in important sites of IIS regulation, including amphidial neurons, are conserved between the two species (Figure 3.3C, Figure 3.4C). Conservation of expression in these tissues, which sense and direct responses to environmental cues in both species, is consistent with the hypothesis that the function of AGE-1 in directing dauer and L3i development is conserved between *C. elegans* and *S. stercoralis*. Furthermore, the *C. elegans* intestine is an important endocrine tissue [160] and expresses antagonistic insulin-like ligands [144]. Strong expression of *Ss-age-1* in the intestine (Figure 3.4A, Table 3.1) suggests that the intestine may also be a site of IIS regulation during L3i development in *S. stercoralis*.

PI3 kinase inhibition blocks *S. stercoralis* L3i activation

Previous work in *C. elegans* has demonstrated that pharmacological inhibition of IIS, using the PI3 kinase inhibitor LY294002, leads to dauer arrest under well-fed conditions [59]. This work was extended to clade V parasitic nematodes, the same clade as *C. elegans*, by Brand and Hawdon, who demonstrated that LY294002 could inhibit feeding of *Ancylostoma caninum* and *A. ceylanicum* L3i [68]. LY294002 has a similar effect on larval development in another clade V nematode, *Nippostrongylus brasiliensis* [71]. However, it has never been demonstrated that inhibition of IIS signaling prevents resumption of feeding by infective larvae in any other clade of parasitic nematode in phylum Nematoda, in which animal parasitism is thought to have evolved independently at least four times [109].

To determine whether IIS regulates activation of clade IV *S. stercoralis* L3i under host-like conditions, we performed an *in vitro* L3i activation assay [57,69]. Host-like conditions included incubation in DMEM, supplemented with 10% canine serum and 12.5 mM reduced glutathione, for 24 hours at 37°C and 5% CO_2. Resumption of feeding, a hallmark of activation, was assessed by the ingestion of FITC dye into the pharynx.

We assessed the percentage of L3i feeding in three concentrations of LY294002, 10-100 μM, and compared this to a DMSO (carrier) positive control. We observed a significant, dose-dependent reduction in L3i activation in response to LY294002 (Figure 3.5). Logistic regression analysis revealed a 90% decrease (odds ratio: 0.10, 95% confidence interval: 0.08-0.13) in the odds of resumption of feeding for L3i at 100 μM, a 67% decrease (odds ratio: 0.33, 95% confidence interval: 0.28-0.40) in the odds of resumption of feeding for L3i at 50 μM, and a 25% decrease (odds ratio: 0.75, 95% confidence interval: 0.63-0.89) in the odds of resumption of feeding for L3i at 10 μM, all in comparison to the DMSO positive control. All odds ratios were significant at conventional statistical probabilities ($p < 0.001$). At 100 μM of the PI3 kinase inhibitor, resumption of feeding by L3i was nearly inhibited to the level observed in the M9 buffer negative control. These data support the hypothesis that IIS signaling through the PI3 kinase, composed of *Ss-age-1* and *Ss-aap-1*, is necessary for resumption of L3i development in *S. stercoralis* upon encountering a host.

To our knowledge, these data demonstrate, for the first time, that PI3 kinase function and IIS is important in L3i activation in nematodes outside of clade V. This suggests that IIS may regulate activation of L3i in other parasitic nematode species upon encountering their respective

hosts. Future studies may provide additional insight into the role of IIS in modulating L3i activation.

Implications for the 'dauer hypothesis' and future directions

We have previously demonstrated that the *S. stercoralis* ortholog of the *Ce*-DAF-16 forkhead transcription factor is required for L3i arrest [78]. This is consistent with the function of *Ce*-DAF-16, which translocates to the nucleus when IIS is diminished under dauer-promoting conditions [85]. In this study, we have presented evidence that the *S. stercoralis* homolog of *Ce*-AGE-1 regulates L3i activation. This is also consistent with the function of *Ce*-AGE-1, which mediates an increase in IIS when dauer larvae encounter favorable conditions and resume development [147,165]. Together, these data suggest that an IIS pathway, similar to that in *C. elegans*, mediates both developmental arrest of *S. stercoralis* L3i as well as activation of these infective larvae when a suitable host is encountered. Thus, we find the "dauer hypothesis" to be a relevant and informative framework for investigating the mechanisms governing L3i development in the parasitic nematode *S. stercoralis*.

Future progress towards defining the role of *Ss-age-1* in the development of *S. stercoralis* L3i will require new or enhanced functional genomic tools. Knock-down of the *Ss-age-1* message using RNA interference, which has previously been of limited utility in many parasitic nematodes including *S. stercoralis* [93,94,237], could provide an excellent means of assessing the role of *Ss-age-1* throughout the life cycle. Previously, gene function in parasitic nematodes has also been inferred from heterologous complementation of mutations in *C. elegans*, an approach we have taken to assess the function of *Ss-daf-16* [79]. However, using established methods [79,83], we have been unable to express *Ss-age-1* sequences in the *C. elegans* CY246 strain to ascertain heterologous complementation. Future studies may reveal the mechanism that accounts for this lack of expression and allow us to pursue this line of experimentation.

Improvements in *S. stercoralis* transgenesis would also provide several more definitive means of assessing the function of *Ss-age-1*. Currently, we are able to observe effects of transgene expression in only small numbers of transiently transformed *S. stercoralis* in the post free-living generation [78]. Inducible expression of dominant loss- or gain-of-function constructs targeting *Ss-age-1* or other IIS components, preferably in stable transgenic lines, would allow us to interrogate functions of specific genes and to assess the epistatic relationships between components of the IIS pathway in regulating development of *S. stercoralis* L3i. Similar constructs could also be used to determine the role of *Ss-age-1* in homogonic versus heterogonic

development of *S. stercoralis* post-parasitic L1. Our studies to elucidate the role of *Ss-age-1* in post-parasitic development using the PI3 kinase inhibitor LY294002 have thus far been uninterpretable due, we believe, to our inability to procure developmentally uncommitted L1 [43]. As we establish more robust methods, including the ability to generate stable transgenic lines and undertake conditional transgene expression, we will address additional questions regarding the role of *Ss-age-1* and of IIS generally in *S. stercoralis* development. A greater understanding of the role of IIS in L3i development may lead to novel control strategies as well as new treatments for strongyloidiasis and other diseases caused by parasitic nematodes.

3.5 Figures

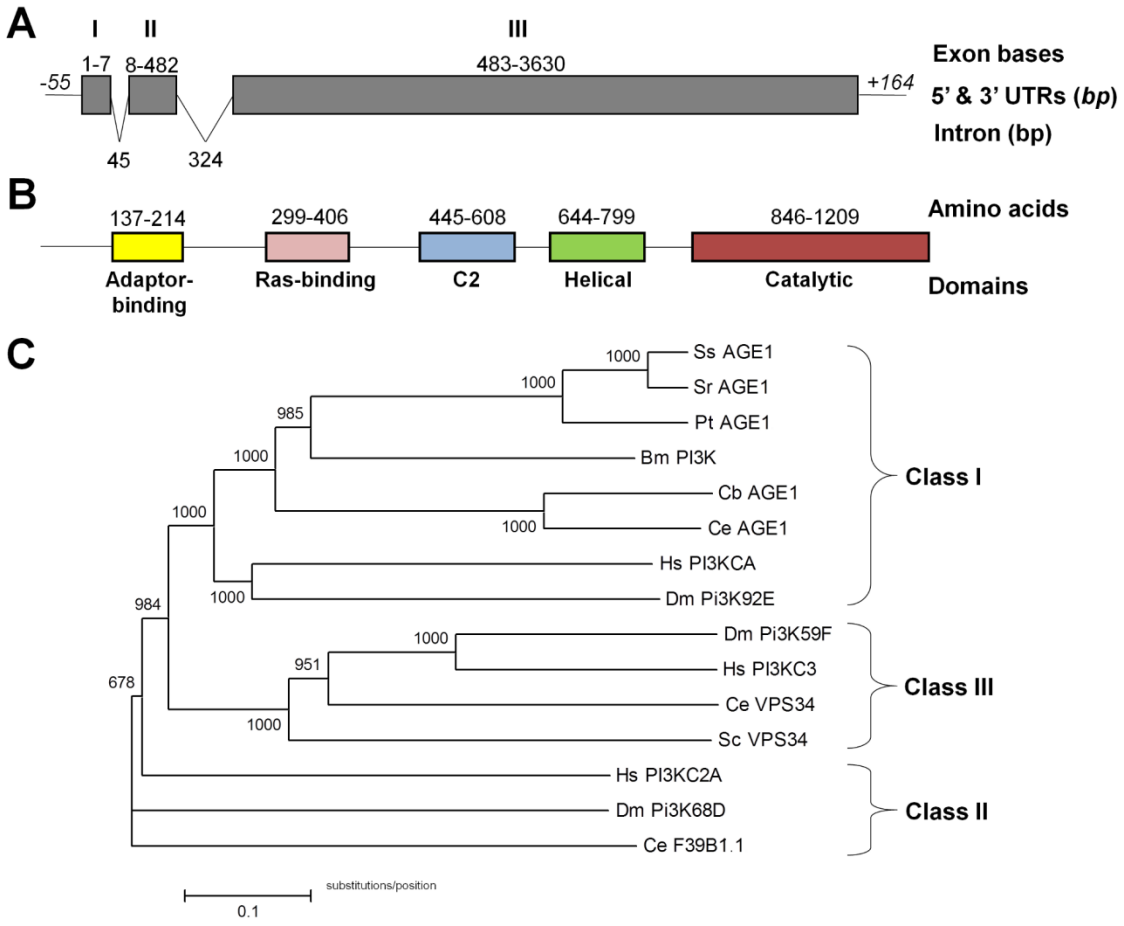

Figure 3.1. *Ss*-AGE-1 is a homolog of the *Ce*-AGE-1 PI3 kinase catalytic subunit.
(A) Intron-exon structure of the *Ss-age-1* unspliced mRNA sequence. Grey boxes indicate the three exons, with the numbers above indicating the first and last base pairs of the exon. Introns are indicated by slanted lines between the exons, with the numbers indicating the total intron length. The 5' and 3' untranslated regions (UTR) are indicated with horizontal lines, with the italicized numbers indicating the total length of the UTR in base-pairs (bp). (B) Domain structure of the *Ss*-AGE-1 predicted protein. Shaded boxes represent the five protein family domains, with the numbers indicating the first and last amino acids of the domain. (C) Phylogenetic analysis of *Ss*-AGE-1. The predicted *Ss*-AGE-1 protein groups with other class I PI3 kinase catalytic subunits, including *Ce*-AGE-1. Abbreviations: *Strongyloides stercoralis* (Ss), *Strongyloides ratti* (Sr), *Parastrongyloides trichosuri* (Pt), *Brugia malayi* (Bm), *Caenorhabditis briggsae* (Cb), *Caenorhabditis elegans* (Ce), *Homo sapiens* (Hs), *Drosophila melanogaster* (Dm), and *Saccharomyces cerevisiae* (Sc).

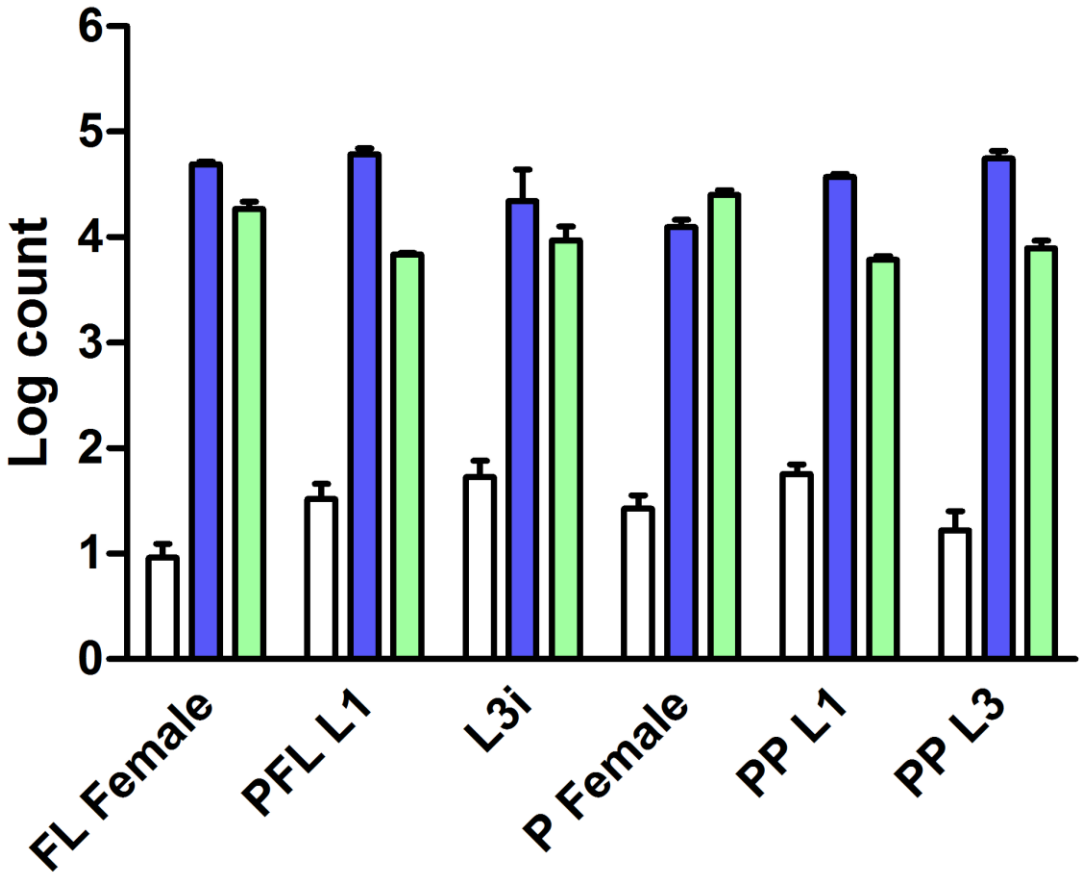

Figure 3.2. *Ss-age-1* is expressed at a low level in all examined *S. stercoralis* life stages.
Ss-age-1 (white bars) transcript levels in comparison to transcript levels of two reference genes, *Ss-act-2* (dark blue bars) and *Ss-gapdh* (light green bars), in six *S. stercoralis* developmental stages: free-living females (FL Female), post-free-living first-stage larvae (PFL L1), infectious third-stage larvae (L3i), parasitic females (P Female), predominantly (>95%) heterogonically developing post-parasitic first-stage larvae (PP L1), and post-parasitic approximately third-stage larvae heterogonically developing to free-living adults (PP L3). Transcript levels were normalized to *Ss-age-1* in free-living females and log transformed. Error bars represent + 1 SEM.

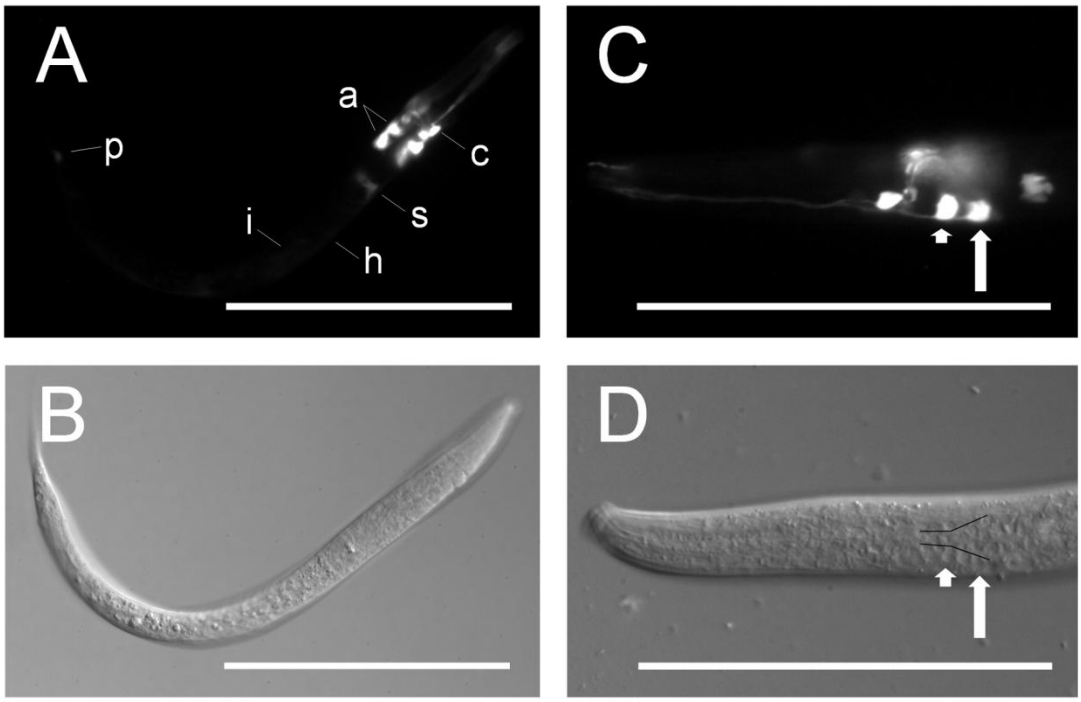

Figure 3.3. *Ce-age-1* is expressed in amphidial neurons and other tissues.
Fluorescence (A,C) and DIC (B,D) images of transgenic *C. elegans* first-stage larvae expressing *Ce-age-1p::Ce-age-1(102bp)::egfp::Ce-age-1t* from an extra-chromosomal array. (A,B) Strong expression of the EGFP reporter was present in amphidial neurons (a), a neuron or support cell anterior to the nerve ring (c), and the sphincter connecting the pharynx to the intestine (s). Weak expression was present in the intestine (i), hypodermis (h), and a phasmidial neuron (p). (C,D) EGFP reporter expression was present in the amphidial neurons AWC (short arrow) and ASJ (long arrow). Cell bodies of the amphidial neurons align just lateral to the black lines in panel D [58]. Scale bars = 100 μm.

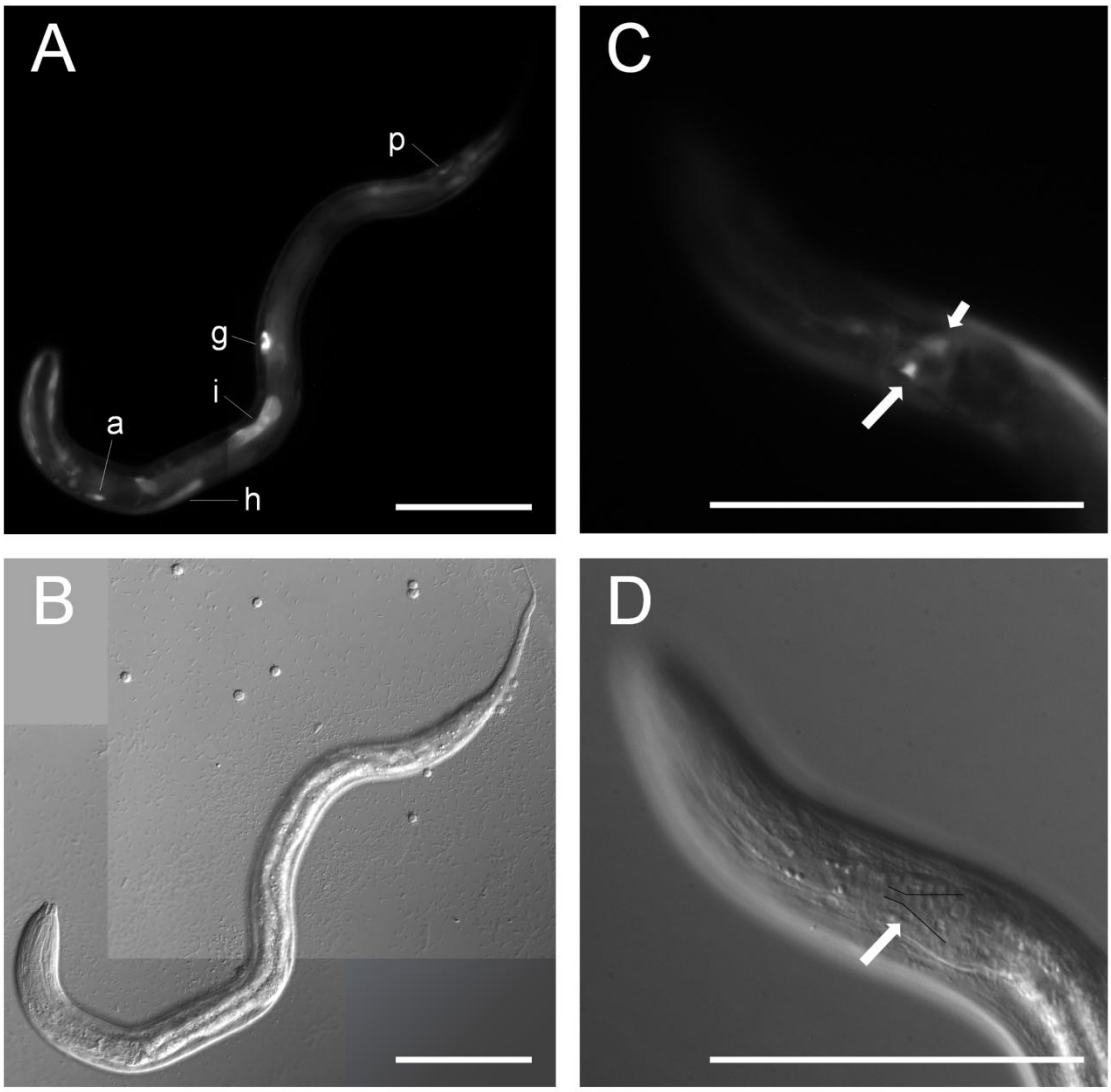

Figure 3.4. *Ss-age-1* is expressed in amphidial neurons, the intestine, and other tissues.
Fluorescence (A,C) and DIC (B,D) images of transgenic *S. stercoralis* post-free-living first-stage larvae expressing *Ss-age-1p::egfp::Ss-era-1t* from an extra-chromosomal array. (A,B) Expression of the EGFP reporter was present in the intestine (i), gonadal primordium (g), amphidial/head neuron (a), hypodermis (h), and phasmidial/tail neuron (p). (C,D) Expression of the EGFP reporter was present in an amphidial neuron (long arrow), with positional homology to AWC in *C. elegans*. The other cell body of the amphidial neuron pair is out of the plane of focus (short arrow). Cell bodies of the amphidial neurons align just lateral to the black lines in panel D [58]. Scale bars = 100 μm.

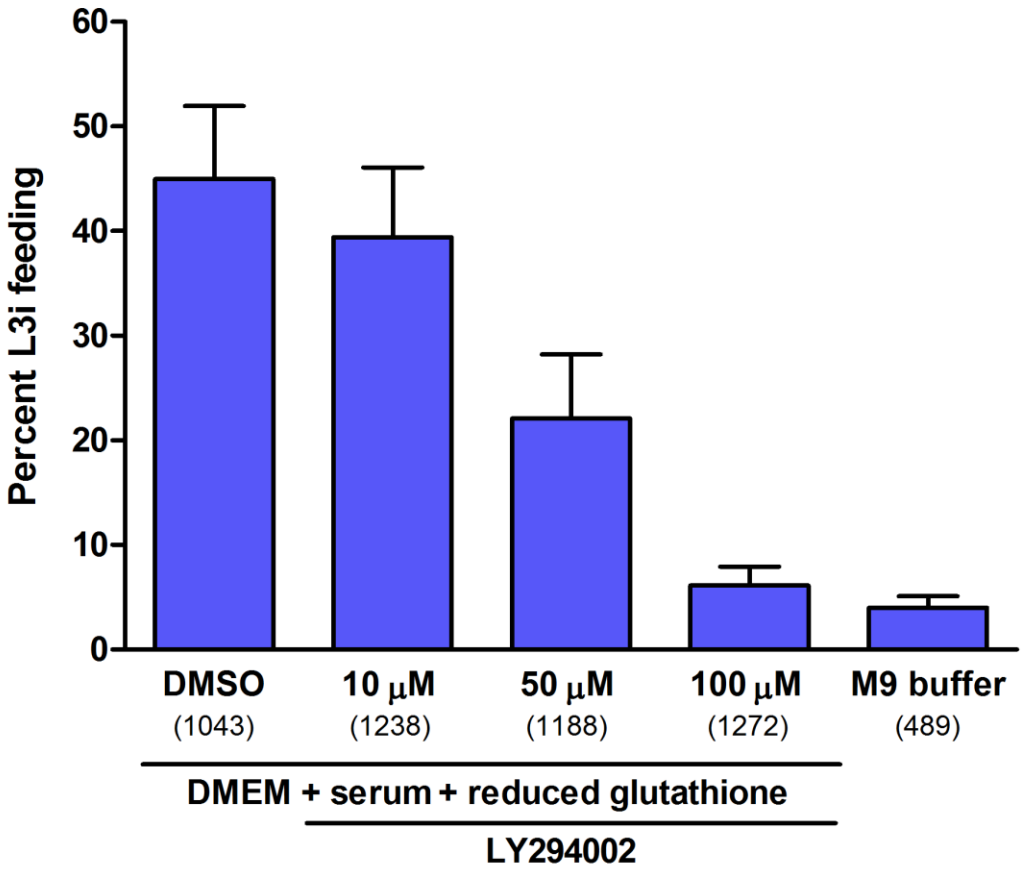

Figure 3.5. *S. stercoralis* L3i activation is attenuated by the PI3 kinase inhibitor LY294002.
In vitro activation of *S. stercoralis* L3i under host-like culture conditions by incubation in DMEM, 10% canine serum, and 12.5 mM reduced glutathione for 24 hours at 37°C and 5% CO_2. The percentage of L3i that resumed feeding, a hallmark of activation, was scored by ingestion of FITC into the pharynx. Conditions included DMSO (carrier) positive control and M9 buffer negative control. The PI3 kinase inhibitor LY294002 was evaluated at 100 μM, 50 μM, and 10 μM, with each condition compared to the DMSO control using a logistic regression analysis. Error bars represent + 1 SEM and parenthetical integers show the total number of L3i evaluated for each condition.

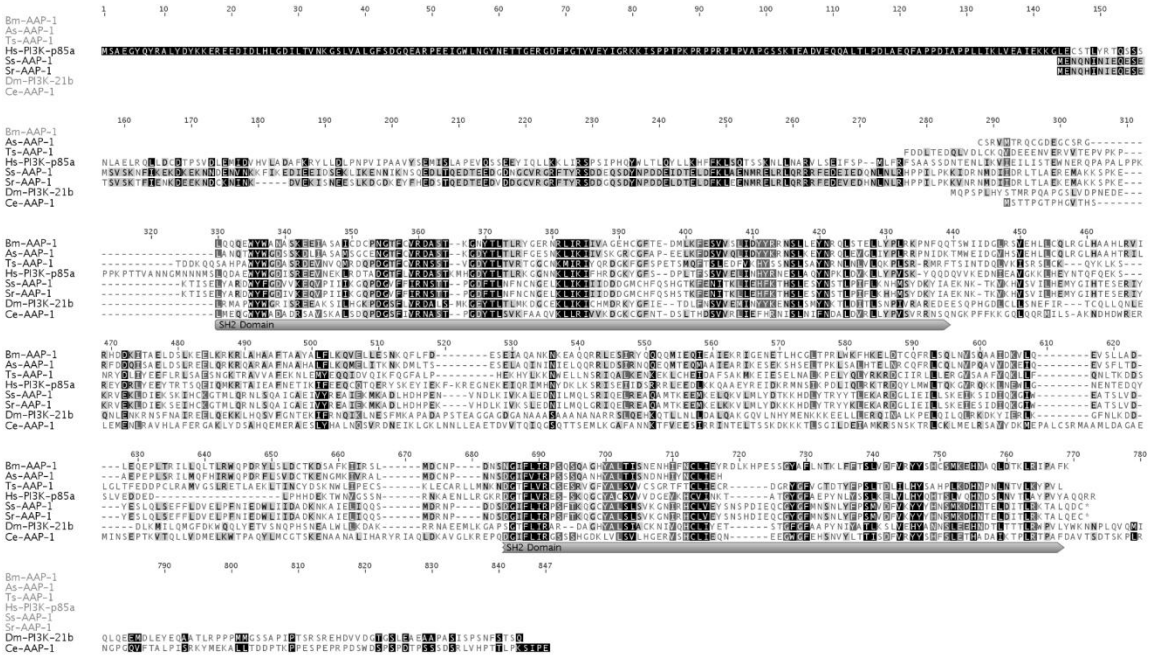

Figure 3.S1. *Ss*-AAP-1 is a PI3 kinase accessory/regulatory subunit.
Protein alignment of PI3 kinase accessory/regulatory subunits. The two Scr homology 2 (SH2) domains (grey bars) have the highest conservation of residues (black highlights) between all sequences. Abbreviations: *Strongyloides stercoralis* (Ss), *Strongyloides ratti* (Sr), *Brugia malayi* (Bm), *Ascaris suum* (As), *Trichinella spiralis* (Ts), *Caenorhabditis elegans* (Ce), *Homo sapiens* (Hs), and *Drosophila melanogaster* (Dm).

3.6 Table

Table 3.1: Sites of *Ss-age-1* expression in transgenic *S. stercoralis* post-free-living first-stage larvae.

	Intestine	Gonadal Primorium	Head Neuron(s)	Tail Neuron(s)	Sheath/Socket Cell(s)	Hypodermis	Pharynx	Other Cell Body	Total
Expt 1 n, (%)	11 (73%)	11 (73%)	8 (53%)	4 (27%)	5 (33%)	6 (40%)	6 (40%)	3 (20%)	15
Expt 2 n, (%)	15 (79%)	7 (37%)	7 (37%)	4 (21%)	8 (42%)	7 (37%)	4 (21%)	2 (11%)	19
Expt 3 n, (%)	15 (71%)	12 (57%)	5 (24%)	4 (19%)	5 (24%)	6 (29%)	6 (29%)	2 (10%)	21
Total n, (%)	**41 (75%)**	**30 (55%)**	**20 (36%)**	**12 (22%)**	**18 (33%)**	**19 (35%)**	**16 (29%)**	**7 (13%)**	**55**

CHAPTER 4 - *Strongyloides stercoralis* cGMP Pathway Signaling Regulates Insulin- and TGFβ-like Peptide Transcripts and Development of Infective Third-stage Larvae

The contents of this chapter is a manuscript in preparation:

> Stoltzfus JD, Bart S, Lok JB (2013) *Strongyloides stercoralis* cGMP Pathway Signaling Regulates Insulin- and TGFβ-like Peptide Transcripts and Development of Infective Third-stage Larvae.

4.1 Abstract

The infectious form of the parasitic nematode *Strongyloides stercoralis* is a developmentally arrested third-stage larva (L3i), which is morphologically similar to the developmentally arrested dauer larva in the free-living nematode *Caenorhabditis elegans*. We hypothesize that the molecular pathways regulating *C. elegans* dauer development also control L3i arrest and activation in *S. stercoralis*. Previously, we demonstrated a role for insulin/IGF-1-like signaling (IIS) in regulating L3i arrest and activation. In a recent RNAseq study, we identified the major components of the four canonical dauer pathways in *S. stercoralis*. In this study, we describe G protein-coupled receptor (GPCR) signaling components in *S. stercoralis* and examine the role of cyclic guanosine monophosphate (cGMP) pathway signaling in regulating L3i activation. We found that application of the membrane permeable cGMP analogue 8-bromo-cGMP resulted in potent activation of *S. stercoralis* L3i, as measured by resumption of feeding, with 85.1±2.2% of L3i feeding in 200 μM 8-bromo-cGMP in comparison to 0.6±0.3% in the buffer diluent. L3i stimulated with 8-bromo-cGMP positively regulated transcript levels of the insulin-like peptide (ILP) -encoding gene *Ss-ilp-1* (ratio 46.8±19.7) and negatively regulated transcript levels of the dauer transforming growth factor β (TGFβ) -encoding gene *Ss-tgh-1* (ratio 0.32±0.08) in comparison to unstimulated controls. Expression of promoter::*egfp* reporter constructs in the *S. stercoralis* post-free-living generation revealed *Ss-ilp-1* and *Ss-ilp-6* promoter activity in the hypodermis and neurons and *Ss-ilp-7* promoter activity in the intestine and a pair of head neurons. Together, these data provide evidence that a cGMP signaling pathway regulates *S. stercoralis* L3i development.

4.2 Introduction

Parasitic nematodes infect approximately one in four persons globally, with the vast burden of disease concentrated in tropical and developing regions [4]. The parasitic nematode *Strongyloides stercoralis* infects an estimated 30-100 million people worldwide [5]; infection can result in disseminated strongyloidiasis and potentially fatal hyperinfection in immunocompromised persons [11]. Like many soil-transmitted helminths, the infectious form of *S. stercoralis* is a developmentally arrested third-stage larva (L3i), which is non-feeding, long-lived, and stress-resistant [8]. *S. stercoralis* L3i exhibit thermotaxis and chemotaxis to a range of host-like cues [56], including body temperature [19], carbon dioxide [16], sodium chloride [17], and urocanic acid [18]. Upon entering a suitable host, L3i quickly activate and resume feeding and development [8]. However, the molecular mechanisms by which *S. stercoralis* L3i sense and transduce host cues and subsequently signal resumption of development are poorly understood.

The free-living nematode *Caenorhabditis elegans* has a facultative developmentally arrested third-stage larva, known as the dauer larva, which forms during stressful conditions including high temperature, low food levels, and high dauer pheromone levels; when conditions improve, *C. elegans* exits dauer and resumes reproductive development [23,130]. The molecular pathways regulating dauer entry have been well studied and include: a cyclic guanosine monophosphate (cGMP) signaling pathway, an insulin/IGF-1-like signaling (IIS) pathway, a dauer transforming growth factor β (TGFβ) signaling pathway, and a DAF-12 nuclear hormone receptor regulated by dafachronic acid (DA) steroid ligands [30,41]. We have demonstrated that components of these four pathways are present in *S. stercoralis* [238], that elements of the IIS pathway control L3i arrest and activation [78,111], and that Δ7-DA is a potent activator of L3i [69]. However, a role for cGMP signaling in regulating *S. stercoralis* L3i development has not been previously examined.

In *C. elegans*, cGMP signaling is crucial for transducing dauer pheromone signals, which indicate population density [239]. Dauer pheromone, a complex mixture of ascarosides [131,132,240,241], is continuously secreted, and high concentrations potently induce dauer formation [28,130]. Several chemosensory seven-transmembrane G protein-coupled receptors (7TM GPCRs) sense specific or combinations of dauer-inducing ascarosides; these include *Ce*-SRBC-64 and *Ce*-SRBC-66 [33], *Ce*-SRG-36 and *Ce*-SRG-37 [133], and *Ce*-DAF-37 and *Ce*-DAF-38 [242]. At least two of these chemosensory 7TM GPCRs signal through the G protein α subunits *Ce*-GPA-2 and *Ce*-GPA-3 [33]. Constitutively activated forms of *Ce*-GPA-2 or *Ce*-

GPA-3 result in constitutive dauer formation, while mutations that inactivate the proteins encoded by these genes result in decreased dauer entry under dauer-inducing conditions [89].

Under dauer-inducing conditions, such as high dauer pheromone levels, *Ce*-GPA-2 and *Ce*-GPA-3 are thought to inhibit the transmembrane guanylyl cyclase encoded by *Ce-daf-11*, thereby decreasing concentrations of the second messenger cGMP [33]. Mutations in *Ce-daf-11* result in dauer constitutive (Daf-c) phenotypes [36,60,136]. Some downstream effects of cGMP signaling are mediated by *Ce*-TAX-4 and *Ce*-TAX-2, the α and β subunits, respectively, of a heteromeric cyclic-nucleotide gated ion channel, which both regulates chemosensation and thermosensation and can also inhibit or stimulate dauer larva formation in different contexts [134,135,243].

Exogenous application of the membrane permeable cGMP analog 8-bromo-cGMP rescues the Daf-c phenotype of *Ce-daf-11* mutants, but does not rescue the Daf-c phenotypes of *Ce-tax-4*, IIS pathway, or dauer TGFβ pathway mutants [60]. Furthermore, addition of 8-bromo-cGMP results in increased *Ce-ins-7* and *Ce-daf-28* transcript abundances [139]. Both *Ce-ins-7* and *Ce-daf-28* encode agonistic insulin-like peptides (ILPs) in the IIS pathway [138,149]. Signaling mediated by cGMP also regulates the dauer TGFβ pathway, since *Ce-daf-11* acts cell autonomously to regulate *Ce-daf-7* expression in ASI chemosensory neurons [123,137]. These data suggest that cGMP signaling acts upstream of both IIS and TGFβ signaling.

While ascaroside pheromones have been detected in many nematode species [141,142,244], it is difficult to envision a role for these compounds in regulating L3i development for many warm-blooded animal parasitic nematodes, particularly in species where all post-parasitic larvae invariably developmentally arrest in the infectious form [13]. In *S. stercoralis*, where post-parasitic larvae can facultatively develop heterogonically to a single free-living generation, the post-free-living larvae invariably develop to L3i regardless of population density. However, a dauer-like pheromone that regulates L3i formation has recently been described in the parasitic nematode *Parastrongyloides trichosuri*, which can undergo multiple rounds of free-living replication outside its animal host [48].

As a second messenger for a wide variety of chemosensory 7TM GPCRs, and not limited to the 7TM GPCRs that bind ascarosides as described above, cGMP represents a crucial transducer of environmental signals. Indeed, the *C. elegans* genome encodes over 1,600 chemosensory 7TM GPCRs [245], which are thought to signal through the 21 G protein α (G_α) subunits, two G protein β (G_β) subunits, and two G protein γ (G_γ) subunits encoded in the genome [91]. One of the primary functions of these G proteins is to regulate guanylyl cyclases, including

Ce-DAF-11, which in turn produce cGMP [246]. Thus, a wide variety of environmental stimuli, including but not limited to ascarosides, can regulate cGMP levels in *C. elegans*.

Increased cGMP signaling activates L3i in parasitic nematode species closely related to *C. elegans* [66,68,71]. Additionally, next-generation deep-sequencing of the transcriptome (RNAseq) of *S. stercoralis* revealed increased transcript levels of many cGMP signaling pathway components in L3i [238]. Together, these data led us to hypothesize that chemosensory 7TM GPCRs sense host cues and that cGMP pathway signaling is important for transducing host-like cues in L3i as well as triggering resumption of development once it is inside the host.

In this study, we identify a large subset of *S. stercoralis* chemosensory 7TM GPCRs and note that transcripts for many of these genes are found only in L3i and/or *in vivo* activated third-stage larvae (L3+). We also identify all of the G proteins present in the draft *S. stercoralis* genome and observe that transcripts for many G_{α} subunits are at their maximal levels in L3i. We then demonstrate that the membrane permeable analog of cGMP potently activates *S. stercoralis* L3i and regulates transcript levels of the ILP-encoding gene *Ss-ilp-1* and the dauer TGFβ ligand-encoding gene *Ss-tgh-1*. Additionally, we show that several of the ILP gene promoters are active in amphidial neurons and the intestine, tissues that are important for IIS in *C. elegans*.

4.3 Materials and Methods

Ethics statement

The *S. stercoralis* PV001 and UPD strains were maintained in prednisone-treated beagles in accordance with protocols 702342, 801905, and 802593 approved by the University of Pennsylvania Institutional Animal Care and Use Committee (IACUC). All IACUC protocols, as well as routine husbandry care of the animals, were carried out in strict accordance with the *Guide for the Care and Use of Laboratory Animals of the National Institutes of Health*.

S. stercoralis maintenance

The *S. stercoralis* PV001 and UPD strains were maintained and cultured as previously described [9,10,111].

S. stercoralis RNAseq and *de novo* transcript assembly

S. stercoralis developmental stages used for RNA isolation, dsDNA library construction and sequencing, and read alignment to the *S. stercoralis* draft genome (6 December 2011 version)

have been described previously [238]. *De novo* assembly of RNAseq reads from *S. stercoralis* developmental stages has also been described previously [238].

Transcript abundances of manually annotated *S. stercoralis* genes were calculated using Cufflinks version 2.0.2 (http://cufflinks.cbcb.umd.edu/) as fragments per kilobase of exon per million mapped reads (FPKM), with paired-end reads counted as single sampling events [120]. FPKM values for coding sequences (CDS) of both genes and individual isoforms, along with ± 95% confidence intervals, were calculated for each gene in each of the 21 samples using Cuffdiff version 2.0.2. Log10 transformed values were plotted in Prism version 5.03 (GraphPad Software, Inc., http://www.graphpad.com/), and the y-axis was uniformly scaled for each gene family to aid comparisons between genes. Significant differences in FPKM values between developmental stages and p-values were determined using Cuffdiff version 2.0.2, a program with the Cufflinks package [121]; p-values <0.05 were considered statistically significant.

Identification of *S. stercoralis* GPCRs and G proteins.

BLAST searches of the *S. stercoralis* (ftp://ftp.sanger.ac.uk/pub/pathogens/HGI/) genomic contigs, as well as *S. stercoralis de novo* assembled transcripts (ArrayExpress accession number E-MTAB-1184; http://www.ebi.ac.uk/arrayexpress/experiments/E-MTAB-1184), using *C. elegans* protein sequences (http://www.wormbase.org/) were performed using Geneious version 6.0 (www.geneious.com) set to the least restrictive parameters. A total of 76 *C. elegans* chemosensory 7TM GPCRs, four from each of the 19 families, were used to BLAST search the *S. stercoralis* genomic contigs, resulting in a total of 227 hits. The 21 *C. elegans* G_{α} proteins, the two G_{β} proteins, and the two G_{γ} proteins, were used to search both the *S. stercoralis* genomic contigs and *de novo* assembled transcripts.

BLAST hits were manually annotated using aligned reads from all seven developmental stages by a combination of the Integrated Genome Viewer (IGV) version 2.0.34 (http://www.broadinstitute.org/igv/) and Geneious. Putative *S. stercoralis* homologs were identified through reverse BLAST searches using NCBI's pBLAST (http://blast.ncbi.nlm.nih.gov/Blast.cgi) [118] against *C. elegans* sequences. Putative *S. stercoralis* homologs of chemosensory 7TM GPCRs were also checked for transmembrane domains using TMHMM Server version 2.0 (http://www.cbs.dtu.dk/services/TMHMM/) and assigned to a *C. elegans* superfamily based on reverse BLAST search results. Manually annotated *S. stercoralis* transcripts were used to determine predicted protein sequences.

Phylogenetic analysis of *C. briggsae*, *C. elegans*, and *S. stercoralis* G_α proteins was performed by alignment of protein sequences with Clustal W and a BLOSUM matrix using Geneious. A neighbor-joining phylogenetic tree, with 1000 iterations of bootstrapping, was then constructed using Geneious. *S. stercoralis* G_α protein-encoding genes were named by relationship to *C. briggsae* and *C. elegans* proteins.

S. stercoralis L3i *in vitro* activation

In vitro activation of *S. stercoralis* L3i was performed as previously described [57,111] with the following adaptations. All conditions were supplemented with antibiotics (100 U/ml penicillin, 10 μg/ml streptomycin, and 12.5 μg/ml tetracycline). M9 Buffer was used as the medium for both the experimental conditions and the negative control [116], except where indicated.

For the titration of 8-bromo-cGMP, L3i were isolated from six-day-old charcoal coprocultures (incubated at 25°C) by the Baermann technique at 27°C. L3i were subsequently washed twice in deionized water and incubated in M9 buffer supplemented with antibiotics for three hours at room temperature before distributing the L3i amongst the different conditions. The positive control was composed of DMEM (supplemented with L-glutamine, 4.5 g/L glucose, and sodium pyruvate) (Corning, www.cellgro.com), 10% naive canine serum, and 12.5 mM L-glutathione reduced (CAS 70-18-8) (Sigma-Aldrich, www.sigmaaldrich.com). The negative control was M9 buffer. The experimental conditions, using 8-bromo-cGMP (CAS 51116-01-9) (Sigma) at 800 μM, 200 μM, 100 μM, and 50 μM, were carried out in M9 buffer. Each condition consisted of three wells in a 96-well plate, with approximately 100 L3i in 100 μl total volume in each well. L3i were incubated at 37°C in 5% CO_2 in air for 21 hours; 2.5 μl of fluorescein isothiocyanate (FITC; CAS 3326-32-7) (Sigma) dissolved in N,N-dimethylformamide (CAS 68-12-2) (Sigma) at 20 mg/ml and aged for ≥ one month was then added to each well, and the cultures were incubated an additional three hours at 37°C and 5% CO_2 in air (24 hours total). L3i for each condition were pooled and washed five times in 14 ml of M9 buffer, with centrifugation at 75 x g for five minutes at room temperature. L3i were then mounted on glass slides with grease edged cover-slips, immobilized by a 20 second heat-shock at 60°C or with 10 mM levamisole (Sigma), and viewed by fluorescence microscopy. Only L3i with FITC in the pharynx were scored as "positive" for feeding.

For L3i activation kinetics, conditions included both 200 μM 8-bromo-cGMP and host-like cues, consisting of DMEM, 10% canine serum, and 3.75 mM L-glutathione reduced. L3i

were isolated as previously described. L3i in all conditions were incubated at 37°C and 5% CO_2 in air for a total of 24 hours, with chemical cues added at appropriate intervals such that L3i were exposed to activating compounds for 4, 6, 12, 18, or 24 hours total. L3i were incubated with FITC and scored for feeding as previously described.

RT-qPCR

S. stercoralis L3i were prepared as previously described in the *in vitro* activation kinetic assay, except that L3i were obtained from seven-day-old PV001 strain coprocultures and were incubated at 37°C and 5% CO_2 in air using 500 L3i in 100 µl of liquid in each well with 24 wells per condition. Unstimulated L3i were soaked in antibiotics for three hours at room temperature. L3i from each condition were pooled and the pellet frozen at -80°C in 100 µl TRIzol reagent (Life Technologies, www.lifetechnologies.com); the L3i pellet was ground using a pestle, and total RNA was extracted per the manufacturer's protocol. RNA concentrations were determined using a NanoDrop 2000 spectrophotometer (Thermo Scientific, www.nanodrop.com).

Gene-specific primer sets, which only amplified spliced cDNA, included Ssilp1RT-2aF and -2R, Sstgh1RT-2F and -R, and Ss-gapdhRT-2F and -R [99,111,224]. Primer sets were calibrated using a five dilution series of total RNA and efficiencies calculated using standard methods [225]. Gene-specific one-step RT-qPCR was performed on four biological replicates, each in technical duplicate, using the Brilliant II SYBR Green QRT-PCR kit (Agilent Technologies, www.agilent.com) with 40 ng of total RNA on an Applied Biosystems 7500 (Life Technologies) instrument as previously described [111]. Controls omitting template or reverse transcriptase were also included.

Mean fold-changes were calculated using the Pfaffl Method [247], with the "no stimulation" condition as the calibrator and *Ss-gapdh* as the reference gene. Mean ratios as well as the mean percentage of L3i ingesting FITC dye, + 1 SD, were plotted in Prism version 5.03 (GraphPad Software, Inc., www.graphpad.com).

Plasmid construction and transformation of *S. stercoralis*

Plasmids for microinjection of *S. stercoralis* were constructed by Gateway cloning technology (Life Technologies). The *Ss-ilp-1* promoter region, containing 2,327 bp 5' of the start site, was PCR amplified from *S. stercoralis* genomic DNA, using the primers Ssilp1-1F and Ssilp1-1R, and recombined into pDONR P4-P1R, forming pPV483. The *Ss-ilp-6* promoter region, containing 2,566 bp 5' of the start site, was PCR amplified from *S. stercoralis* genomic

DNA, using the primers Ssilp6-1F and Ssilp6-1R, and recombined into pDONR P4-P1R, forming pPV484. The *Ss-ilp-7* promoter region, containing 1,270 bp 5' of the start site, was PCR amplified from *S. stercoralis* genomic DNA, using the primers Ssilp7-1F and Ssilp7-1R, and recombined into pDONR P4-P1R, forming pPV485. The 870 bp coding sequence and stop codon for enhanced green fluorescent protein (*egfp*) was PCR amplified from pJA257 (Addgene, www.addgene.org), using the primers EGFPGW-1F and EGFPGW-1R, and recombined into pDONR 221, forming pPV477. The *Ss-era-1* terminator, consisting of 598 bp 3' of *Ss-era-1*, was PCR amplified from pAJ08 (Addgene), using the primers Ss-era-1-1FattB2r and Ss-era-1-1RattB3, and recombined into pDONR P2R-P3, forming pPV475. *S. stercoralis* genomic DNA was prepared from mixed-stage worms using the Qiagen DNeasy Blood and Tissue kit (www.qiagen.com). All pDONR plasmid inserts were confirmed by complete sequencing.

S. stercoralis insulin-like peptide promoter::*egfp* reporter plasmids were constructed by LR recombination reactions using Gateway. The *Ss-ilp-1* promoter::*egfp*::*Ss-era-1* terminator plasmid was constructed by recombining the plasmids pPV483, pPV477, and pPV475 into pDEST R4-R3, forming pPV487. The *Ss-ilp-6* promoter::*egfp*::*Ss-era-1* terminator plasmid was constructed by recombining the plasmids pPV484, pPV477, and pPV475 into pDEST R4-R3, forming pPV488. The *Ss-ilp-7* promoter::*egfp*::*Ss-era-1* terminator plasmid was constructed by recombining the plasmids pPV485, pPV477, and pPV475 into pDEST R4-R3, forming pPV489. All pDEST plasmid inserts were confirmed by complete sequencing.

S. stercoralis was transformed by gonadal micro-injection of adult free-living females as previously described [10]. A mix of 50 ng/µl of either pPV487, pPV488, or pPV489 and 20 ng/µl of pAJ08 (Addgene) as a co-injection marker was micro-injected into the distal gonad of gravid females. Injected females were paired with an equal number of males and incubated on an NGM agar plate, with *E. coli* OP50 as a food source, at 22°C. The F1 post-free-living progeny were screened for fluorescence both 48 and 72 hours after microinjection. Larvae were screened for expression of fluorescent reporter transgenes using an Olympus SZX12 stereomicroscope with coaxial epifluorescence (www.olympus.com). Each transgenic larva was subsequently mounted on a 2% agarose pad (Lonza, www.lonza.com), anesthetized with 10 mM levamisole (Sigma), and examined in detail using an Olympus BX60 compound microscope equipped with Nomarski Differential Interference Contrast (DIC) optics and epifluorescence. Specimens were imaged using a Spot RT Color digital camera and Spot Advanced v5.1 image analysis software (Diagnostic Instruments, Inc., www.spotimaging.com). Captured images were processed using GIMP version 2.6 (www.gimp.org) and Microsoft PowerPoint 2007 (www.microsoft.com).

4.4 Results

S. stercoralis chemosensory 7TM GPCRs

We previously noted that in *S. stercoralis*, transcripts of genes encoding putative cGMP signaling proteins are up-regulated in L3i; we speculated that cGMP signaling may be important in L3i for relaying host cues and controlling resumption of development upon entering a permissive host [238]. Since chemosensory 7TM GPCRs are known to regulate cGMP signaling and to be crucial for *C. elegans*' response to environmental cues [245,248,249], including the sensing of ascarosides [33,133,242], we hypothesized that homologs in *S. stercoralis* might play a role in sensing environmental and host cues, especially in L3i. Thus, we surveyed homologs of chemosensory 7TM GPCRs in *S. stercoralis* to determine whether the transcripts are developmentally regulated in a manner consistent with a role in sensing host cues.

Using reciprocal BLAST searches, with four disparate members from each of the 19 *C. elegans* chemosensory 7TM GPCR families used to conduct the initial search [248], we identified a total of 85 genes in the *S. stercoralis* genome that encode putative chemosensory 7TM GPCRs (Table 4.1). These 85 putative *S. stercoralis* chemosensory 7TM GPCRs almost certainly compose an incomplete list of the total number of *S. stercoralis* chemosensory 7TM GPCRs; however, this list likely includes the majority of the chemosensory 7TM GPCRs in the genome, given the open parameters of the BLAST searches. Although we included four members from each of the *C. elegans* SRW, SRZ, and SRBC superfamilies in our BLAST searches, we did not find homologs from any of these superfamilies in *S. stercoralis*. This search also identified other conserved classes of 7TM receptors (data not shown). We determined which of the seven *C. elegans* superfamilies each of the *S. stercoralis* chemosensory 7TM GPCRs were homologous to using BLAST scores (Table 4.1). However, we were unable to assign *S. stercoralis* homologs to specific *C. elegans* families due to large sequence differences.

Utilizing RNAseq data from seven different *S. stercoralis* developmental stages, we determined the transcript abundance patterns for each of the 85 putative *S. stercoralis* chemosensory 7TM GPCR homologs (Table 4.1). Surprisingly, nearly all of the transcript abundance profiles fit just a few patterns: transcripts detected only in L3i, only in *in vivo* activated L3+, in both L3i and L3+, or in none of the developmental stages examined. Furthermore, the normalized transcript abundance for nearly all of these transcripts was lower than for many other genes we have examined in *S. stercoralis*.

S. stercoralis heterotrimeric G proteins

In *C. elegans*, as well as other metazoans, chemosensory 7TM GPCRs signal through heterotrimeric G proteins to intracellular effectors [91,250]. G proteins are composed of three separately transcribed peptides: the G_α subunit that confers functional specificity, the G_β subunit, and the G_γ subunit [246]. The *C. elegans* genome contains 21 G_α subunit-, two G_β subunit-, and two G_γ subunit-encoding genes; the promoters for the majority of the G_α subunit-encoding genes are active in chemosensory amphidial neurons [91]. Two of the *C. elegans* G_α subunit-encoding genes, *Ce-gpa-2* and *Ce-gpa-3*, play a role in larval commitment to dauer development [33,89]. Our lab has previously identified orthologs of these two genes in *S. stercoralis*, named *Ss-gpa-2* and *Ss-gpa-3*, the transcripts of which are at a maximum in L3i [88,238]. Additionally, the promoter for *Ss-gpa-3* is active in the amphidial neurons of transgenic *S. stercoralis* post-free-living larvae, suggesting that it plays a role in relaying chemosensory cues [90]. Thus, we sought to identify all the G proteins in *S. stercoralis* and examine their transcript abundance patterns to determine whether the transcripts of other G proteins in the parasite are also at a maximum in L3i.

Using reciprocal BLAST searches, we identified a total of 14 G_α subunit, two G_β subunit, and two G_γ subunit-encoding genes in *S. stercoralis* (Table 4.2). By comparing the putative protein sequences for the *S. stercoralis* G_α subunits with *C. elegans* and *C. briggsae* sequences in a phylogenetic analysis, we were able to determine the G_α gene class [250] for each of the *S. stercoralis* G_α subunits as well as their orthologous relationships with their *Caenorhabditis* spp. counterparts (Table 4.2, Figure 4.S1). Noticeably absent from the *S. stercoralis* genomic contigs, as well as the *de novo* assembled transcripts, were orthologs for *gpa-1*, *-8*, *-9*, *-11*, *-14*, *-15*, and *-16*.

We then examined the transcript abundance patterns for each of the G protein-encoding genes, using RNAseq data from seven *S. stercoralis* developmental stages. We found that for many of the nematode-specific G_α subunit orthologs [250], transcript abundance reached a peak in L3i (Table 4.2, Figure 4.S2). In contrast, transcripts for *Ss-gpa-4* were detected in all developmental stages examined, except L3i. Transcripts from the conserved G_β subunit and G_γ subunit genes were found in all developmental stages examined (Table 4.2, Figure 4.S3).

8-bromo-cGMP activates *S. stercoralis* L3i

In previous studies, we observed an increase in transcripts encoding guanylyl cyclases in L3i [238], suggesting that one of the downstream effects of chemosensory 7TM GPCR signaling

through heterotrimeric G proteins, upon L3i encountering a permissive host, is an increase in the second-messenger cGMP. A similar pathway—and accompanying increase in cGMP—has been described in *C. elegans* in response to odorants [251]. Additionally, other research groups have used the membrane-permeable analog of cGMP, 8-bromo-cGMP, to test whether increases in cGMP can activate L3i in place of host-like cues in *Ancylostoma caninum* [66], *Ancylostoma ceylanicum* [68], and *Nippostrongylus brasiliensis* [71]. For each of these three hookworm species (clade 9B) [252], which are closely related to *C. elegans* (clade 9A), 8-bromo-cGMP results in activation of L3i at 5 mM for *A. caninum* and *A. ceylanicum* and 500 μM for *N. brasiliensis*.

To test whether increases in cGMP can activate L3i in place of host-like cues in *S. stercoralis* (clade 10B), where parasitism is thought to have arisen independently of the hookworm species [109], we applied 8-bromo-cGMP to *S. stercoralis* L3i and assessed activation in an *in vitro* activation assay [57,111]. We incubated *S. stercoralis* L3i in a mixture of biochemical host-like cues as a positive control, composed of DMEM supplemented with 10% canine serum and 12.5 mM reduced glutathione, M9 buffer as a negative control, and a range of 8-bromo-cGMP concentrations in M9 buffer for a total of 24 hours at 37°C and 5% CO_2 in air; we then assessed resumption of feeding, a hallmark of activation, by ingestion of a FITC fluorescent dye.

S. stercoralis L3i were activated by 8-bromo-cGMP, with 200 μM 8-bromo-cGMP resulting in 85.1% (±2.2, SD) of L3i feeding in comparison to 0.6% (±0.3, SD) for the M9 buffer negative control (Figure 4.1A). At much higher concentrations of 8-bromo-cGMP (e.g., 2 mM or greater), we observed L3i that were radially constricted in alternating segments along the longitudinal axis and that had a compromised cuticle, as evidenced by permeability to the FITC dye (data not shown).

To compare the kinetics of activation for *S. stercoralis* L3i in host-like cues with 8-bromo-cGMP, we examined the frequency of feeding over a 24-hour time course (Figure 4.1B). We determined the percentage of L3i feeding after incubation in 200 μM 8-bromo-cGMP or a mixture of DMEM, 10% canine serum, and 3.75 mM reduced glutathione, for 4, 6, 12, 18, and 24 hours at 37°C and 5% CO_2 in air. We found that 8-bromo-cGMP activated L3i much more rapidly than the mixture of biochemical host-like cues.

8-bromo-cGMP activation regulates expression of insulin-like peptide and TGFβ ligand transcripts in L3i

Studies in *C. elegans* have revealed that cGMP pathway signaling lies upstream of IIS and regulates transcript levels of *Ce-daf-28* and *Ce-ins-7*, both proposed to be *Ce*-DAF-2 insulin-like receptor agonists [138,139]. Previously, we identified seven ILPs in *S. stercoralis* and noted that the transcripts for several of these are developmentally regulated [238]. Additional studies in *C. elegans* have shown that cGMP pathway signaling also regulates the dauer TGFβ pathway, including transcript levels of the single dauer TGFβ ligand-encoding gene *Ce-daf-7* [137]. We previously described seven *daf-7*-like genes in *S. stercoralis*, named *Ss-tgh-1* through *-7*, and noted that *Ss-tgh-1*, *-2*, and *-3* transcripts were only detected in L3i [76,238]. In *A. caninum*, 8-bromo-cGMP activation has been correlated with the transcriptional profile observed with serum stimulation; however, no canonical dauer pathway component transcripts were examined in this study [70]. To determine whether cGMP signaling also regulates transcript levels of genes encoding ILP and dauer TGFβ ligands in *S. stercoralis* upon L3i activation, we performed reverse transcription quantitative PCR (RT-qPCR) to examine changes in transcript levels for *Ss-ilp-1* and *Ss-tgh-1* following L3i activation with 8-bromo-cGMP.

We found that *Ss-ilp-1* transcript levels were positively correlated with L3i activation, while *Ss-tgh-1* transcript levels were negatively correlated with L3i activation (Figure 4.2A-B). Indeed, *Ss-ilp-1* transcripts were increased 46.8 (±19.7, SD)-fold over unstimulated L3i when exposed to 8-bromo-cGMP (Figure 4.2A). Conversely, *Ss-tgh-1* transcripts decreased to a ratio of 0.32 (±0.08, SD) when L3i exposed to 8-bromo-cGMP were compared to unstimulated L3i (Figure 4.2B).

S. stercoralis ILP promoters are active in the nervous system and other tissues

In *C. elegans*, cGMP signaling regulates ILP transcript levels and the promoters of genes encoding ILPs are often active in the nervous system, intestine, and/or gonad [138,144]. These tissues are known to play important roles in regulating dauer development, longevity, and responses to environmental stresses [138,144,230]. Previously, we reported that the transcript abundances of three *S. stercoralis* ILPs, *Ss-ilp-1*, *-6*, and *-7*, are differentially regulated during post-free-living development [238]. To determine whether these three *S. stercoralis* ILPs are expressed in similar tissues as *C. elegans* ILPs, we made promoter::enhanced green fluorescent protein (*egfp*) reporter constructs for *Ss-ilp-1*, *-6*, and *-7* and expressed these in transgenic *S. stercoralis* post-free-living larvae.

We observed EGFP under control of the *Ss-ilp-1* promoter in the hypodermis/body wall as well as a single pair of head neurons (Table 4.3, Figure 4.3A-D). The promoter activity for *Ss-*

ilp-6 was similar to *Ss-ilp-1*, with EGFP observed in the hypodermis/body wall and head neurons; however, *Ss-ilp-6* promoter activity was observed in several pairs of head neurons and tail neuron(s), while *Ss-ilp-1* promoter activity was limited to a single pair of head neurons (Table 4.3, Figure 4.3E-H). EGFP under control of the *Ss-ilp-7* promoter was localized to the intestine as well as a single pair of head neurons with a single process that extended dorsally almost to the anterior portion of the intestine (Table 4.3, Figure 4.3M-P). The location and shape of this pair of neurons is most consistent with SIAV in *C. elegans*.

Unexpectedly, we observed that in a small number of larvae (4/39) expressing the *Ss-ilp-6* promoter::*egfp* reporter construct, tail development was abnormal, resulting in a "club-like" tail (Figure 4.3I-L). This phenotype was observed regardless of whether EGFP was observed in a tail neuron (Figure 4.3I-L) and was not observed in any larvae for either the *Ss-ilp-1* or *Ss-ilp-7* constructs. We have also never observed this phenotype in non-transformed larvae.

4.5 Discussion

In this study, we sought to determine whether cGMP pathway signaling regulates *S. stercoralis* L3i activation and the IIS and dauer TGFβ signaling pathways through modulation of their cognate ligands. Additionally, we sought to describe the upstream components that regulate the second messenger cGMP, including chemosensory 7TM GPCRs and heterotrimeric G proteins. We hypothesized that this chemosensory pathway may be one of the first to transduce host cues when *S. stercoralis* L3i encounter a permissive host. This hypothesis was based on our previous observation that the transcripts of multiple cGMP pathway components are increased in *S. stercoralis* L3i, suggesting that this pathway may be "poised" to transduce host cues [238], and studies demonstrating that exogenous application of 8-bromo-cGMP activates L3i of hookworm species [66,68,71]. We therefore sought to describe the components of a chemosensory 7TM GPCR signaling pathway in *S. stercoralis* and determine whether cGMP signaling regulates L3i activation as well as IIS and/or TGFβ pathways.

Using RNAseq data from seven *S. stercoralis* developmental stages and draft *S. stercoralis* genomic contigs, we identified and characterized the developmental transcript profiles for many of the *S. stercoralis* chemosensory 7TM GPCRs. For these 85 chemosensory 7TM GPCRs, the vast majority had transcripts found in L3i and/or L3+ (Table 4.1), and transcripts were found at low abundances in comparison to other *S. stercoralis* genes; these data are highly suggestive of a role for these receptors acting in a few chemosensory cells to sense host cues.

Our RNAseq data set does not include the free-living male or autoinfective L3 (L3a) developmental stages, which must use chemosensory cues to seek out females or migrate within the host, respectively. These developmental stages may express specific chemosensory 7TM GPCRs that control these functions, the transcripts of which may only be found in these stages and thus absent in our data set.

The paucity of chemosensory 7TM GPCR-encoding genes in *S. stercoralis* in comparison to *C. elegans* is not entirely surprising given the evolutionary distance separating *S. stercoralis* (clade 10B) and *C. elegans* (clade 9A) [252] and the large differences in the number of chemosensory 7TM GPCRs among even closely related nematode species [248]. The differences in the number of chemosensory 7TM GPCR genes within the well-studied *Caenorhabditis* genus is illustrated by the fact that there are approximately 40% more chemosensory 7TM GPCR-encoding genes in the *C. elegans* genome (1,646 genes) than in the *C. briggsae* genome (1,151 genes) [248]. Thus, the chemosensory 7TM GPCR family of receptors appears to have a great deal of evolutionary plasticity in terms of absolute number and ligand specificity. Additionally, *S. stercoralis*, like many parasitic nematodes, predominately resides inside a nutrient-rich host or in bacteria-rich feces and thus does not need to continually navigate and adapt to a complex external environment with limited resources. Thus, the need for chemosensory 7TM GPCRs in *S. stercoralis* is mainly limited to L3i sensing a host, larval migration within the host, and free-living male and female mate attraction during heterogonic development. These differences in lifestyle between *S. stercoralis* and *C. elegans* may partially account for the smaller number of 7TM GPCR-encoding genes in *S. stercoralis*.

We used a similar strategy to identify G proteins in *S. stercoralis*; however, the sequence divergence between *S. stercoralis* and *C. elegans* of the proteins these genes encode is far less than for the chemosensory 7TM GPCRs. By phylogenetic analysis, we were able to identify the *C. elegans* ortholog for each of the *S. stercoralis* G_{α}-, G_{β}-, and G_{y}-encoding genes (Table 4.2, Figures S4.1, S4.2, & S4.3). Interestingly, *S. stercoralis* appears to only have 14 G_{α}-encoding genes in comparison to the 21 in *C. elegans*. This observation is congruous with the smaller number of chemosensory 7TM GPCRs in *S. stercoralis*, since fewer receptors would need fewer signal transduction molecules. Many of the nematode-specific G_{α}-encoding genes have transcripts that are at their peak in L3i (Table 4.2, Figure S4.2). Along with our previous observation that the *Ss-gpa-3* promoter is active in amphidial neurons [90], these data are consistent with a role for *S. stercoralis* G_{α} subunits in relaying environmental and host chemosensory cues in L3i.

Using a previously established *S. stercoralis* L3i feeding assay [57,111], we demonstrated that exogenous application of the membrane-permeable cGMP analog 8-bromo-cGMP stimulates L3i activation (Figure 4.1A) with a higher potency than that observed in experiments with other parasitic nematodes [66,68,71]. Furthermore, application of 8-bromo-cGMP activated L3i more quickly than a mixture of biochemical host-like cues (Figure 4.1B). These data suggest that increases in endogenous cGMP levels accompany *S. stercoralis* L3i activation upon encountering a permissive host. Since previous work has demonstrated 8-bromo-cGMP activation only in hookworm species [66,68,71], which are closely related to *C. elegans* [252], these findings from the distantly related *S. stercoralis*, where parasitism is thought to have arisen independently from the hookworm species [109], suggest a more broadly conserved mechanism of L3i activation in parasitic nematodes.

In *C. elegans*, cGMP pathway signaling regulates both the IIS pathway as well as the dauer TGFβ pathway [137-139]. Using RT-qPCR, we demonstrated that activation of *S. stercoralis* L3i by 8-bromo-cGMP was accompanied by a dramatic increase in *Ss-ilp-1* transcripts as well as a decrease in *Ss-tgh-1* transcripts (Figure 4.2). In previous work, we described *Ss-ilp-1* as a putative IIS agonist, due to protein sequence similarities with *C. elegans* agonistic ILPs and a decrease in transcript levels during parasitic development [238]; thus, our data suggest that *Ss-ilp-1* transcripts increase immediately following L3i activation, but then decrease again during development to the parasitic female, consistent with a role as an agonistic ILP. Although developmental regulation of dauer TGFβ pathway homologs and an increase in the number of dauer TGFβ ligands from one to seven in *S. stercoralis* suggests a different role for this pathway than in *C. elegans*, the dauer TGFβ pathway does appear to be important in L3i, since three of the TGFβ ligands have transcripts only detected in L3i [238]. Our observation that *Ss-tgh-1* transcripts are decreased following L3i activation is consistent with these previously described data, which have described a role for TGFβ signaling in parasitic nematodes that is opposite to its apparent role in *C. elegans* dauer regulation [72-76]. Together, our RT-qPCR results suggest that, as in *C. elegans*, cGMP pathway signaling is upstream of both IIS and dauer TGFβ signaling in *S. stercoralis*.

Since our data demonstrate that ILP transcript levels are modulated during L3i activation with 8-bromo-cGMP, we expressed *S. stercoralis* ILP promoter::*egfp* reporter constructs in the post-free-living generation to determine the tissues in which ILP promoters are active. We found that *Ss-ilp-1* and *Ss-ilp-6* promoters are active in head neurons as well as the hypodermis/body wall (Figure 4.3A-H); in previous work, we hypothesized that both of these ILPs act as IIS

agonists [238]. Interestingly, our data suggest that mis-regulation of the native *Ss-ilp-6* locus results in abnormal tail formation (Figure 4.3I-L). Since the *Ss-ilp-6* promoter::*egfp* reporter construct does not contain any coding sequence for *Ss-ilp-6*, this phenotype may be a result of alterations in transcription factor binding at the endogenous *Ss-ilp-6* locus, potentially caused by transcriptional co-factors being recruited away from the endogenous promoter to the multiple copies of the promoter present in the extra-chromosomal array. Additionally, we found that the *Ss-ilp-7* promoter is active in both a single pair of head neurons as well as the intestine (Figure 4.3M-P). We previously hypothesized that *Ss-ilp-7* acts as an IIS antagonist [238]. The promoter activity of *S. stercoralis* ILPs in hypodermal, neuronal, and intestinal tissues is consistent with anatomical locations of *C. elegans* ILP promoter activity [144].

Our model, whereby cGMP signaling regulates *S. stercoralis* L3i activation, is not entirely analogous to the role of cGMP signaling in regulating *C. elegans* dauer development. In *C. elegans*, elevated levels of ascarosides, which accompany high population density, bind chemosensory 7TM GPCRs that activate inhibitory G proteins that repress the guanylyl cyclase *Ce*-DAF-11, ultimately decreasing cGMP levels and promoting dauer entry [33]. In contrast, we hypothesize that in *S. stercoralis* L3i, host compounds bind chemosensory 7TM GPCRs, which activate G proteins that in turn activate guanylyl cyclases that increase cGMP levels; this ultimately triggers L3i to activate and resume development, in part through increased IIS and decreased dauer TGFβ signaling. Although this hypothesized chain of events is strongly supported by this work and previous studies, future studies are still needed to rigorously demonstrate the specific roles of these pathways in regulating L3i development.

4.6 Figures

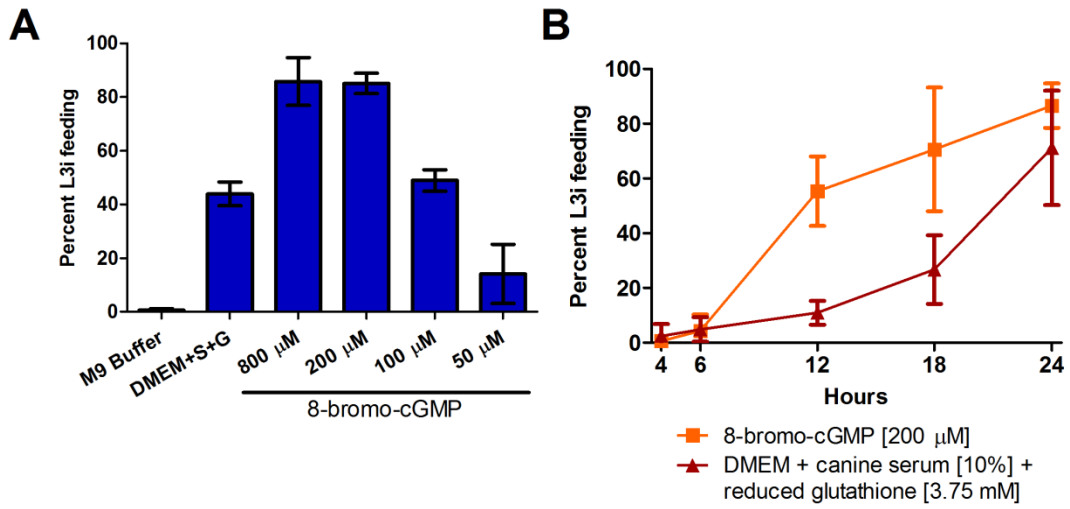

Figure 4.1. *S. stercoralis* L3i are activated by 8-bromo-cGMP.
The membrane permeable cGMP analog, 8-bromo-cGMP, induced resumption of feeding, a hallmark of activation, in *S. stercoralis* L3i. Feeding was assessed by ingestion of a FITC dye after incubation at 37°C and 5% CO_2 in air for 24 hours for all conditions. (A) At 200 μM, 8-bromo-cGMP dissolved in M9 buffer results in potent resumption of feeding in L3i, with 85.1% (±2.2, SD) of larvae feeding after 24 hours. In comparison, host-like cues consisting of DMEM, 10% canine serum (S), and 12.5 mM reduced glutathione (G), resulted in 43.9% (±2.6, SD) of L3i feeding, while the M9 buffer negative control resulted in 0.6% (±0.3, SD) of L3i feeding, after 24 hours. (B) Kinetics of activation were determined for both 200 μM 8-bromo-cGMP and host-like cues, consisting of DMEM, 10% canine serum, and 3.75 mM reduced glutathione, after incubation for 4, 6, 12, 18, or 24 hours. All conditions were incubated for a total of 24 hours at 37°C and 5% CO_2 in air. Error bars represent ± 1 standard deviation (SD).

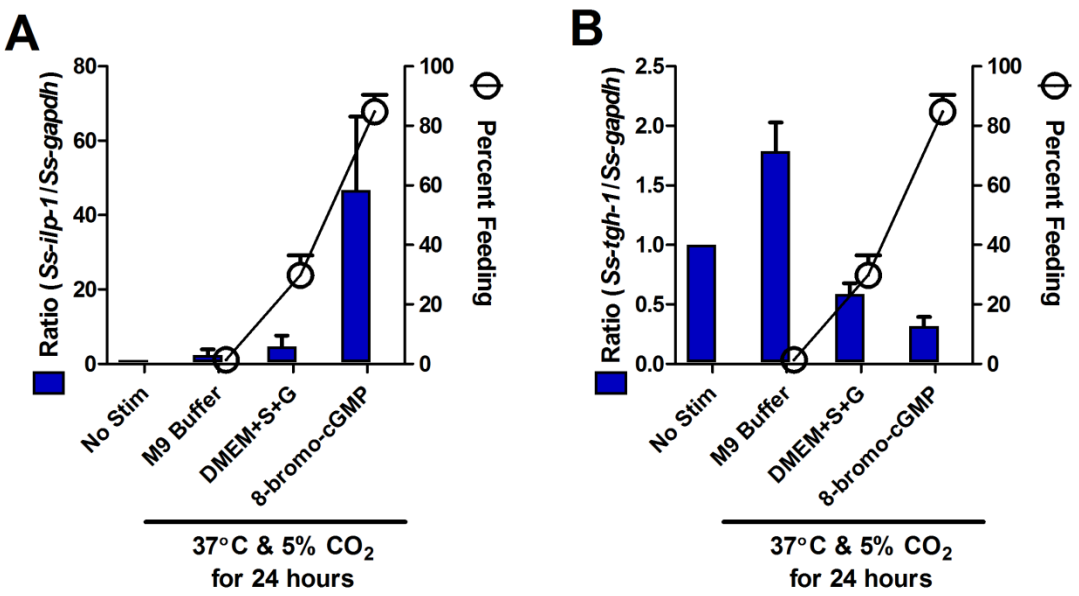

Figure 4.2. 8-bromo-cGMP L3i activation modulates ILP and TGFβ ligand transcript levels. Transcript levels of the insulin-like peptide (ILP) ligand-encoding gene *Ss-ilp-1* and dauer transforming growth factor β (TGFβ) ligand-encoding gene *Ss-tgh-1* were quantified using RT-qPCR following *S. stercoralis* L3i activation in 8-bromo-cGMP. Conditions included L3i that had no stimulation (only exposed to room temperature conditions in M9 buffer) as well as L3i incubated at 37°C and 5% CO2 for 24 hours in either M9 buffer; DMEM, 10% canine serum, and 3.75 mM reduced glutathione; or 200 μM 8-bromo-cGMP. Gene-specific transcript levels were normalized to *Ss-gapdh* transcript levels and the unstimulated control using the Pfaffl Method and the ratio plotted as the mean +1 SD (left y-axis). The mean percentage of L3i that resumed feeding in each of the stimulated conditions was also plotted +1 SD (right y-axis).

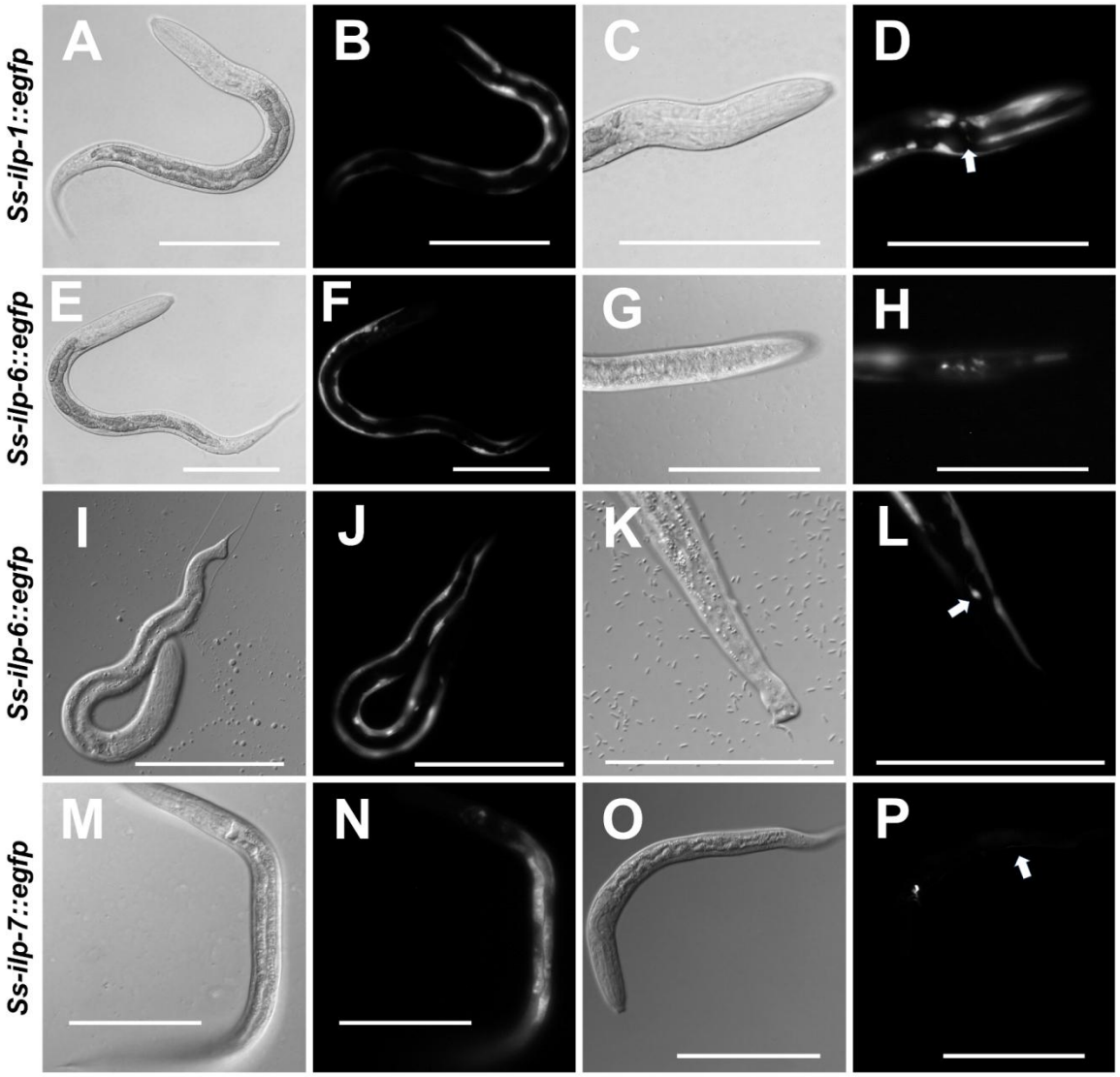

Figure 4.3. *S. stercoralis* ILP promoters are active in the nervous system and other tissues. Transgenic *S. stercoralis* post-free-living larvae expressing enhanced green fluorescent protein (EGFP) under the control of three insulin-like peptide (ILP) promoters were assessed for tissue-specific expression. (A-D) Transgenic larvae carrying the *Ss-ilp-1* promoter::*egfp* reporter construct; (A,C) DIC images and (B, D) fluorescent images. The *Ss-ilp-1* promoter is active in the hypodermis/body wall and a single pair of head neurons (D, arrow). (E-L) Transgenic larvae carrying the *Ss-ilp-6* promoter::*egfp* reporter construct; (E,G,I,K) DIC images and (F,H,J,L) fluorescent images. The *Ss-ilp-6* promoter is active in the hypodermis/body wall, several head neurons, and a tail neuron (L, arrow). (I-L) A minority (4/39) of transgenic larvae carrying the *Ss-ilp-6* promoter::*egfp* reporter construct had abnormal tail development, resulting in a "club-like" tail. (M-P) Transgenic larvae carrying the *Ss-ilp-7* promoter::*egfp* reporter construct; (M,O) DIC images and (N,P) fluorescent images. The *Ss-ilp-7* promoter is active in the intestine and a single pair of head neurons, with a single process that extends dorsally almost to the anterior portion of the intestine (P, arrow), most consistent with SIAV in *C. elegans*.

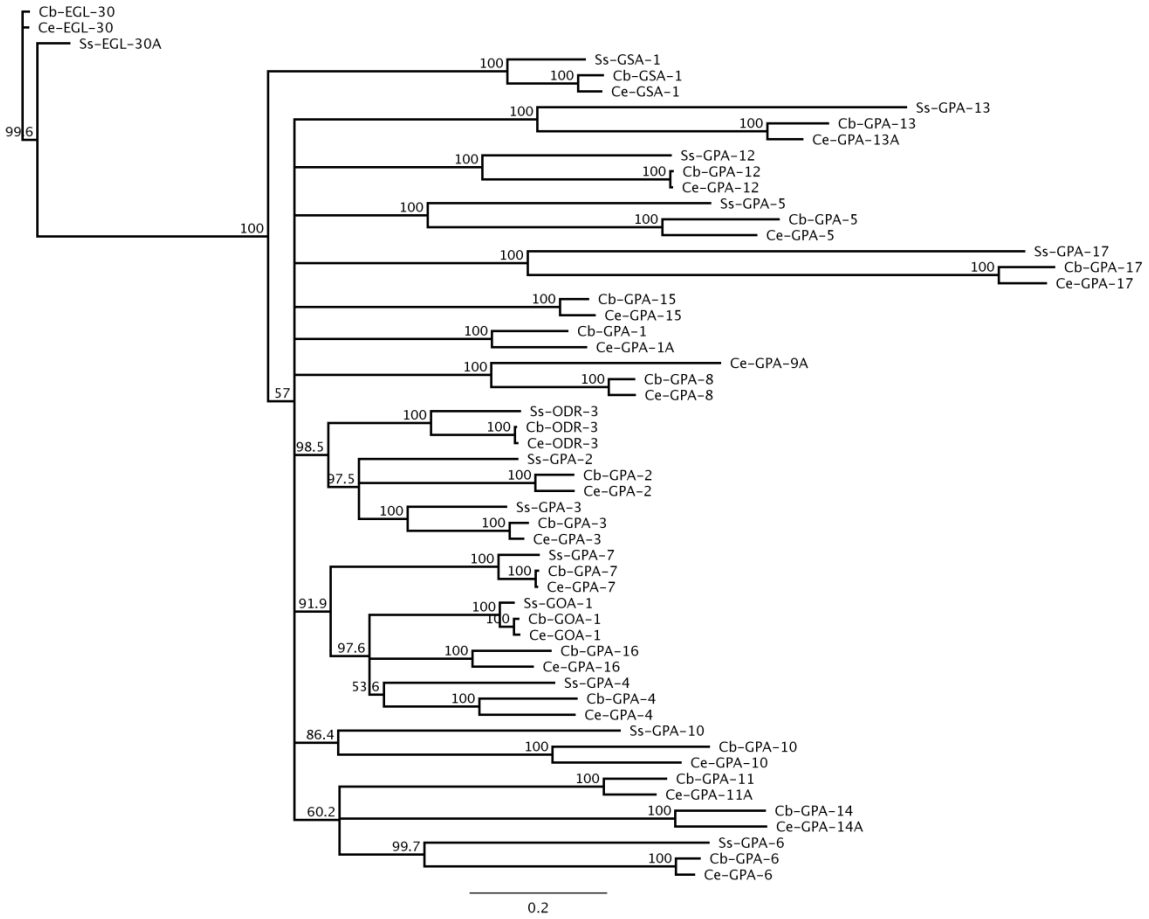

Figure 4.S1. Phylogenetic analysis of *S. stercoralis* and *Caenorhabditis* spp. Gα proteins.
A protein alignment, generated with Clustal W, of *S. stercoralis* (Ss), *C. briggsae* (Cb), and *C. elegans* (Ce) heterotrimeric G protein α subunit (Gα) homologs was used to construct a neighbor-joining tree with 100 iterations of boot-strapping. Orthologs for several *C. briggsae* and *C. elegans* Gα-encoding genes (*gpa-1*, *-8*, *-9*, *-11*, *-14*, *-15*, and *-16*) were not identified in the *S. stercoralis* draft genome or *de novo* assembled transcripts. The scale bar represents substitutions per position.

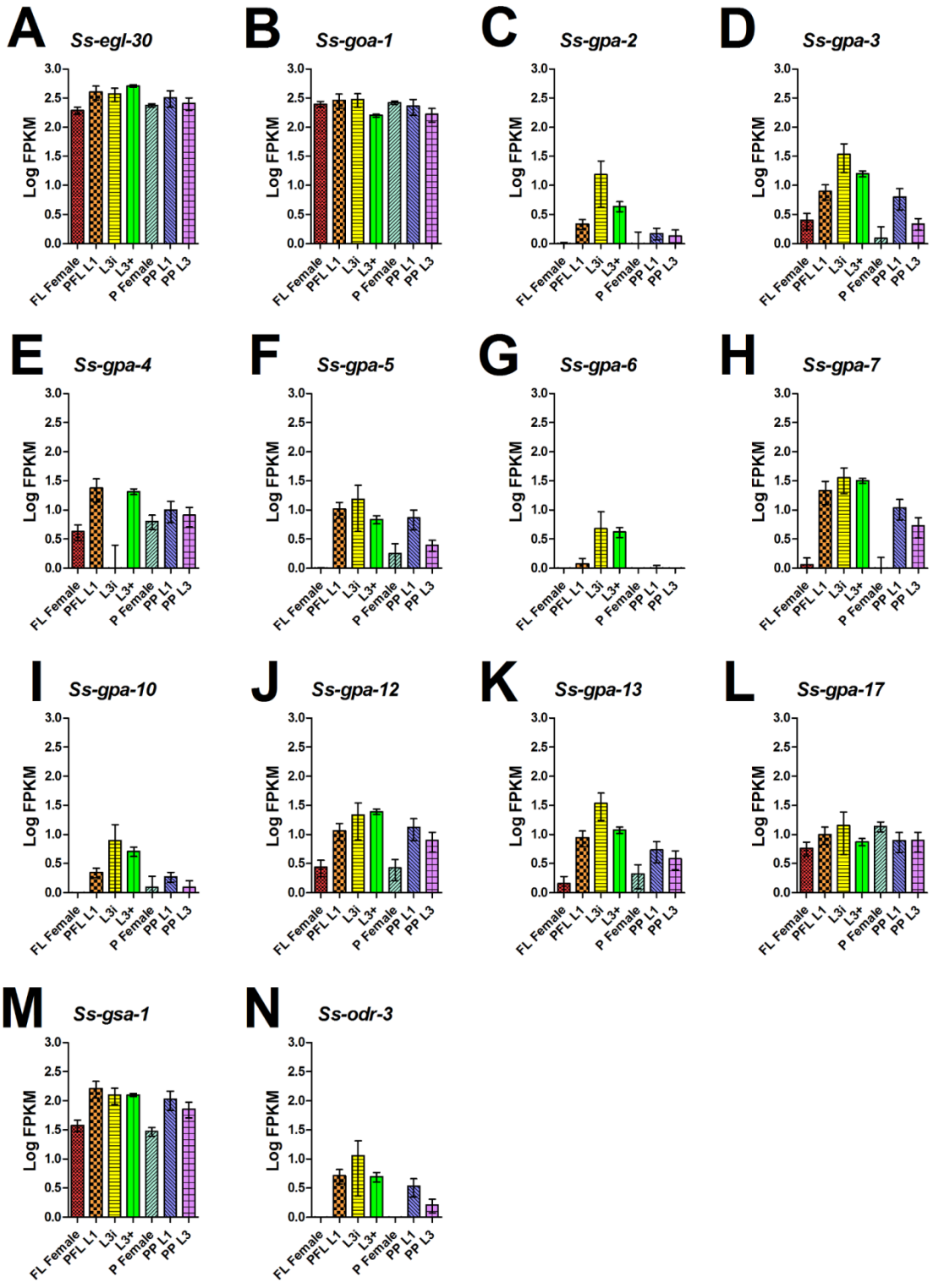
A
Ss-egl-30
B
Ss-goa-1
C
Ss-gpa-2
D
Ss-gpa-3
E
Ss-gpa-4
F
Ss-gpa-5
G
Ss-gpa-6
H
Ss-gpa-7
I
Ss-gpa-10
J
Ss-gpa-12
K
Ss-gpa-13
L
Ss-gpa-17
M
Ss-gsa-1
N
Ss-odr-3
Log FPKM
3.0
2.5
2.0
1.5
1.0
0.5
0.0
FL Female
PFL L1
L3i
L3+
P Female
PP L1
PP L3

Figure 4.S2. Developmental regulation of transcripts encoding *S. stercoralis* Gα subunits.
(A-N) Transcript abundance patterns in *S. stercoralis* developmental stages were determined by RNAseq for genes encoding orthologs of heterotrimeric G protein α subunits (Gα). Transcript abundances were quantified in seven developmental stages: free-living females (FL Female), post-free-living first-stage larvae (PFL L1), infectious third-stage larvae (L3i), *in vivo* activated third-stage larvae (L3+), parasitic females (P Female), post-parasitic first-stage larvae (PP L1), and post-parasitic third-stage larvae (PP L3). Transcript abundances were calculated as fragments per kilobase of coding exon per million mapped reads (FPKM) and log transformed. Error bars represent 95% confidence intervals. The y-axes were scaled from 0 to 3.0 to aid comparison between genes.

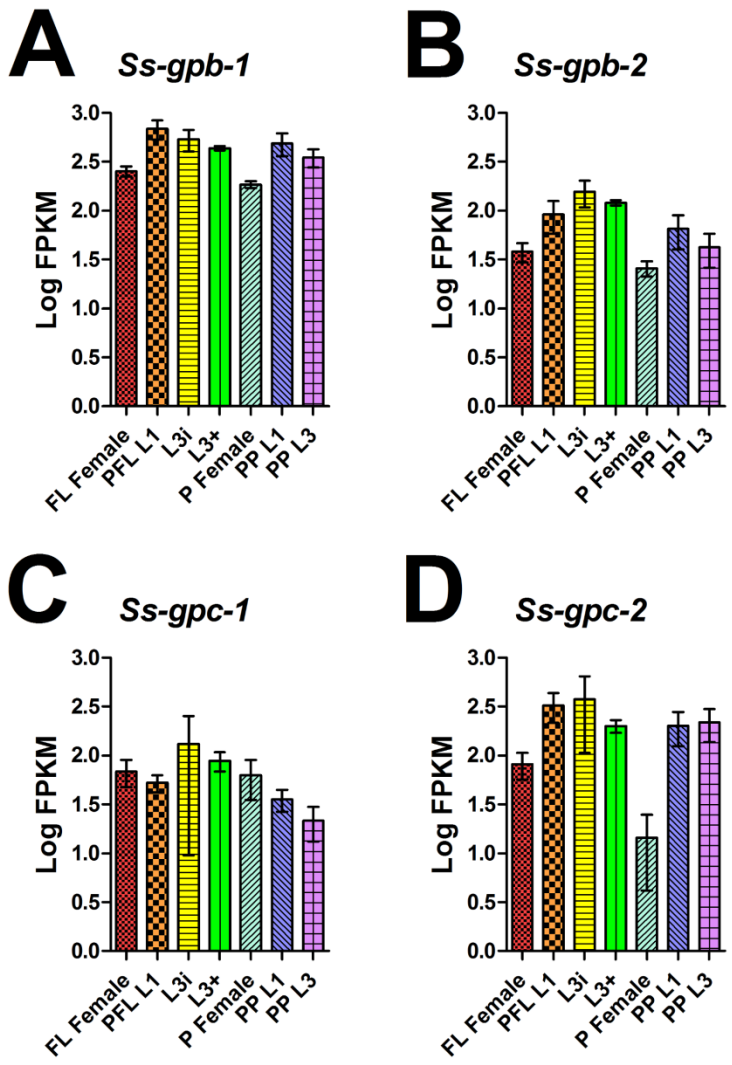

Figure 4.S3. Developmental regulation of transcripts encoding *S. stercoralis* G_β and G_γ subunits. (A-D) Transcript abundance patterns in *S. stercoralis* developmental stages were determined by RNAseq for genes encoding homologs of heterotrimeric G-protein β (G_β) subunits (A,B) and γ (G_γ) subunits (C,D). Transcript abundances were quantified in seven developmental stages: free-living females (FL Female), post-free-living first-stage larvae (PFL L1), infectious third-stage larvae (L3i), *in vivo* activated third-stage larvae (L3+), parasitic females (P Female), post-parasitic first-stage larvae (PP L1), and post-parasitic third-stage larvae (PP L3). Transcript abundances were calculated as fragments per kilobase of coding exon per million mapped reads (FPKM) and log transformed. Error bars represent 95% confidence intervals. The y-axes were scaled from 0 to 3.0 to aid comparison between genes.

4.7 Tables

Table 4.1. Transcript abundance of *S. stercoralis* homologs of *C. elegans* chemosensory 7TM GPCRs.

C. elegans superfamily	Transcripts in L3i only	Transcripts in L3+ only	Transcripts in L3i & L3+	Transcripts in other stages	Transcripts not detected	Total number
***Ss*-SRA**	1	1	3	1	5	11
***Ss*-SRG**	6*	2	9	7	29	53*
***Ss*-SRSX**	-	-	-	1	1	2
***Ss*-STR**	5	2	2	1	9	19

*Includes one gene with a premature "stop" codon.

Table 4.2. Identification of *S. stercoralis* heterotrimeric G protein orthologs.

G protein	*C. elegans*	*S. stercoralis*	*S. stercoralis* transcript abundance profile
G_{α} subunits			
G_{ns}	*Ce*-GPA-1	np	
	Ce-GPA-2	*Ss*-GPA-2	peak in L3i
	Ce-GPA-3	*Ss*-GPA-3	peak in L3i
	Ce-GPA-7	*Ss*-GPA-7	peak in L3i
	Ce-GPA-8	np	
	Ce-GPA-9	np	
	Ce-GPA-10	*Ss*-GPA-10	peak in L3i
	Ce-GPA-15	np	
	Ce-ODR-3	*Ss*-ODR-3	peak in L3i
G_{nsd}	*Ce*-GPA-11	np	
	Ce-GPA-13	*Ss*-GPA-13	peak in L3i
	Ce-GPA-14	np	
	Ce-GPA-17	*Ss*-GPA-17	present in all stages examined
$G_{i/o}$	*Ce*-GOA-1	*Ss*-GOA-1	present in all stages examined
	Ce-GPA-4	*Ss*-GPA-4	absent in L3i
	Ce-GPA-16	np	
G_{q}	*Ce*-EGL-30	*Ss*-EGL-30	present in all stages examined
G_{s}	*Ce*-GSA-1	*Ss*-GSA-1	present in all stages examined
G_{12}	*Ce*-GPA-5	*Ss*-GPA-5	peak in L3i
	Ce-GPA-6	*Ss*-GPA-6	only detected in PFL L1, L3i, and L3+
	Ce-GPA-12	*Ss*-GPA-12	peak in L3i
G_{β} subunits	*Ce*-GPB-1	*Ss*-GPB-1	present in all stages examined
	Ce-GPB-2	*Ss*-GPB-2	present in all stages examined
G_{γ} subunits	*Ce*-GPC-1	*Ss*-GPC-1	present in all stages examined
	Ce-GPC-2	*Ss*-GPC-2	nadir in P female

Note: G_{ns}, nematode-specific G_{α} subunit; G_{nsd}, divergent nematode-specific G_{α} subunit; np, not present in the *S. stercoralis* genomic contigs or *de novo* assembled transcripts.

Table 4.3. Location of EGFP expression in transgenic *S. stercoralis* post-free-living larvae under the control of ILP promoters.

Promoter	Intestine	Hypodermis/ body wall	Head neuron(s)	Tail neuron(s)	Pharnyx	Other cell body	Total number
Ss-ilp-1	0 (0%)	40 (100%)	20 (50%)	1 (3%)	0 (0%)	2 (5%)	n=40
Ss-ilp-6	0 (0%)	39 (100%)	20 (51%)	6 (15%)	1 (3%)	0 (0%)	n=39
Ss-ilp-7	21 (100%)	1 (5%)	18 (81%)	1 (5%)	0 (0%)	1 (5%)	n=21

CHAPTER 5 - Discussion

Since parasitic nematodes are responsible for a vast global disease burden in not only humans, but also animals and plants of agricultural importance, understanding the mechanisms by which these organisms infect their hosts is of significant health and economic importance [3]. In humans, soil-transmitted parasitic nematodes that cause hookworm disease and strongyloidiasis, as well as vector-transmitted parasitic nematodes that cause filariasis, have devastating health impacts worldwide [5,6]. The infectious form of the species that cause each of these diseases is a developmentally arrested third-stage larva (L3i) [2]. Understanding the molecular mechanisms regulating the developmental arrest as well as activation of L3i once they enter a host may lead to new therapeutics and control strategies.

One of the guiding paradigms in the field to understand the mechanisms controlling L3i development has been the "dauer hypothesis," which posits that the comparatively well-understood mechanisms controlling developmental arrest of the dauer third-stage larva, a facultative life stage of the free-living nematode *Caenorhabditis elegans*, are similar to those controlling L3i arrest and activation in parasitic nematodes. Limited studies have suggested that the same pathways regulating dauer entry act in reverse to govern dauer exit in *C. elegans* [60,147], but relative to the large body of data on dauer entry, the data on mechanisms governing dauer exit are few. This caveat is of direct importance to the study of L3i development in parasitic nematodes, since the pathways controlling dauer exit (analogous to L3i activation) may differ from the well-studied pathways controlling dauer entry (analogous to L3i developmental arrest). However, this thesis, and the tests of the dauer hypothesis carried out therein, has operated under the assumption that the pathways controlling *C. elegans* dauer arrest are also crucial for governing dauer exit.

In *C. elegans*, four cellular signaling pathways control dauer development [30,41]. Prior to the work described in this thesis, it had been unclear whether all components in these four canonical dauer pathways are present in parasitic nematodes or what role they play in regulating L3i development. While previous studies had cloned a few components from each of the four pathways in parasitic nematodes [75,80,87,88], this work had left in question whether each entire pathway is present and functional; this is a well-warranted question, since critic al components of other evolutionarily conserved signaling pathways are absent in many parasitic nematode species [93]. Additionally, previous work on one particular pathway, the dauer transforming growth factor β (TGFβ) signaling pathway, provided evidence that in parasitic nematodes this pathway

functions in a manner directly opposite to that predicted from the dauer hypothesis [77]. Together, these uncertainties have led to much speculation about the validity of the dauer hypothesis and about the actual mechanisms controlling L3i development.

Although this thesis does not fully resolve all of these questions, it does shed significant new light on the components and potential functions of the canonical dauer pathways in the parasitic nematode *Strongyloides stercoralis*. This parasitic nematode was chosen as a model due to unique facets of the life cycle, including a single facultative free-living generation, and the availability of molecular tools unavailable in other parasitic nematode species, which together facilitate investigation of the factors controlling L3i development [10]. Specifically, the developmental checkpoint in the post-parasitic generation, leading to either direct (parasitic via the L3i) or indirect (free-living) development, the invariant development directly to L3i in the post-free-living generation, and the rapid resumption of development inside a host each provide unique aspects of the life cycle to probe for factors regulating L3i development [8].

The work covered in chapter 2 used next-generation deep sequencing of the *S. stercoralis* transcriptome (RNAseq) in seven developmental stages to identify homologs for each of the components in the four canonical dauer signaling pathways [238]. This work represented, for the first time, a complete identification of all the canonical dauer signaling pathway components in any parasitic nematode species. Additionally, the RNAseq data generated in this study allowed for the precise quantification of transcript abundance for each of the canonical dauer pathway components, thereby enabling an inference of the function of these pathways in *S. stercoralis*. As with any study examining changes in transcript abundance, this RNAseq study assumed that changes in transcript abundance are directly correlated with changes in protein levels, thereby regulating biological function. However, many additional mechanisms of regulating protein levels and function exist, including regulation of transcripts by microRNAs or other non-coding RNAs, rates of mRNA translation, post-translational modifications, and protein stability. For many of the signaling proteins examined, phosphorylation is the primary means of regulating biological activity, not transcript abundance; however, for other genes, particularly ligands and receptors, developmental regulation of transcripts is crucial for regulating biological function.

Several key observations were made in the RNAseq study described in chapter 2. First, transcripts from all components of the cyclic guanosine monophosphate (cGMP) signaling pathway examined were up-regulated in L3i, suggesting a role for this pathway in transducing host cues. These observations directly led to the studies described in chapter 4. Second, a paucity of insulin-like peptides (ILPs) in the insulin/IGF-1-like signaling (IIS) pathway, in

comparison to *C. elegans*, was striking, suggesting a less complicated modulation of IIS in S. *stercoralis* than in *C. elegans*. Furthermore, transcripts for several of these *S. stercoralis* ILPs (e.g., *Ss-ilp-1*, *Ss-ilp-6*, and *Ss-ilp-7*) were differentially regulated during L3i development, providing further evidence that this pathway is involved in regulating *S. stercoralis* L3i arrest and activation. Third, seven homologs of the single *C. elegans daf-7* dauer TGFβ ligand were discovered in *S. stercoralis*. The transcripts for three of these genes were present only in L3i, suggesting a role in regulating L3i arrest and/or host immune system modulation—a role divergent from *C. elegans daf-7*. Finally, *S. stercoralis* homologs of dafachronic acid (DA) biosynthetic enzymes were not coordinately regulated during L3i development leading to equivocal results about endogenous DA regulation of the DAF-12 nuclear hormone receptor (NHR) homolog. Together, this RNAseq study presented the first comprehensive picture of canonical dauer pathway regulation in any parasitic nematode species and demonstrated that two of these pathways (IIS and cGMP pathway signaling) likely have conserved function with their *C. elegans* counterparts, while at least one (dauer TGFβ signaling) likely has a different function. However, it remains undetermined whether these pathways are present in other parasitic nematode species and how their transcriptional regulation compares with both *S. stercoralis* and *C. elegans*.

The IIS pathway in *S. stercoralis* has been well-studied in comparison to the other canonical dauer signaling pathways. Previous work had established that the downstream FOXO-like DAF-16 homolog in *S. stercoralis* is important in L3i morphogenesis and arrest [78], similar to the role of *C. elegans* DAF-16 in IIS and dauer development [217]. However, prior to this thesis, it was unknown whether IIS is involved in L3i activation. Thus, chapter 3 focused on the *S. stercoralis age-1* phosphatidylinositol-3 kinase (PI3K) homolog—a critical mediator of IIS in *C. elegans*. These studies demonstrated that *S. stercoralis age-1* is expressed in similar tissues as *C. elegans age-1* and that transcripts are present in all developmental stages, as would be expected for a signaling pathway component. Most importantly, this work demonstrated that a PI3K inhibitor, LY294002, prevents L3i activation in the presence of host-like cues, suggesting a role for IIS in regulating the infectious process. These studies reinforced the hypothesis that with regard to regulation of larval development, IIS in *S. stercoralis* functions similarly to IIS in *C. elegans*, as would be predicted from the dauer hypothesis [111].

In spite of this progress, there are several unanswered questions regarding IIS in *S. stercoralis* and other parasitic nematodes. Experiments to determine whether IIS controls switching between direct or indirect development in *S. stercoralis* have been inconclusive, in part

due to the inability to procure developmentally uncommitted larvae. Additionally, the role of IIS in L3i activation has been limited to pharmacological studies; genetic evidence would greatly increase the robustness of this conclusion. With only seven ILPs in *S. stercoralis*, redundancy is reduced in comparison to *C. elegans*, and it should be possible to determine specific roles for several of these ILPs using existing tools. Although IIS has been examined in three species of hookworm [81,82,84], this pathway has remained largely unexamined in other parasitic nematode species.

While the amphidial neurons and the host cues that L3i sense have been well studied in *S. stercoralis* [16-19,54,57], the molecular pathway(s) that transduce these host cue signals have been relatively neglected. In *C. elegans*, environmental cues are largely sensed by over 1,600 chemosensory seven transmembrane G-protein coupled receptors (7TM GPCRs) [248], several of which are known to signal through a cGMP pathway [33,133,242]. Transcripts of many components in this pathway were significantly increased in L3i, as described in chapter 2. Thus, chapter 4 focused on the role of cGMP pathway signaling in regulating L3i activation.

These studies demonstrated that exogenous application of 8-bromo-cGMP, a membrane-permeable analog of the second messenger cGMP, potently activated L3i. Additional work demonstrated that L3i activation with 8-bromo-cGMP regulates transcript levels of both an ILP and a dauer TGFβ ligand in *S. stercoralis*. These results suggest that cGMP pathway signaling plays an important role in *S. stercoralis* L3i activation, similar to hookworms [66,68,71], and that this pathway is upstream of both IIS and dauer TGFβ signaling, as in *C. elegans* [41]. While cGMP pathway signaling in parasitic nematodes and *C. elegans* appears to be important for sensing "environmental" cues (host cues or dauer pheromones, respectively), the actual ligands appear to differ markedly between *C. elegans* and its parasitic counterparts.

Although cGMP pathway signaling is important for L3i activation in both *S. stercoralis* and hookworms, no specific 7TM GPCR and host cue ligand interactions have been investigated. Chapter 4, which focuses on *S. stercoralis*, presents the most comprehensive survey of parasitic nematode chemosensory 7TM GPCRs to date and describes the developmental stages where their transcripts are expressed. However, this type of survey has not yet been conducted in any other parasitic nematode species. Nevertheless, from this limited information, it is clear that chemosensory 7TM GPCRs are highly divergent between different nematode species and that their transcripts are precisely regulated during different developmental stages. Since 7TM GPCRs are the targets of a large percentage of current chemotherapeutics [253], these would present excellent targets against which to screen new highly specific anthelmintics. However,

new chemotherapeutics with wide anthelminthic activity would be best screened against members of more conserved 7TM GPCR families.

While the studies encompassed in chapters 2, 3, and 4 have neither resolved all aspects of the dauer hypothesis nor elucidated all mechanisms regulating L3i arrest and activation, they have shed considerable light in these two areas. In *S. stercoralis*, the canonical dauer pathway homologs and transcript regulation of these components have been well characterized, and significant progress has been made in demonstrating roles for IIS and cGMP pathway signaling in regulating L3i development. Additionally, data in chapter 4 suggest that the epistatic relationships in *C. elegans* between cGMP signaling and downstream IIS and dauer TGFβ signaling are conserved in *S. stercoralis*. Together, these data suggest that the dauer hypothesis is a useful paradigm for generating hypotheses regarding the pathways controlling L3i development in parasitic nematodes. The striking exception to this conclusion is dauer TGFβ signaling. Both the increase in the number of dauer TGFβ ligands in *S. stercoralis* in comparison to *C. elegans* as well as the developmental regulation of several of these transcripts in diametric opposition to *Ce-daf-7* transcripts suggest that dauer TGFβ signaling has been co-opted by *S. stercoralis* for a process entirely different from its pro-reproductive function in *C. elegans*. These data, therefore do not support that aspect of the dauer hypothesis that pertains to dauer TGFβ signaling, a result which emphasizes the necessity of directly testing this hypothesis in the parasitic nematodes of interest.

In future studies, two additional lines of experimentation would aid further elucidation of mechanisms regulating L3i development in parasitic nematodes. First, in contrast to the present hypothesis-driven study, an unbiased genome-wide examination of transcripts differentially regulated during L3i development using existing RNAseq data could elucidate additional pathways that control L3i arrest and activation. A pathway with transcripts that are differentially regulated in these processes may be amenable to direct examination using existing tools, including pharmacological inhibitors/activators or expression of dominant loss- or gain-of-function transgene constructs. Second, a forward genetic screen, preferably using transposon-mediated mutagenesis, to find *S. stercoralis* mutants that do not undergo L3i arrest in the post-free-living generation (and develop to a second free-living generation of females) would provide unbiased genetic evidence of genes necessary for L3i development. It is hoped that this knowledge will aid in understanding pathways governing the developmental regulation of all parasitic nematodes and thereby contribute to new treatment strategies and control measures.

REFERENCES

1. Noble ER, Noble GA, Schad GA, MacInnes AJ (1989) Parasitology: The Biology of Animal Parasites. Philadelphia: Lea & Febiger.
2. Anderson RC (2000) Nematode Parasites of Vertebrates: Their Development and Transmission. New York: CABI Publishing.
3. Martin J, Abubucker S, Heizer E, Taylor CM, Mitreva M (2011) Nematode.net update 2011: addition of data sets and tools featuring next-generation sequencing data. Nucleic Acids Res 40: D720-728.
4. Miguel E, Kremer M (2004) Worms: Identifying Impacts on Education and Health in the Presence of Treatment Externalities. Econometrica 72: 159-217.
5. Bethony J, Brooker S, Albonico M, Geiger SM, Loukas A, et al. (2006) Soil-transmitted helminth infections: ascariasis, trichuriasis, and hookworm. Lancet 367: 1521-1532.
6. Taylor MJ, Hoerauf A, Bockarie M (2010) Lymphatic filariasis and onchocerciasis. Lancet 376: 1175-1185.
7. Yamada M, Matsuda S, Nakazawa M, Arizono N (1991) Species-specific differences in heterogonic development of serially transferred free-living generations of *Strongyloides planiceps* and *Strongyloides stercoralis*. J Parasitol 77: 592-594.
8. Schad GA (1989) Morphology and life history of *Strongyloides stercoralis*. In: Grove DI, editor. Strongyloidiasis a major roundworm infection of man. London: Taylor and Francis. pp. 85–104.
9. Schad GA, Hellman ME, Muncey DW (1984) *Strongyloides stercoralis*: hyperinfection in immunosuppressed dogs. Exp Parasitol 57: 287-296.
10. Lok JB (2007) *Strongyloides stercoralis*: a model for translational research on parasitic nematode biology, WormBook, ed. The *C. elegans* Research Community, WormBook, doi/10.1895/wormbook.1.134.1, http://www.wormbook.org.
11. Marcos LA, Terashima A, Canales M, Gotuzzo E (2011) Update on strongyloidiasis in the immunocompromised host. Curr Infect Dis Rep 13: 35-46.
12. Schad GA, Chowdhury AB, Dean CG, Kochar VK, Nawalinski TA, et al. (1973) Arrested development in human hookworm infections: an adaptation to a seasonally unfavorable external environment. Science 180: 502-504.
13. Hotez P, Hawdon J, Schad GA (1993) Hookworm larval infectivity, arrest and amphiparatenesis: the *Caenorhabditis elegans* Daf-c paradigm. Parasitol Today 9: 23-26.
14. Croll NA (1972) Feeding and lipid synthesis of *Ancylostoma tubaeforme* preinfective larvae. Parasitology 64: 369-378.
15. Croll NA (1972) Energy utilization of infective *Ancylostoma tubaeforme* larvae. Parasitology 64: 355-368.
16. Sciacca J, Forbes WM, Ashton FT, Lombardini E, Gamble HR, et al. (2002) Response to carbon dioxide by the infective larvae of three species of parasitic nematodes. Parasitol Int 51: 53-62.
17. Forbes WM, Ashton FT, Boston R, Zhu X, Schad GA (2004) Chemoattraction and chemorepulsion of *Strongyloides stercoralis* infective larvae on a sodium chloride

gradient is mediated by amphidial neuron pairs ASE and ASH, respectively. Vet Parasitol 120: 189-198.
18. Safer D, Brenes M, Dunipace S, Schad G (2007) Urocanic acid is a major chemoattractant for the skin-penetrating parasitic nematode *Strongyloides stercoralis*. Proc Natl Acad Sci U S A 104: 1627-1630.
19. Lopez PM, Boston R, Ashton FT, Schad GA (2000) The neurons of class ALD mediate thermotaxis in the parasitic nematode, *Strongyloides stercoralis*. Int J Parasitol 30: 1115-1121.
20. Croll NA, Matthews BE (1977) Biology of Nematodes: Halstead Press.
21. Hotez P, Haggerty J, Hawdon J, Milstone L, Gamble HR, et al. (1990) Metalloproteases of infective *Ancylostoma* hookworm larvae and their possible functions in tissue invasion and ecdysis. Infect Immun 58: 3883-3892.
22. Hotez PJ, Narasimhan S, Haggerty J, Milstone L, Bhopale V, et al. (1992) Hyaluronidase from infective *Ancylostoma* hookworm larvae and its possible function as a virulence factor in tissue invasion and in cutaneous larva migrans. Infect Immun 60: 1018-1023.
23. Cassada RC, Russell RL (1975) The dauerlarva, a post-embryonic developmental variant of the nematode *Caenorhabditis elegans*. Dev Biol 46: 326-342.
24. Burglin TR, Lobos E, Blaxter ML (1998) *Caenorhabditis elegan*s as a model for parasitic nematodes. Int J Parasitol 28: 395-411.
25. Aboobaker AA, Blaxter ML (2000) Medical significance of *Caenorhabditis elegans*. Ann Med 32: 23-30.
26. Mitreva M, McCarter JP, Martin J, Dante M, Wylie T, et al. (2004) Comparative genomics of gene expression in the parasitic and free-living nematodes *Strongyloides stercoralis* and *Caenorhabditis elegans*. Genome Res 14: 209-220.
27. Viney ME (2009) How did parasitic worms evolve? Bioessays 31: 496-499.
28. Golden JW, Riddle DL (1984) The *Caenorhabditis elegans* dauer larva: developmental effects of pheromone, food, and temperature. Dev Biol 102: 368-378.
29. Golden JW, Riddle DL (1984) A pheromone-induced developmental switch in *Caenorhabditis elegans*: Temperature-sensitive mutants reveal a wild-type temperature-dependent process. Proc Natl Acad Sci U S A 81: 819-823.
30. Hu PJ (2007) Dauer, WormBook, ed. The *C. elegans* Research Community, WormBook, doi/10.1895/wormbook.1.144.1, http://www.wormbook.org.
31. Ward S, Thomson N, White JG, Brenner S (1975) Electron microscopical reconstruction of the anterior sensory anatomy of the nematode *Caenorhabditis elegans*. J Comp Neurol 160: 313-337.
32. Bargmann CI, Horvitz HR (1991) Control of larval development by chemosensory neurons in *Caenorhabditis elegans*. Science 251: 1243-1246.
33. Kim K, Sato K, Shibuya M, Zeiger DM, Butcher RA, et al. (2009) Two chemoreceptors mediate developmental effects of dauer pheromone in *C. elegans*. Science 326: 994-998.
34. Schackwitz WS, Inoue T, Thomas JH (1996) Chemosensory neurons function in parallel to mediate a pheromone response in *C. elegans*. Neuron 17: 719-728.

35. Ouellette M (2001) Biochemical and molecular mechanisms of drug resistance in parasites. Trop Med Int Health 6: 874-882.
36. Riddle DL, Swanson MM, Albert PS (1981) Interacting genes in nematode dauer larva formation. Nature 290: 668-671.
37. Albert PS, Brown SJ, Riddle DL (1981) Sensory control of dauer larva formation in *Caenorhabditis elegans*. J Comp Neurol 198: 435-451.
38. Lewis JA, Hodgkin JA (1977) Specific neuroanatomical changes in chemosensory mutants of the nematode *Caenorhabditis elegans*. J Comp Neurol 172: 489-510.
39. Perkins LA, Hedgecock EM, Thomson JN, Culotti JG (1986) Mutant sensory cilia in the nematode *Caenorhabditis elegans*. Dev Biol 117: 456-487.
40. Bargmann CI, Hartwieg E, Horvitz HR (1993) Odorant-selective genes and neurons mediate olfaction in *C. elegans*. Cell 74: 515-527.
41. Fielenbach N, Antebi A (2008) *C. elegans* dauer formation and the molecular basis of plasticity. Genes Dev 22: 2149-2165.
42. Shiwaku K, Chigusa Y, Kadosaka T, Kaneko K (1988) Factors influencing development of free-living generations of *Strongyloides stercoralis*. Parasitology 97 (Pt 1): 129-138.
43. Nolan TJ, Brenes M, Ashton FT, Zhu X, Forbes WM, et al. (2004) The amphidial neuron pair ALD controls the temperature-sensitive choice of alternative developmental pathways in the parasitic nematode, *Strongyloides stercoralis*. Parasitology 129: 753-759.
44. Arizono N (1976) Studies on the free-living generations of *Strongyloides planiceps*, 1943 II. Effect of temperature on the developmental types. Japanese Journal of Parasitology 25: 328-335.
45. Nwaorgu O (1983) The development of the free-living stages of *Strongyloides papillosus*: I. Effect of temperature on the development of the heterogonic and homogenic nematodes in faecal culture. Veterinary Parasitology 13: 213-223.
46. Viney ME (1996) Developmental switching in the parasitic nematode *Strongyloides ratti*. Proc Biol Sci 263: 201-208.
47. Grant WN, Stasiuk S, Newton-Howes J, Ralston M, Bisset SA, et al. (2006) *Parastrongyloides trichosuri*, a nematode parasite of mammals that is uniquely suited to genetic analysis. Int J Parasitol 36: 453-466.
48. Stasiuk SJ, Scott MJ, Grant WN (2012) Developmental plasticity and the evolution of parasitism in an unusual nematode, *Parastrongyloides trichosuri*. Evodevo 3: 1.
49. Viney ME, Matthews BE, Walliker D (1992) On the biological and biochemical nature of cloned populations of *Strongyloides ratti*. J Helminthol 66: 45-52.
50. Galliard H. Pathogenesis of *Strongyloides*; 1967. pp. 247-260.
51. Moncol D, Triantaphyllou A (1978) *Strongyloides ransomi*: Factors influencing the in vitro development of the free-living generation. The Journal of Parasitology: 220-225.
52. Arizono N (1976) Studies on the free-living generations of *Strongyloides planiceps* Rogers, 1943. I. Effects of quantity of food and population density on the developmental types. Japanese Journal of Parasitology 25: 274-282.

53. Ashton FT, Bhopale VM, Fine AE, Schad GA (1995) Sensory neuroanatomy of a skin-penetrating nematode parasite: *Strongyloides stercoralis*. I. Amphidial neurons. J Comp Neurol 357: 281-295.
54. Ashton FT, Bhopale VM, Holt D, Smith G, Schad GA (1998) Developmental switching in the parasitic nematode *Strongyloides stercoralis* is controlled by the ASF and ASI amphidial neurons. J Parasitol 84: 691-695.
55. Ashton FT, Schad GA (1996) Amphids in *Strongyloides stercoralis* and other parasitic nematodes. Parasitol Today 12: 187-194.
56. Ashton FT, Li J, Schad GA (1999) Chemo- and thermosensory neurons: structure and function in animal parasitic nematodes. Vet Parasitol 84: 297-316.
57. Ashton FT, Zhu X, Boston R, Lok JB, Schad GA (2007) *Strongyloides stercoralis*: Amphidial neuron pair ASJ triggers significant resumption of development by infective larvae under host-mimicking in vitro conditions. Exp Parasitol 115: 92-97.
58. Srinivasan J, Durak O, Sternberg PW (2008) Evolution of a polymodal sensory response network. BMC Biol 6: 52.
59. Babar P, Adamson C, Walker GA, Walker DW, Lithgow GJ (1999) PI3-kinase inhibition induces dauer formation, thermotolerance and longevity in *C. elegans*. Neurobiol Aging 20: 513-519.
60. Birnby DA, Link EM, Vowels JJ, Tian H, Colacurcio PL, et al. (2000) A transmembrane guanylyl cyclase (DAF-11) and Hsp90 (DAF-21) regulate a common set of chemosensory behaviors in *Caenorhabditis elegans*. Genetics 155: 85-104.
61. Hawdon JM, Volk SW, Rose R, Pritchard DI, Behnke JM, et al. (1993) Observations on the feeding behaviour of parasitic third-stage hookworm larvae. Parasitology 106 (Pt 2): 163-169.
62. Hawdon JM, Schad GA (1993) *Ancylostoma caninum*: glutathione stimulates feeding in third-stage larvae by a sulfhydryl-independent mechanism. Exp Parasitol 77: 489-491.
63. Hawdon JM, Schad GA (1990) Serum-stimulated feeding in vitro by third-stage infective larvae of the canine hookworm *Ancylostoma caninum*. J Parasitol 76: 394-398.
64. Hawdon JM, Schad GA (1991) Albumin and a dialyzable serum factor stimulate feeding in vitro by third-stage larvae of the canine hookworm *Ancylostoma caninum*. J Parasitol 77: 587-591.
65. Hawdon JM, Volk SW, Pritchard DI, Schad GA (1992) Resumption of feeding in vitro by hookworm third-stage larvae: a comparative study. J Parasitol 78: 1036-1040.
66. Hawdon JM, Datu B (2003) The second messenger cyclic GMP mediates activation in *Ancylostoma caninum* infective larvae. Int J Parasitol 33: 787-793.
67. Tissenbaum HA, Hawdon J, Perregaux M, Hotez P, Guarente L, et al. (2000) A common muscarinic pathway for diapause recovery in the distantly related nematode species *Caenorhabditis elegans* and *Ancylostoma caninum*. Proc Natl Acad Sci USA 97: 460-465.

68. Brand A, Hawdon JM (2004) Phosphoinositide-3-OH-kinase inhibitor LY294002 prevents activation of *Ancylostoma caninum* and *Ancylostoma ceylanicum* third-stage infective larvae. Int J Parasitol 34: 909-914.
69. Wang Z, Zhou XE, Motola DL, Gao X, Suino-Powell K, et al. (2009) Identification of the nuclear receptor DAF-12 as a therapeutic target in parasitic nematodes. Proc Natl Acad Sci U S A 106: 9138-9143.
70. Datu BJ, Loukas A, Cantacessi C, O'Donoghue P, Gasser RB (2009) Investigation of the regulation of transcriptional changes in *Ancylostoma caninum* larvae following serum activation, with a focus on the insulin-like signalling pathway. Vet Parasitol 159: 139-148.
71. Huang SC, Chan DT, Smyth DJ, Ball G, Gounaris K, et al. (2010) Activation of *Nippostrongylus brasiliensis* infective larvae is regulated by a pathway distinct from the hookworm *Ancylostoma caninum*. Int J Parasitol 40: 1619-1628.
72. Brand AM, Varghese G, Majewski W, Hawdon JM (2005) Identification of a DAF-7 ortholog from the hookworm *Ancylostoma caninum*. Int J Parasitol 35: 1489-1498.
73. Crook M, Thompson FJ, Grant WN, Viney ME (2005) *daf-7* and the development of *Strongyloides ratti* and *Parastrongyloides trichosuri*. Mol Biochem Parasitol 139: 213-223.
74. Freitas TC, Arasu P (2005) Cloning and characterisation of genes encoding two transforming growth factor-beta-like ligands from the hookworm, *Ancylostoma caninum*. Int J Parasitol 35: 1477-1487.
75. Gomez-Escobar N, Gregory WF, Maizels RM (2000) Identification of *tgh-2*, a filarial nematode homolog of *Caenorhabditis elegans daf-7* and human transforming growth factor beta, expressed in microfilarial and adult stages of *Brugia malayi*. Infect Immun 68: 6402-6410.
76. Massey HC, Castelletto ML, Bhopale VM, Schad GA, Lok JB (2005) *Sst-tgh-1* from *Strongyloides stercoralis* encodes a proposed ortholog of *daf-7* in *Caenorhabditis elegans*. Mol Biochem Parasitol 142: 116-120.
77. Viney ME, Thompson FJ, Crook M (2005) TGF-beta and the evolution of nematode parasitism. Int J Parasitol 35: 1473-1475.
78. Castelletto ML, Massey HC, Jr., Lok JB (2009) Morphogenesis of *Strongyloides stercoralis* infective larvae requires the DAF-16 ortholog FKTF-1. PLoS Pathog 5: e1000370.
79. Massey HC, Jr., Bhopale MK, Li X, Castelletto M, Lok JB (2006) The fork head transcription factor FKTF-1b from *Strongyloides stercoralis* restores DAF-16 developmental function to mutant *Caenorhabditis elegans*. Int J Parasitol 36: 347-352.
80. Massey HC, Jr., Nishi M, Chaudhary K, Pakpour N, Lok JB (2003) Structure and developmental expression of *Strongyloides stercoralis fktf-1*, a proposed ortholog of *daf-16* in *Caenorhabditis elegans*. Int J Parasitol 33: 1537-1544.
81. Gao X, Frank D, Hawdon JM (2009) Molecular cloning and DNA binding characterization of DAF-16 orthologs from *Ancylostoma* hookworms. Int J Parasitol 39: 407-415.

82. Gao X, Wang Z, Martin J, Abubucker S, Zhang X, et al. (2010) Identification of hookworm DAF-16/FOXO response elements and direct gene targets. PLoS One 5: e12289.
83. Hu M, Lok JB, Ranjit N, Massey HC, Jr., Sternberg PW, et al. (2010) Structural and functional characterisation of the fork head transcription factor-encoding gene, *Hc-daf-16*, from the parasitic nematode *Haemonchus contortus* (Strongylida). Int J Parasitol 40: 405-415.
84. Gelmedin V, Brodigan T, Gao X, Krause M, Wang Z, et al. (2011) Transgenic *C. elegans* dauer larvae expressing hookworm phospho null DAF-16/FoxO exit dauer. PLoS One 6: e25996.
85. Cahill CM, Tzivion G, Nasrin N, Ogg S, Dore J, et al. (2001) Phosphatidylinositol 3-kinase signaling inhibits DAF-16 DNA binding and function via 14-3-3-dependent and 14-3-3-independent pathways. J Biol Chem 276: 13402-13410.
86. Ogawa A, Streit A, Antebi A, Sommer RJ (2009) A conserved endocrine mechanism controls the formation of dauer and infective larvae in nematodes. Curr Biol 19: 67-71.
87. Siddiqui AA, Stanley CS, Skelly PJ, Berk SL (2000) A cDNA encoding a nuclear hormone receptor of the steroid/thyroid hormone-receptor superfamily from the human parasitic nematode *Strongyloides stercoralis*. Parasitol Res 86: 24-29.
88. Massey HC, Jr., Ball CC, Lok JB (2001) PCR amplification of putative *gpa-2* and *gpa-3* orthologs from the (A+T)-rich genome of *Strongyloides stercoralis*. Int J Parasitol 31: 377-383.
89. Zwaal RR, Mendel JE, Sternberg PW, Plasterk RH (1997) Two neuronal G proteins are involved in chemosensation of the *Caenorhabditis elegans* dauer-inducing pheromone. Genetics 145: 715-727.
90. Junio AB, Li X, Massey HC, Jr., Nolan TJ, Todd Lamitina S, et al. (2008) *Strongyloides stercoralis*: cell- and tissue-specific transgene expression and co-transformation with vector constructs incorporating a common multifunctional 3' UTR. Exp Parasitol 118: 253-265.
91. Jansen G, Thijssen KL, Werner P, van der Horst M, Hazendonk E, et al. (1999) The complete family of genes encoding G proteins of *Caenorhabditis elegans*. Nat Genet 21: 414-419.
92. Lans H, Rademakers S, Jansen G (2004) A network of stimulatory and inhibitory Galpha-subunits regulates olfaction in *Caenorhabditis elegans*. Genetics 167: 1677-1687.
93. Dalzell JJ, McVeigh P, Warnock ND, Mitreva M, Bird DM, et al. (2011) RNAi effector diversity in nematodes. PLoS Negl Trop Dis 5: e1176.
94. Lok JB (2012) Nucleic acid transfection and transgenesis in parasitic nematodes. Parasitology 139: 574-588.
95. Li X, Massey HC, Jr., Nolan TJ, Schad GA, Kraus K, et al. (2006) Successful transgenesis of the parasitic nematode *Strongyloides stercoralis* requires endogenous non-coding control elements. Int J Parasitol 36: 671-679.
96. Mello CC, Kramer JM, Stinchcomb D, Ambros V (1991) Efficient gene transfer in *C.elegans*: extrachromosomal maintenance and integration of transforming sequences. EMBO J 10: 3959-3970.

97. Lok JB (2009) Transgenesis in parasitic nematodes: building a better array. Trends Parasitol 25: 345-347.
98. Shao H, Li X, Nolan TJ, Massey HC, Jr., Pearce EJ, et al. (2012) Transposon-mediated Chromosomal Integration of Transgenes in the Parasitic Nematode *Strongyloides ratti* and Establishment of Stable Transgenic Lines. PLoS Pathogens 8: e1002871.
99. Ramanathan R, Varma S, Ribeiro JM, Myers TG, Nolan TJ, et al. (2011) Microarray-based analysis of differential gene expression between infective and noninfective larvae of *Strongyloides stercoralis*. PLoS Negl Trop Dis 5: e1039.
100. Choi YJ, Ghedin E, Berriman M, McQuillan J, Holroyd N, et al. (2011) A deep sequencing approach to comparatively analyze the transcriptome of lifecycle stages of the filarial worm, *Brugia malayi*. PLoS Negl Trop Dis 5: e1409.
101. Moreno Y, Gros PP, Tam M, Segura M, Valanparambil R, et al. (2011) Proteomic analysis of excretory-secretory products of *Heligmosomoides polygyrus* assessed with next-generation sequencing transcriptomic information. PLoS Negl Trop Dis 5: e1370.
102. Cantacessi C, Young ND, Nejsum P, Jex AR, Campbell BE, et al. (2011) The transcriptome of *Trichuris suis*--first molecular insights into a parasite with curative properties for key immune diseases of humans. PLoS One 6: e23590.
103. Laing R, Hunt M, Protasio AV, Saunders G, Mungall K, et al. (2011) Annotation of two large contiguous regions from the *Haemonchus contortus* genome using RNA-seq and comparative analysis with *Caenorhabditis elegans*. PLoS One 6: e23216.
104. Cantacessi C, Mitreva M, Campbell BE, Hall RS, Young ND, et al. (2010) First transcriptomic analysis of the economically important parasitic nematode, *Trichostrongylus colubriformis*, using a next-generation sequencing approach. Infect Genet Evol 10: 1199-1207.
105. Nagayasu E, Ogura Y, Itoh T, Yoshida A, Chakraborty G, et al. (2013) Transcriptomic analysis of four developmental stages of *Strongyloides venezuelensis*. Parasitol Int 62: 57-65.
106. Britton C, Redmond DL, Knox DP, McKerrow JH, Barry JD (1999) Identification of promoter elements of parasite nematode genes in transgenic *Caenorhabditis elegans*. Mol Biochem Parasitol 103: 171-181.
107. Dieterich C, Sommer RJ (2009) How to become a parasite - lessons from the genomes of nematodes. Trends Genet 25: 203-209.
108. Riddle DL (1988) The dauer larva. In: Wood WB, editor. The nematode *Caenorhabditis elegans*. New York: Cold Spring Harbour Laboratory Press. pp. 393-412.
109. Blaxter ML, De Ley P, Garey JR, Liu LX, Scheldeman P, et al. (1998) A molecular evolutionary framework for the phylum Nematoda. Nature 392: 71-75.
110. Holterman M, van der Wurff A, van den Elsen S, van Megen H, Bongers T, et al. (2006) Phylum-wide analysis of SSU rDNA reveals deep phylogenetic relationships among nematodes and accelerated evolution toward crown Clades. Mol Biol Evol 23: 1792-1800.

111. Stoltzfus JD, Massey HC, Jr., Nolan TJ, Griffith SD, Lok JB (2012) *Strongyloides stercoralis age-1*: a potential regulator of infective larval development in a parasitic nematode. PLoS ONE 7: e38587.
112. Marcilla A, Garg G, Bernal D, Ranganathan S, Forment J, et al. (2012) The transcriptome analysis of *Strongyloides stercoralis* L3i larvae reveals targets for intervention in a neglected disease. PLoS Negl Trop Dis 6: e1513.
113. Jex AR, Liu S, Li B, Young ND, Hall RS, et al. (2011) *Ascaris suum* draft genome. Nature 479: 529-533.
114. Nolan TJ, Megyeri Z, Bhopale VM, Schad GA (1993) *Strongyloides stercoralis*: the first rodent model for uncomplicated and hyperinfective strongyloidiasis, the Mongolian gerbil (*Meriones unguiculatus*). J Infect Dis 168: 1479-1484.
115. Herbert DR, Nolan TJ, Schad GA, Lustigman S, Abraham D (2002) Immunoaffinity-isolated antigens induce protective immunity against larval *Strongyloides stercoralis* in mice. Exp Parasitol 100: 112-120.
116. Stiernagle T (2006) Maintenance of *C. elegans*, WormBook, ed. The *C. elegans* Research Community, WormBook, doi/10.1895/wormbook.1.101.1, http://www.wormbook.org.
117. Drummond AJ AB, Buxton S, Cheung M, Cooper A, Duran C, Field M, Heled J, Kearse M, Markowitz S, Moir R, Stones-Havas S, Sturrock S, Thierer T, Wilson A (2011) Geneious v5.5, Available from http://www.geneious.com.
118. Marchler-Bauer A, Lu S, Anderson JB, Chitsaz F, Derbyshire MK, et al. (2011) CDD: a Conserved Domain Database for the functional annotation of proteins. Nucleic Acids Res 39: D225-229.
119. Pang K, Ryan JF, Baxevanis AD, Martindale MQ (2011) Evolution of the TGF-beta signaling pathway and its potential role in the ctenophore, *Mnemiopsis leidyi*. PLoS One 6: e24152.
120. Mortazavi A, Williams BA, McCue K, Schaeffer L, Wold B (2008) Mapping and quantifying mammalian transcriptomes by RNA-Seq. Nat Methods 5: 621-628.
121. Trapnell C, Roberts A, Goff L, Pertea G, Kim D, et al. (2012) Differential gene and transcript expression analysis of RNA-seq experiments with TopHat and Cufflinks. Nat Protoc 7: 562-578.
122. Baugh LR, Kurhanewicz N, Sternberg PW (2011) Sensitive and precise quantification of insulin-like mRNA expression in *Caenorhabditis elegans*. PLoS One 6: e18086.
123. Ren P, Lim CS, Johnsen R, Albert PS, Pilgrim D, et al. (1996) Control of *C. elegans* larval development by neuronal expression of a TGF-beta homolog. Science 274: 1389-1391.
124. Wang J, Kim SK (2003) Global analysis of dauer gene expression in *Caenorhabditis elegans*. Development 130: 1621-1634.
125. Motola DL, Cummins CL, Rottiers V, Sharma KK, Li T, et al. (2006) Identification of ligands for DAF-12 that govern dauer formation and reproduction in *C. elegans*. Cell 124: 1209-1223.
126. Trapnell C, Pachter L, Salzberg SL (2009) TopHat: discovering splice junctions with RNA-Seq. Bioinformatics 25: 1105-1111.

127. Langmead B, Trapnell C, Pop M, Salzberg SL (2009) Ultrafast and memory-efficient alignment of short DNA sequences to the human genome. Genome Biol 10: R25.
128. Grabherr MG, Haas BJ, Yassour M, Levin JZ, Thompson DA, et al. (2011) Full-length transcriptome assembly from RNA-Seq data without a reference genome. Nat Biotechnol 29: 644-652.
129. Trapnell C, Williams BA, Pertea G, Mortazavi A, Kwan G, et al. (2010) Transcript assembly and quantification by RNA-Seq reveals unannotated transcripts and isoform switching during cell differentiation. Nat Biotechnol 28: 511-515.
130. Golden JW, Riddle DL (1982) A pheromone influences larval development in the nematode *Caenorhabditis elegans*. Science 218: 578-580.
131. Jeong PY, Jung M, Yim YH, Kim H, Park M, et al. (2005) Chemical structure and biological activity of the *Caenorhabditis elegans* dauer-inducing pheromone. Nature 433: 541-545.
132. Butcher RA, Fujita M, Schroeder FC, Clardy J (2007) Small-molecule pheromones that control dauer development in *Caenorhabditis elegans*. Nat Chem Biol 3: 420-422.
133. McGrath PT, Xu Y, Ailion M, Garrison JL, Butcher RA, et al. (2011) Parallel evolution of domesticated *Caenorhabditis* species targets pheromone receptor genes. Nature 477: 321-325.
134. Coburn CM, Mori I, Ohshima Y, Bargmann CI (1998) A cyclic nucleotide-gated channel inhibits sensory axon outgrowth in larval and adult *Caenorhabditis elegans*: a distinct pathway for maintenance of sensory axon structure. Development 125: 249-258.
135. Komatsu H, Mori I, Rhee JS, Akaike N, Ohshima Y (1996) Mutations in a cyclic nucleotide-gated channel lead to abnormal thermosensation and chemosensation in *C. elegans*. Neuron 17: 707-718.
136. Thomas JH, Birnby DA, Vowels JJ (1993) Evidence for parallel processing of sensory information controlling dauer formation in *Caenorhabditis elegans*. Genetics 134: 1105-1117.
137. Murakami M, Koga M, Ohshima Y (2001) DAF-7/TGF-beta expression required for the normal larval development in *C. elegans* is controlled by a presumed guanylyl cyclase DAF-11. Mech Dev 109: 27-35.
138. Li W, Kennedy SG, Ruvkun G (2003) *daf-28* encodes a *C. elegans* insulin superfamily member that is regulated by environmental cues and acts in the DAF-2 signaling pathway. Genes Dev 17: 844-858.
139. Hahm JH, Kim S, Paik YK (2009) Endogenous cGMP regulates adult longevity via the insulin signaling pathway in *Caenorhabditis elegans*. Aging Cell 8: 473-483.
140. Jensen VL, Bialas NJ, Bishop-Hurley SL, Molday LL, Kida K, et al. (2010) Localization of a guanylyl cyclase to chemosensory cilia requires the novel ciliary MYND domain protein DAF-25. PLoS Genet 6: e1001199.
141. Noguez JH, Conner ES, Zhou Y, Ciche TA, Ragains JR, et al. (2012) A novel ascaroside controls the parasitic life cycle of the entomopathogenic nematode *Heterorhabditis bacteriophora*. ACS Chem Biol.

142. Choe A, von Reuss SH, Kogan D, Gasser RB, Platzer EG, et al. (2012) Ascaroside signaling is widely conserved among nematodes. Curr Biol 22: 772-780.
143. McKay SJ, Johnsen R, Khattra J, Asano J, Baillie DL, et al. (2003) Gene expression profiling of cells, tissues, and developmental stages of the nematode *C. elegans*. Cold Spring Harb Symp Quant Biol 68: 159-169.
144. Pierce SB, Costa M, Wisotzkey R, Devadhar S, Homburger SA, et al. (2001) Regulation of DAF-2 receptor signaling by human insulin and *ins-1*, a member of the unusually large and diverse *C. elegans* insulin gene family. Genes Dev 15: 672-686.
145. Duckert P, Brunak S, Blom N (2004) Prediction of proprotein convertase cleavage sites. Protein Eng Des Sel 17: 107-112.
146. Tian S, Huajun W, Wu J (2012) Computational prediction of furin cleavage sites by a hybrid method and understanding mechanism underlying diseases. Sci Rep 2: 261.
147. Cornils A, Gloeck M, Chen Z, Zhang Y, Alcedo J (2011) Specific insulin-like peptides encode sensory information to regulate distinct developmental processes. Development 138: 1183-1193.
148. Hua QX, Nakagawa SH, Wilken J, Ramos RR, Jia W, et al. (2003) A divergent INS protein in *Caenorhabditis elegans* structurally resembles human insulin and activates the human insulin receptor. Genes Dev 17: 826-831.
149. Murphy CT, McCarroll SA, Bargmann CI, Fraser A, Kamath RS, et al. (2003) Genes that act downstream of DAF-16 to influence the lifespan of *Caenorhabditis elegans*. Nature 424: 277-283.
150. Tomioka M, Adachi T, Suzuki H, Kunitomo H, Schafer WR, et al. (2006) The insulin/PI 3-kinase pathway regulates salt chemotaxis learning in *Caenorhabditis elegans*. Neuron 51: 613-625.
151. Kodama E, Kuhara A, Mohri-Shiomi A, Kimura KD, Okumura M, et al. (2006) Insulin-like signaling and the neural circuit for integrative behavior in *C. elegans*. Genes Dev 20: 2955-2960.
152. Gregoire FM, Chomiki N, Kachinskas D, Warden CH (1998) Cloning and developmental regulation of a novel member of the insulin-like gene family in *Caenorhabditis elegans*. Biochem Biophys Res Commun 249: 385-390.
153. Smit AB, Vreugdenhil E, Ebberink RH, Geraerts WP, Klootwijk J, et al. (1988) Growth-controlling molluscan neurons produce the precursor of an insulin-related peptide. Nature 331: 535-538.
154. Kawano T, Ito Y, Ishiguro M, Takuwa K, Nakajima T, et al. (2000) Molecular cloning and characterization of a new insulin/IGF-like peptide of the nematode *Caenorhabditis elegans*. Biochem Biophys Res Commun 273: 431-436.
155. Massey HC, Jr., Ranjit N, Stoltzfus JD, Lok JB (2013) *Strongyloides stercoralis* daf-2 encodes a divergent ortholog of *Caenorhabditis elegans* DAF-2. Int J Parasitol 43: 515-520.
156. Wolkow CA, Munoz MJ, Riddle DL, Ruvkun G (2002) Insulin receptor substrate and p55 orthologous adaptor proteins function in the *Caenorhabditis elegans daf-2*/insulin-like signaling pathway. J Biol Chem 277: 49591-49597.

157. Rouault JP, Kuwabara PE, Sinilnikova OM, Duret L, Thierry-Mieg D, et al. (1999) Regulation of dauer larva development in *Caenorhabditis elegans* by *daf-18*, a homologue of the tumour suppressor PTEN. Curr Biol 9: 329-332.
158. Paradis S, Ailion M, Toker A, Thomas JH, Ruvkun G (1999) A PDK1 homolog is necessary and sufficient to transduce AGE-1 PI3 kinase signals that regulate diapause in *Caenorhabditis elegans*. Genes Dev 13: 1438-1452.
159. Paradis S, Ruvkun G (1998) *Caenorhabditis elegans* Akt/PKB transduces insulin receptor-like signals from AGE-1 PI3 kinase to the DAF-16 transcription factor. Genes Dev 12: 2488-2498.
160. Lin K, Hsin H, Libina N, Kenyon C (2001) Regulation of the *Caenorhabditis elegans* longevity protein DAF-16 by insulin/IGF-1 and germline signaling. Nat Genet 28: 139-145.
161. Padmanabhan S, Mukhopadhyay A, Narasimhan SD, Tesz G, Czech MP, et al. (2009) A PP2A regulatory subunit regulates *C. elegans* insulin/IGF-1 signaling by modulating AKT-1 phosphorylation. Cell 136: 939-951.
162. Hertweck M, Gobel C, Baumeister R (2004) *C. elegans* SGK-1 is the critical component in the Akt/PKB kinase complex to control stress response and life span. Dev Cell 6: 577-588.
163. Wang W, Shakes DC (1997) Expression patterns and transcript processing of *ftt-1* and *ftt-2*, two *C. elegans* 14-3-3 homologues. J Mol Biol 268: 619-630.
164. Li J, Tewari M, Vidal M, Lee SS (2007) The 14-3-3 protein FTT-2 regulates DAF-16 in *Caenorhabditis elegans*. Dev Biol 301: 82-91.
165. Kao G, Nordenson C, Still M, Ronnlund A, Tuck S, et al. (2007) ASNA-1 positively regulates insulin secretion in *C. elegans* and mammalian cells. Cell 128: 577-587.
166. Barbieri M, Bonafe M, Franceschi C, Paolisso G (2003) Insulin/IGF-I-signaling pathway: an evolutionarily conserved mechanism of longevity from yeast to humans. Am J Physiol Endocrinol Metab 285: E1064-1071.
167. Jones SJ, Riddle DL, Pouzyrev AT, Velculescu VE, Hillier L, et al. (2001) Changes in gene expression associated with developmental arrest and longevity in *Caenorhabditis elegans*. Genome Res 11: 1346-1352.
168. Lee SS, Kennedy S, Tolonen AC, Ruvkun G (2003) DAF-16 target genes that control *C. elegans* life-span and metabolism. Science 300: 644-647.
169. McElwee J, Bubb K, Thomas JH (2003) Transcriptional outputs of the *Caenorhabditis elegans* forkhead protein DAF-16. Aging Cell 2: 111-121.
170. Oh SW, Mukhopadhyay A, Dixit BL, Raha T, Green MR, et al. (2006) Identification of direct DAF-16 targets controlling longevity, metabolism and diapause by chromatin immunoprecipitation. Nat Genet 38: 251-257.
171. Hunter T, Bannister WH, Hunter GJ (1997) Cloning, expression, and characterization of two manganese superoxide dismutases from *Caenorhabditis elegans*. J Biol Chem 272: 28652-28659.
172. Honda Y, Honda S (1999) The *daf-2* gene network for longevity regulates oxidative stress resistance and Mn-superoxide dismutase gene expression in *Caenorhabditis elegans*. Faseb J 13: 1385-1393.

173. Jia K, Chen D, Riddle DL (2004) The TOR pathway interacts with the insulin signaling pathway to regulate *C. elegans* larval development, metabolism and life span. Development 131: 3897-3906.
174. Savage-Dunn C (2005) TGF-beta signaling, WormBook, ed. The *C. elegans* Research Community, WormBook. Available: http://www.wormbook.org/chapters/www_tgfbsignal/tgfbsignal.html.
175. McSorley HJ, Grainger JR, Harcus Y, Murray J, Nisbet AJ, et al. (2010) *daf-7*-related TGF-beta homologues from Trichostrongyloid nematodes show contrasting life-cycle expression patterns. Parasitology 137: 159-171.
176. Freitas TC, Jung E, Pearce EJ (2007) TGF-beta signaling controls embryo development in the parasitic flatworm *Schistosoma mansoni*. PLoS Pathog 3: e52.
177. Patterson GI, Padgett RW (2000) TGF beta-related pathways. Roles in *Caenorhabditis elegans* development. Trends Genet 16: 27-33.
178. Park D, Estevez A, Riddle DL (2010) Antagonistic Smad transcription factors control the dauer/non-dauer switch in *C. elegans*. Development 137: 477-485.
179. Narasimhan SD, Yen K, Bansal A, Kwon ES, Padmanabhan S, et al. (2011) PDP-1 links the TGF-beta and IIS pathways to regulate longevity, development, and metabolism. PLoS Genet 7: e1001377.
180. Georgi LL, Albert PS, Riddle DL (1990) *daf-1*, a *C. elegans* gene controlling dauer larva development, encodes a novel receptor protein kinase. Cell 61: 635-645.
181. Estevez M, Attisano L, Wrana JL, Albert PS, Massague J, et al. (1993) The *daf-4* gene encodes a bone morphogenetic protein receptor controlling *C. elegans* dauer larva development. Nature 365: 644-649.
182. Morita K, Shimizu M, Shibuya H, Ueno N (2001) A DAF-1-binding protein BRA-1 is a negative regulator of DAF-7 TGF-beta signaling. Proc Natl Acad Sci U S A 98: 6284-6288.
183. Inoue T, Thomas JH (2000) Targets of TGF-beta signaling in *Caenorhabditis elegans* dauer formation. Dev Biol 217: 192-204.
184. Patterson GI, Koweek A, Wong A, Liu Y, Ruvkun G (1997) The DAF-3 Smad protein antagonizes TGF-beta-related receptor signaling in the *Caenorhabditis elegans* dauer pathway. Genes Dev 11: 2679-2690.
185. da Graca LS, Zimmerman KK, Mitchell MC, Kozhan-Gorodetska M, Sekiewicz K, et al. (2004) DAF-5 is a Ski oncoprotein homolog that functions in a neuronal TGF beta pathway to regulate *C. elegans* dauer development. Development 131: 435-446.
186. Gunther CV, Georgi LL, Riddle DL (2000) A *Caenorhabditis elegans* type I TGF beta receptor can function in the absence of type II kinase to promote larval development. Development 127: 3337-3347.
187. Gunther CV, Riddle DL (2004) Alternative polyadenylation results in a truncated *daf-4* BMP receptor that antagonizes DAF-7-mediated development in *Caenorhabditis elegans*. J Biol Chem 279: 39555-39564.
188. Herpin A, Lelong C, Favrel P (2004) Transforming growth factor-beta-related proteins: an ancestral and widespread superfamily of cytokines in metazoans. Dev Comp Immunol 28: 461-485.

189. Suzuki Y, Yandell MD, Roy PJ, Krishna S, Savage-Dunn C, et al. (1999) A BMP homolog acts as a dose-dependent regulator of body size and male tail patterning in *Caenorhabditis elegans*. Development 126: 241-250.
190. Morita K, Chow KL, Ueno N (1999) Regulation of body length and male tail ray pattern formation of *Caenorhabditis elegans* by a member of TGF-beta family. Development 126: 1337-1347.
191. Krishna S, Maduzia LL, Padgett RW (1999) Specificity of TGFbeta signaling is conferred by distinct type I receptors and their associated SMAD proteins in *Caenorhabditis elegans*. Development 126: 251-260.
192. Dumas KJ, Guo C, Wang X, Burkhart KB, Adams EJ, et al. (2010) Functional divergence of dafachronic acid pathways in the control of *C. elegans* development and lifespan. Dev Biol 340: 605-612.
193. Antebi A, Yeh WH, Tait D, Hedgecock EM, Riddle DL (2000) *daf-12* encodes a nuclear receptor that regulates the dauer diapause and developmental age in *C. elegans*. Genes Dev 14: 1512-1527.
194. Li J, Brown G, Ailion M, Lee S, Thomas JH (2004) NCR-1 and NCR-2, the *C. elegans* homologs of the human Niemann-Pick type C1 disease protein, function upstream of DAF-9 in the dauer formation pathways. Development 131: 5741-5752.
195. Rottiers V, Motola DL, Gerisch B, Cummins CL, Nishiwaki K, et al. (2006) Hormonal control of *C. elegans* dauer formation and life span by a Rieske-like oxygenase. Dev Cell 10: 473-482.
196. Wollam J, Magner DB, Magomedova L, Rass E, Shen Y, et al. (2012) A novel 3-hydroxysteroid dehydrogenase that regulates reproductive development and longevity. PLoS Biol 10: e1001305.
197. Gerisch B, Weitzel C, Kober-Eisermann C, Rottiers V, Antebi A (2001) A hormonal signaling pathway influencing *C. elegans* metabolism, reproductive development, and life span. Dev Cell 1: 841-851.
198. Jia K, Albert PS, Riddle DL (2002) DAF-9, a cytochrome P450 regulating *C. elegans* larval development and adult longevity. Development 129: 221-231.
199. Patel DS, Fang LL, Svy DK, Ruvkun G, Li W (2008) Genetic identification of HSD-1, a conserved steroidogenic enzyme that directs larval development in *Caenorhabditis elegans*. Development 135: 2239-2249.
200. Hannich JT, Entchev EV, Mende F, Boytchev H, Martin R, et al. (2009) Methylation of the sterol nucleus by STRM-1 regulates dauer larva formation in *Caenorhabditis elegans*. Dev Cell 16: 833-843.
201. Ludewig AH, Kober-Eisermann C, Weitzel C, Bethke A, Neubert K, et al. (2004) A novel nuclear receptor/coregulator complex controls *C. elegans* lipid metabolism, larval development, and aging. Genes Dev 18: 2120-2133.
202. Snow MI, Larsen PL (2000) Structure and expression of *daf-12*: a nuclear hormone receptor with three isoforms that are involved in development and aging in *Caenorhabditis elegans*. Biochim Biophys Acta 1494: 104-116.
203. Shostak Y, Van Gilst MR, Antebi A, Yamamoto KR (2004) Identification of *C. elegans* DAF-12-binding sites, response elements, and target genes. Genes Dev 18: 2529-2544.

204. Lim LP, Lau NC, Weinstein EG, Abdelhakim A, Yekta S, et al. (2003) The microRNAs of *Caenorhabditis elegans*. Genes Dev 17: 991-1008.
205. Bethke A, Fielenbach N, Wang Z, Mangelsdorf DJ, Antebi A (2009) Nuclear hormone receptor regulation of microRNAs controls developmental progression. Science 324: 95-98.
206. Sinha A, Sommer RJ, Dieterich C (2012) Divergent gene expression in the conserved dauer stage of the nematodes *Pristionchus pacificus* and *Caenorhabditis elegans*. BMC Genomics 13: 254.
207. Kim SK, Lund J, Kiraly M, Duke K, Jiang M, et al. (2001) A gene expression map for *Caenorhabditis elegans*. Science 293: 2087-2092.
208. Viney ME, Lok JB (2007) *Strongyloides* spp., *WormBook*, ed. The *C. elegans* Research Community, WormBook, Available: http://www.wormbook.org/chapters/www_genomesStrongyloides/genomesStrongyloides.html.
209. Grainger JR, Smith KA, Hewitson JP, McSorley HJ, Harcus Y, et al. (2010) Helminth secretions induce de novo T cell Foxp3 expression and regulatory function through the TGF-beta pathway. J Exp Med 207: 2331-2341.
210. Chan MS (1997) The global burden of intestinal nematode infections--fifty years on. Parasitol Today 13: 438-443.
211. Montes M, Sawhney C, Barros N (2010) *Strongyloides stercoralis*: there but not seen. Curr Opin Infect Dis 23: 500-504.
212. Blaxter M (1998) *Caenorhabditis elegans* is a nematode. Science 282: 2041-2046.
213. Kimura KD, Tissenbaum HA, Liu Y, Ruvkun G (1997) *daf-2*, an insulin receptor-like gene that regulates longevity and diapause in *Caenorhabditis elegans*. Science 277: 942-946.
214. Weinkove D, Halstead JR, Gems D, Divecha N (2006) Long-term starvation and ageing induce AGE-1/PI 3-kinase-dependent translocation of DAF-16/FOXO to the cytoplasm. BMC Biol 4: 1.
215. Morris JZ, Tissenbaum HA, Ruvkun G (1996) A phosphatidylinositol-3-OH kinase family member regulating longevity and diapause in *Caenorhabditis elegans*. Nature 382: 536-539.
216. Ogg S, Paradis S, Gottlieb S, Patterson GI, Lee L, et al. (1997) The Fork head transcription factor DAF-16 transduces insulin-like metabolic and longevity signals in *C. elegans*. Nature 389: 994-999.
217. Gottlieb S, Ruvkun G (1994) *daf-2*, *daf-16* and *daf-23*: genetically interacting genes controlling Dauer formation in *Caenorhabditis elegans*. Genetics 137: 107-120.
218. Tissenbaum HA, Ruvkun G (1998) An insulin-like signaling pathway affects both longevity and reproduction in *Caenorhabditis elegans*. Genetics 148: 703-717.
219. Viney ME (1994) A genetic analysis of reproduction in *Strongyloides ratti*. Parasitology 109 (Pt 4): 511-515.
220. Triantaphyllou AC, Moncol DJ (1977) Cytology, reproduction, and sex determination of *Strongyloides ransomi* and *S. papillosus*. J Parasitol 63: 961-973.
221. Larkin MA, Blackshields G, Brown NP, Chenna R, McGettigan PA, et al. (2007) Clustal W and Clustal X version 2.0. Bioinformatics 23: 2947-2948.

222. Tamura K, Dudley J, Nei M, Kumar S (2007) MEGA4: Molecular Evolutionary Genetics Analysis (MEGA) software version 4.0. Mol Biol Evol 24: 1596-1599.
223. Rose J, Eisenmenger F (1991) A fast unbiased comparison of protein structures by means of the Needleman-Wunsch algorithm. J Mol Evol 32: 340-354.
224. Soblik H, Younis AE, Mitreva M, Renard BY, Kirchner M, et al. (2011) Life cycle stage-resolved proteomic analysis of the excretome/secretome from *Strongyloides ratti*--identification of stage-specific proteases. Mol Cell Proteomics 10: M111 010157.
225. Real-Time PCR Applications Guide (2006). Bio-Rad Laboratories.
226. Evans TC (2006) Transformation and microinjection, WormBook, ed. The *C. elegans* Research Community, WormBook, Available: http://www.wormbook.org/chapters/www_transformationmicroinjection/transformationmicroinjection.html.
227. R Development Core Team (2011) R: A language and environment for statistical computing. R Foundation for Statistical Computing. Vienna, Austria. Available: http://www.R-project.org/.
228. Engelman JA, Luo J, Cantley LC (2006) The evolution of phosphatidylinositol 3-kinases as regulators of growth and metabolism. Nat Rev Genet 7: 606-619.
229. Fantl WJ, Escobedo JA, Martin GA, Turck CW, del Rosario M, et al. (1992) Distinct phosphotyrosines on a growth factor receptor bind to specific molecules that mediate different signaling pathways. Cell 69: 413-423.
230. Wolkow CA, Kimura KD, Lee MS, Ruvkun G (2000) Regulation of *C. elegans* life-span by insulinlike signaling in the nervous system. Science 290: 147-150.
231. Hunt-Newbury R, Viveiros R, Johnsen R, Mah A, Anastas D, et al. (2007) High-throughput in vivo analysis of gene expression in *Caenorhabditis elegans*. PLoS Biol 5: e237.
232. McGhee JD, Sleumer MC, Bilenky M, Wong K, McKay SJ, et al. (2007) The ELT-2 GATA-factor and the global regulation of transcription in the *C. elegans* intestine. Dev Biol 302: 627-645.
233. McGhee JD, Fukushige T, Krause MW, Minnema SE, Goszczynski B, et al. (2009) ELT-2 is the predominant transcription factor controlling differentiation and function of the *C. elegans* intestine, from embryo to adult. Dev Biol 327: 551-565.
234. Biron D, Wasserman S, Thomas JH, Samuel AD, Sengupta P (2008) An olfactory neuron responds stochastically to temperature and modulates *Caenorhabditis elegans* thermotactic behavior. Proc Natl Acad Sci U S A 105: 11002-11007.
235. Wes PD, Bargmann CI (2001) *C. elegans* odour discrimination requires asymmetric diversity in olfactory neurons. Nature 410: 698-701.
236. Zhu H, Li J, Nolan TJ, Schad GA, Lok JB (2011) Sensory neuroanatomy of *Parastrongyloides trichosuri*, a nematode parasite of mammals: Amphidial neurons of the first-stage larva. J Comp Neurol 519: 2493-2507.
237. Dalzell JJ, Warnock ND, McVeigh P, Marks NJ, Mousley A, et al. (2012) Considering RNAi experimental design in parasitic helminths. Parasitology 139: 589-604.

238. Stoltzfus JD, Minot S, Berriman M, Nolan TJ, Lok JB (2012) RNAseq analysis of the parasitic nematode *Strongyloides stercoralis* reveals divergent regulation of canonical dauer pathways. PLoS Negl Trop Dis 6: e1854.
239. Ludewig AH, Schroeder FC (2013) Ascaroside signaling in *C. elegans*, WormBook, ed. The *C. elegans* Research Community, WormBook, doi/10.1895/wormbook.1.155.1, http://www.wormbook.org.
240. Butcher RA, Ragains JR, Kim E, Clardy J (2008) A potent dauer pheromone component in *Caenorhabditis elegans* that acts synergistically with other components. Proc Natl Acad Sci U S A 105: 14288-14292.
241. Pungaliya C, Srinivasan J, Fox BW, Malik RU, Ludewig AH, et al. (2009) A shortcut to identifying small molecule signals that regulate behavior and development in *Caenorhabditis elegans*. Proc Natl Acad Sci U S A 106: 7708-7713.
242. Park D, O'Doherty I, Somvanshi RK, Bethke A, Schroeder FC, et al. (2012) Interaction of structure-specific and promiscuous G-protein-coupled receptors mediates small-molecule signaling in *Caenorhabditis elegans*. Proc Natl Acad Sci U S A 109: 9917-9922.
243. Coburn CM, Bargmann CI (1996) A putative cyclic nucleotide-gated channel is required for sensory development and function in *C. elegans*. Neuron 17: 695-706.
244. Mayer MG, Sommer RJ (2011) Natural variation in *Pristionchus pacificus* dauer formation reveals cross-preference rather than self-preference of nematode dauer pheromones. Proc Biol Sci 278: 2784-2790.
245. Robertson HM, Thomas JH (2005) The putative chemoreceptor families of *C. elegans*, WormBook, ed. The *C. elegans* Research Community, WormBook, doi/10.1895/wormbook.1.66.1, www.wormbook.org.
246. Bastiani C, Mendel J (2006) Heterotrimeric G proteins in *C. elegans*. WormBook, ed The C elegans Research Community, WormBook, doi/101895/wormbook1751, http://wwwwormbookorg.
247. Pfaffl MW (2001) A new mathematical model for relative quantification in real-time RT-PCR. Nucleic Acids Res 29: e45.
248. Thomas JH, Robertson HM (2008) The *Caenorhabditis* chemoreceptor gene families. BMC Biol 6: 42.
249. Troemel ER, Chou JH, Dwyer ND, Colbert HA, Bargmann CI (1995) Divergent seven transmembrane receptors are candidate chemosensory receptors in *C. elegans*. Cell 83: 207-218.
250. O'Halloran DM, Fitzpatrick DA, McCormack GP, McInerney JO, Burnell AM (2006) The molecular phylogeny of a nematode-specific clade of heterotrimeric G-protein alpha-subunit genes. J Mol Evol 63: 87-94.
251. Bargmann CI (2006) Chemosensation in *C. elegans*, WormBook, ed. The *C. elegans* Research Community, WormBook, doi/10.1895/wormbook.1.123.1, http://www.wormbook.org.
252. von Megen HHB, van den Elsen SJJ, Holterman MHM, Karssen G, Mooijman PJW, et al. (2009) A phylogenetic tree of nematodes based on about 1200 full-length small subunit ribosomal DNA sequences. Nematology 11: 927-950.

253. Overington JP, Al-Lazikani B, Hopkins AL (2006) How many drug targets are there? Nature reviews Drug discovery 5: 993-996.